Immunologic function of Virtual Memory CD8+ T cells & Role of KLF2 in effector CD4+ T cell lineage commitment

A Dissertation
SUBMITTED TO THE FACULTY OF
UNIVERSITY OF MINNESOTA
BY

June-Yong Lee

IN PARTIAL FULFILLMENT OF THE REQUIREMENTS
FOR THE DEGREE OF
DOCTOR OF PHILOSOPHY

Advisor: Stephen C. Jameson, PhD

November 2014

Acknowledgements

I would like to thank Stephen Jameson for be a great mentor throughout my Ph.D. training. The work presented in this thesis would not have been possible without his support and guidance. After 4 years exploring science with him, I realize that I am a blessed graduate student who had a chance to work with such a great scientist, writer as well as teacher. Also, I have been lucky to have another advisor Kris Hogquist who always provided profound feedback for my research.

I would like to thank all the members of the 'Jamequist' lab for their help and support. I would specifically like to thank Sara Hamilton for her help with Listeria infection experiment on my PNAS publication and Yu-Jung Lee for his help with immunofluorescent analysis on my follicular helper T cell project. I would also like to acknowledge Justin Taylor for his help in analyzing germinal center reaction. He was very helpful for the project and with teaching his general flow cytometry expertise.

My thesis committee members Yoji Shimizu, Marc Jenkins, David Masopust, Tim Starr and Bruce Blazer provided critical support and feedback.

Finally, I would like to acknowledge my parents for supporting me through my entire life. They have always believed in me and empowered me to follow my dreams

Dedication

This dissertation is dedicated to my wife, Jinjoo Kang. You are my best friend, as well as lifetime companion. I would not have accomplished this achievement without your sacrifice and support. Thank you for being with me.

Abstract

During my Ph.D. training, my research has been focused on two distinct topics: investigating the immunologic fuction of Virtual Memory CD8+ T cells; and elucidating the role of KLF2 in effector CD4+ T cell lineage commitment.

In the first part (Chaper 2), we investigate the immunologic properties of foreign-antigen specific memory-phenotype T cells, termed Virtual Memory (VM). Our data indicates that VM cells differ functionally from "true memory" cells, yet VM cells efficiently control a bacterial (*Listeria monocytogenes*) infection. These data support the novel concept that naturally occurring VM cells contribute to "pre-immune" resistance to infection.

In the second part (Chapter 3), we find that expression of the transcription factor Kruppel-like factor 2 (KLF2) expression varies in distinct Th subsets, and downregulation of KLF2 and the trafficking molecule S1PR1 (the well-defined target of KLF2) is required for Tfh differentiation. In addition to promoting S1PR1 expression, we also find that KLF2 induces expression of Blimp-1, which is known to oppose Tfh differentiation. Furthermore, KLF2 also promotes expression of T-bet and Gata3, and enhances Th1 differentiation. These data reveal that KLF2 plays an important role in dictating the lineage differentiation of CD4+ T cells.

Table of Contents

List of Figures

Chapter 1

Introduction

In the immune system, multiple cellular components are closely connected with their environment to trigger appropriate immune responses against pathogens. At the same time, these cell populations are tightly regulated to maintain homeostasis of the system and prevent immunopathology. To achieve the goals and ensure the survival of the organism, the mammalian system has developed two complementary, but distinct arms: the innate and adaptive immune systems[1].

The innate immune system is the frontline defense of host that recognizes evolutionary conserved pathogen- and danger- associated molecular patterns (PAMPs and DAMPs) by using several types of pattern recognition receptors[1-5]. Therefore, although the innate immune system is non-specific and can't distinguish individual pathogens, the innate immune response is rapid and able to offer some degree of pathogen elimination in the acute phase of the infection[1,4,5]. However, while innate immunity remains essential for the rapid response to a pathogen, some pathogens cannot be controlled by the non-specific innate immune response alone. When the innate immune system fails to control, the adaptive immune response is initiated by the antigen presenting innate immune cells (e.g. dendritic cells) which induce antigen-specific immune responses. In addition to assisting in elimination of a primary infection, activation of adaptive immune cells results in the generation of "immunologic memory"[1,6]. Therefore, although the adaptive immune response takes a longer period of time to develop than the non-specific innate immune response, the adaptive immune response is antigen-specific and provides long-lasting robust immunity against subsequent infection of same pathogen[1,6]. Hence, understanding how the adaptive

immune system functions is significant to the development of therapeutics and well as vaccines.

Therefore, I have studied the effector mechanisms of the adaptive immune response. Especially, among the adaptive immune system, my thesis researches has focused on investigating the peripheral effector function of T lymphocytes against cognate pathogens, as well as the molecular mechanism of effector lineage differentiation. Therefore, in this chapter, I will introduce background information relevant to these areas of my thesis research.

Adaptive immune response

As described above, one of the biggest differences between the innate and adaptive immune response is antigen-specificity. Innate immune responses initially protect the host against pathogen, but those only work to control pathogens that include certain molecular patterns or that induce host danger signals (e.g. interferon, apoptosis etc.). To efficiently fight the broad range of pathogens, B cells and T cells, which are the two main effector populations in the adaptive immune system, have evolved to recognize a great variety of different non-self antigens from environment. For B cells, membrane-bound immunoglobulin (Ig) on the cell surface serves as the antigen recognition receptor, and is known as the B cell receptor (BCR), which is also secreted as antibody by terminally differentiated plasma cells upon encountering the specific antigen. Similar to B cells, T cells also recognize their specific antigen with membrane-bound T cell

receptors (TCRs). However, unlike BCRs that recognize and bind the specific antigen by itself, TCRs instead recognize peptide fragments of protein antigens that are presented by the major histocompatibility complex (MHC) on host cell surface[1]. Also, T cells do not secrete their antigen receptors, and their function depends on physical localization at sites of antigen presentation or infection. With the specific antigen receptors, the adaptive immune cells can specifically recognize only one cognate antigen and leads to cellular activation and clonal expansion that provide a robust specific response against the invading pathogen[1,6].

General overview of T cell immune response

In the periphery, depending on the antigen experience and activation status, T cells can largely be sub-populated into three: naïve, effector and memory T cells[1]. After differentiation in the thymus, T cells express a trafficking receptor, sphingosine 1-phosphate receptor 1 (S1PR1), and migrate to the bloodstream by following a concentration gradient of its ligand sphingosine 1-phosphate (S1P)[7,8]. On reaching the periphery, the T cells continuously circulate throughout the body between the lymphatic and cardiovascular system by using several other trafficking molecules (e.g. CD62L, CCR7 etc.) on their surface, and patrol secondary lymphoid organs (lymph nodes and the spleen) where they search for APC presenting their specific cognate antigen[7,8]. Mature circulating T cells that haven't encountered their specific antigen are defined as naïve T cells[8].

Once naïve T cells encounter their cognate antigen, they proliferate and differentiate into effector T cells, and acquire new activities that contribute to removal of the antigen. Besides the cognate antigen recognition by specific TCR (sigal 1), effector T cell differentiation is also critically influenced by the type, timing, strength, and duration of costimulatory (signal 2) and cytokine (signal 3) stimulation[9]. Signal 2 is provided by costimulatory molecules (e.g. CD80/CD86) expressed on activated antigen presenting cells (APCs)[10]. When professional APCs (such as DCs, macrophages, and B cells) are primed by PAMPs and DAMPs, they upreguate co-stimulatory molecules which are recognized by CD28 on the T cell. Stimulation through CD28 in addition to TCR signal is required for effector T cell differentiation, and TCR signaling without CD28:CD80/86 interaction results in inducing T cell anergy[10]. The signal 3 is various cytokines. TCR and costimulatory signals initiate proliferation of naïve cells, but in the absence of a specific cytokine signal the cells fail to develop optimal effector functions, survive poorly, and do not form a responsive memory population[9-11]. When all three signals are present, a T cell becomes fully activated and is able to differentiate into an effector T cell that is capable of contributing to the elimination of an invading pathogen.

At last, following the elimination of the infecting pathogen, effector T cells undergo a contraction phase wherein the majority of pathogen-specific effector T cells die by apoptosis, but typically a small percentage (~5–10%) survive to further mature into memory T cells. As described above, this memory T cell population is long lived and gives an enhanced response to cognate antigen, which yields protection from subsequent challenge by the same pathogen[11-13].

CD8 and CD4 T cells

Phenotypically T cells can be categorized into two main subsets, CD4 expressing T cells and CD8 expressing T cells which recognize different types of MHCs[14]. On antigen recognition, naïve T cells differentiate into several functional classes of effector T cells that are specialized for different activities. CD8 T cells recognize pathogen peptides presented by MHC class I molecules, and naïve CD8 T cells differentiate into effector T cells that kill infected cells (through granzymes and perforin) and secrete cytokines such as interferon-γ (IFNγ) and tumour necrosis factor (TNF)[11]. CD4 T cells have a more flexible repertoire of effector activities. After recognition of pathogen peptides presented by MHC class II molecules, naïve CD4 T cells differentiate down distinct pathways that generate effector subsets with different immunological functions. The main CD4 effector subsets currently distinguished are Th1, Th2, Th17 and follicular helper T (Tfh) cells, which promote immune responses, and several regulatory T (Treg) subsets that have inhibitory activity and limits the extent of immune activation[15,16]. Therefore, CD8+ T cells are known as "cytolytic" upon activation and are equipped to directly kill infected cells where as CD4+ "helper" T cells produce cytokines that help activate other cell types that eventually control an infection[11,15,16]. The detailed immune function of each effector T cell lineages will be discussed in later section of this introduction.

Effector and memory CD8 T cell

Effector CD8 T cells perform cytotoxic activities and are essential in host defense against cytosolic, most commonly viruses and intracellular bacteria. These cytotoxic T cells can kill cells harboring such pathogens by recognizing foreign peptides that are transported to the cell surface bound to MHC class I molecules[1,11].

Functionally, effector CD8 T cells can uniformly be categorized as cytotoxic T cells. But, conceptually, effector CD8 T cells have been further divided into at least two subsets based on their memory potential, memory precursor effector cells (MPECs) that can become long-lived memory CD8 T cells and short-lived effector cells (SLECs) that do not[17]. Previous studies using acute infection model (e.g. *Lymphocytic choriomeningitis virus* (LCMV), *Listeria Monocytogenes* (LM)) have found that some effector cell subsets persist long-term and populate the memory cell pool, and in many cases these cells can be identified based on increased expression of interleukin-7Rα (CD127), CD27, and B cell lymphoma 2 (Bcl2) and decreased expression of effector molecule, KLRG1[17]. For the cell fate decision between MPEC and SLEC, the amount and duration of antigenic (signal 1) and inflammatory cytokine (signal 3) stimuli have been suggested as the critical players though regulating expression of effector transcription factors (e.g. T-bet, Eomes, Blimp-1)[17]. These results indicate that the innate immune system sets the relative amounts of a lineage-determining transcription factor in activated CD8 T cells during primary immune response, as well as regulates memory cell potential of the effector CD8 T cells.

It has been classically accepted that there are two main memory T cell populations: central memory T cells (Tcm) and effector memory T cells (Tem), based on their trafficking molecule expression[18,19]. Tcm express high levels of the lymphoid organ homing molecules, CCR7 and CD62L, and Tem express low levels of CCR7 and CD62L. The differential expression of these trafficking molecules on memory T cells suggests localization and functional differences between these two memory subsets[18,19]. With the CCR7 and CD62L expression, Tcm have the potential to recirculate through secondary lymphoid organs due to the expression of CCR7 and CD62L and preferentially migrate into the inflamed lymph nodes to proliferate rapidly, but take longer to differentiate into effector cells[18,19]. On the other hand, $CD62L^{lo}$/ $CCR7^{lo}$ Tem can more preferentially access peripheral non-lymphoid tissues (NLT) where the inflammation occurs, and rapidly induce effector function to eliminate the pathogen[18,19]. More recently, another subset of memory CD8 T cells, called resident memory T cells (Trm), has been identified[18,20]. Although this population shares the NLT migratory capacity of Tem, Trm don't recirculate through the body (like "classic" Tem) but are instead maintained as a long-term resident population in diverse NLTs[20]. More importantly, recent studies clearly have shown that Trm cells provide better protection against local secondary infections than circulating memory cells[21]. Thus, Trm cells are now recognized as critical sentinels in peripheral sites.

Effector CD4 T cell lineages

In contrast to CD8 T cells that mainly differentiate into cytotoxic T cells, CD4 T cells can differentiate into a variety of effector subsets, including Th1, Th2, Th17 cells, follicular helper T (Tfh) cells, and induced regulatory T (iTreg) cells that have unique functional properties[1,15,16]. Functionally, Th1 cells are characterized by their production of IFN-γ and are involved in cellular immunity against intracellular microorganisms. Th2 cells produce IL-4, IL-5, and IL-13 and are required for humoral immunity to control extracellular pathogens. Th17 cells produce IL-17A, IL-17F, and IL-22 and play important roles in clearance of extracellular bacteria and fungi, especially at mucosal surfaces. Tfh cells are a subset of helper T cells that regulate the maturation of B cells and initiate the germinal center responses to generate high-affinity neutralizing antibodies[1,15,16].

The basis for CD4 T cell differentiation decisions are still being defined. But the cytokines in the microenvironment (signal 3) and lineage specific transcription factors induced by the cytokine signaling have been shown as critical players in the lineage commitment[1,15,16]. For Th1 lineage, IL-12 produced by innate immune cells and IFN-γ produced by both NK cells and T cells polarize cells toward the Th1 cell differentiation program through action of STAT4, STAT1, and T box transcription factor T-bet. Th2 cell differentiation requires the action of GATA3 downstream of IL-4 and Stat6. Th17 cell differentiation requires a transcription factor, RORγt that is induced by TGF-β in combination with the pro-inflammatory cytokines IL-6, IL-21, and IL-23, all of which induce STAT3 phosphorylation. The cytokine requirement for Tfh cell differentiation is

less clear than other subsets, but a recent study suggested that TGF-β signaling through STAT3, STAT4 is essential for human Tfh differentiation[22], and the differentiation may be dependent on the transcription factor Bcl-6[1,15,16].

Virtual memory CD8 T cells

It has long been assumed that memory cells are only formed following "naïve" T cell encounter with specific foreign antigen presented on MHC molecule[9,17,23-25]. However, a series of previous studies showed that various homeostatic cues also can induce "naïve" T cells to acquire "memory-like" properties, without foreign antigen induced priming[12,26-31].

During studies on T cell homeostasis, it was found that naive CD8 T cells undergo proliferation in lymphopenic environments (termed homeostatic proliferation or lymphopenia-induced proliferation) by both engagement of the TCR with self-peptide/MHC ligands and signal of various cytokines (including IL-2, IL-4, IL-7 and IL-15)[24,32,33]. And in the process of lymphopenia-induced proliferation, the naïve CD8 T cells obtain memory-like phenotype and function[24,33]. They elevate expression of several functional effector molecules that are highly expressed on antigen-primed conventional memory CD8 T cells (such as CD44, CD122 (IL-2 receptor β) and CXCR3), and provide superior protection against infection[24,33]. Lymphopenia occurs not only in artificial situations (e.g. in immune-deficient or irradiated animals): physiological lymphopenia also occurs during the neonatal period in mice, and induces production of memory-phenotype T cells[24,26]. More importantly, our previous study, using peptide/MHC

tetramers in combination with magnetic enrichment protocol, showed that unimmunized mice contained a population of foreign antigen specific memory-like CD8 T cells, termed Virtual Memory (VM) CD8 T cells[26,27]. These findings do clearly show that antigen non-experienced phenotypic "memory" CD8 T cells arise through homeostatic mechanisms during normal immune system development, and suggest this population of cells may be active participants in "primary" immune responses against "foreign" pathogen. However, the antigen specific function of VM CD8 T cells was poorly characterized during actual cognate pathogen infection, and hence their potential contribution to immune responses was unclear.

Kruppel-like Factor 2 (KLF2) function in T cell

KLF2 is a zinc-finger transcription factor that binds to CACCC domain or other GC-rich DNA sequences allowing them to exert their transcriptional regulation. Since 1995 when KLF2 was originally identified, KLF2 has been shown to have many roles in multiple cells from vascular development to immune cell function[8].

In T cell immunology, my lab and other groups have reported that KLF2 has multiple critical roles in peripheral T cell trafficking though directly regulating key trafficking molecules, such as L-selectin (CD62L) and S1PR1[7,8,20]. KLF2 expression is increased in the late stages of thymocyte development and maintained during naïve T cell stage that subsequently promotes CD62L and S1PR1 expression in mature single positive (SP) thymocyte and naïve T cells[7,8]. As briefly described above, S1PR1 is essential for thymic egress of mature SP T cells, as well as secondary lymphoid organ exit of naïve T

cells in periphery[34,35]. Thus, with increased expression of KLF2 and S1PR1, mature SP T cells can migrate toward blood stream. Indeed, the accumulation of KLF2 deficient mature T cells in the thymus is prevented by overexpression of S1PR1, suggesting that this factor is the key target of KLF2 for thymic emigration[36,37]. In addition, KLF2 also directly promotes expression of CD62L, which is required for access of naive T cells to lymph nodes, indicating that this KLF coordinates opposite aspects (both exit and entry) of lymphocyte trafficking. For this reason, KLF2 can be considered a regulator of naïve T cell circulation, allowing naïve T cells to circulate throughout lymph nodes and back into the blood.

During immune response, KLF2 expression in T cells is dynamic and determined by both the strength and duration of TCR and cytokine signaling[8]. Previous studies have shown that KLF2 is highly expressed in naive T cells but rapidly down-regulated at the protein and mRNA level in response to triggering of the T cell antigen and cytokine receptor, which provides a mechanism for the initial retention of activated T cells in lymphoid tissues[8]. But, the loss of KLF2 in early-activated T cell is recovered in fully differentiated effector T cells that allows them to re-enter the blood stream and migrate to the infected tissues[8,20]. At the memory stage, KLF2 expression in different memory T cell subsets varies, and the differential expression of KLF2 determines recirculation potential of the memory T cell subsets. In recent data, we showed that KLF2 is continuously down-regulated in "Resident Memory" CD8 T cells (Trm), a population that is prominent in non-lymphoid tissues and does not appear to exchange with other sites through recirculation via the blood and lymph. On the other hand, memory CD8 T cells

circulating in the blood or found in lymphoid sites such as lymph node show high KLF2 expression[20]. Moreover, the level of KLF2 impact transcriptional program (e.g. T-Bet, Blimp-1) of effector T cells[38,39], and the down-regulation of KLF2 during effector phase of immune response is required for Trm generation[20]. Collectively, these previous findings have suggested that KLF2 may also have critical immunologic role in T cell differentiation besides trafficking. However, the regulation and function of KLF2 in peripheral effector and memory T cells are still less clear and needed to be further explored.

Statement of thesis

This thesis includes two conceptually different studies. The one is about the immunologic function of Virtual Memory CD8+ T cells (chapter 2), and the other is about the role of KLF2 in effector CD4+ T cell lineage commitment (chapter 3).

In chapter 2, specifically, my study is focused on elucidating the foreign antigen specific response of naturally occurring memory-phenotype CD8 T cells. Our previous studies indicated that foreign antigen specific memory-like CD8 T cell, termed Virtual Memory (VM), populations arise through homeostatic mechanisms during normal immune system development[26,27]. Also, some preliminary data of ours indicated that this VM population also displays some functional properties of antigen-primed "True" memory (TM) cells. Therefore, we hypothesized that the VM CD8 T cells might provide important pre-immune protection against cognate pathogens. To test this hypothesis, I

focused on characterizing the foreign antigen specific response of VM CD8 T cells and comparing them to naïve and TM populations.

In the second project (chapter 3), I studied the transcriptional regulation of KLF2 and its role in effector CD4 T cell determination. My initial collaborative work focused on CD8+T cells showed that KLF2 and its transcriptional target S1PR1 have a critical role in determining memory CD8 T cell lineage between recirculating (Tcm) or tissue-resident memory (Trm) populations (not included in this dissertation)[20]. Also, recent studies from others using CD8 T cells showed KLF2 may directly affect to several effector transcription factors (T-Bet, Blimp-1) which also have a critical role in CD4 T cell effector differentiation[38,39]. Based on these previous studies, we hypothesized that KLF2 might also have a critical regulatory role in effector CD4 T cell lineage commitment during antigen-specific immune response.

Chapter 2

Immunologic function of the foreign antigen specific homeostatic memory (Virtual memory (VM)) CD8+ T cells

Reprinted from the Proceedings of the National Academy of Sciences. June-Yong Lee, Sara E. Hamilton, Adovi D. Akue, Kristin A. Hogquist and Stephen C. Jameson. "Virtual memory CD8 T cells display unique functional properties." Proc Natl Acad Sci U S A. 2013 Aug 13;110(33):13498-503. *Copyright 2013.*

Previous studies revealed the existence of foreign antigen specific memory phenotype CD8 T cells in unimmunized mice. Considerable evidence suggests this population, termed Virtual Memory (VM) CD8 T cells, arise via physiological homeostatic mechanisms. However, the antigen specific function of VM cells is poorly characterized, and hence their potential contribution to immune responses against pathogens is unclear. Here we show that naturally occurring, polyclonal VM cells have unique functional properties, distinct from either naïve or antigen-primed memory CD8 T cells. In striking contrast to conventional memory cells, VM cells showed poor TCR-induced IFN-γ synthesis and preferentially differentiated into central memory phenotype cells after priming. Importantly, VM cells showed efficient control of Listeria monocytogenes (LM) infection, indicating memory-like capacity to eliminate certain pathogens. These data suggest naturally arising VM cells display novel functional traits, allowing them to form a bridge between the innate and adaptive phase of a response to pathogens.

Introduction

While the function of memory T cells generated by exposure to foreign antigens is well studied, far less is understood about the properties of memory-like T cells, which are produced in response to homeostatic processes. Numerous studies have shown that lymphopenic conditions can drive naïve CD4 and CD8 T cells to proliferate and acquire phenotypic traits of memory cells[12,24,28,29,31]. Furthermore, studies on lymphopenia-induced "homeostatic memory" CD8 T cells suggest they also resemble foreign antigen primed "true" memory (TM) cells in their functional properties – including the ability to rapidly produce IFN-γ, and control of bacterial and viral infections[32,33,40]. Yet, differences in phenotype and function have been noted in comparison between the homeostatic memory and TM CD8 T cells, including altered kinetics of responses to pathogen and distinct expression of integrins[27,41]. Such findings indicate that homeostatic processes do not completely mimic the TM pool, and suggests there may be distinct functional capacities of these populations.

In addition, our studies and others indicate that normal animals possess a population of unprimed memory-like CD8 T cells, which we termed "virtual memory (VM)" cells (to distinguish them from the induced homeostatic memory pool discussed above)[27]. These cells appear soon after birth in normal mice[26], and have been found to comprise 5-20% of CD8 T cells specific for diverse foreign antigens[26,27,42-45]. The finding that VM cells arise at similar frequencies in germ-free mice supports the model that such cells are produced by homeostatic mechanisms, rather than stimulation by environmental or commensal microbes[27]. The fact that VM CD8 T cell appear in neonatal

mice might indicate a role in protective immunity at this vulnerable stage[26], but VM cells also increase in frequency during aging, and studies on HSV responsive cells revealed that T cells with high avidity for the viral antigen were selectively maintained in the VM pool[44]. Furthermore, responses by high avidity cells correlated with enhanced pathogen control in older animals, suggesting a mechanism through which VM cells may compensate for functional defects in the aging immune system[44].

However, the functional properties of naturally arising VM cells have not been clearly defined. In earlier studies, we were surprised to observe that in vivo TCR stimulation did not result in production of IFN-γ by antigen specific VM cells[27] – a result indicating that VM CD8 T cells differ from either conventional or lymphopenia-driven homeostatic memory cells (both of which are potent producers of this cytokine)[32,40]. Such findings raised the possibility that, while displaying memory phenotype, the VM pool retains naïve functional properties, or may even be functionally compromised – and hence contribute little to an immune response. Furthermore, several studies suggest that memory-phenotype CD8 T cells (from unimmunized mice) exert a regulatory role, acting to inhibit CD4 and CD8 T cell responses[46-50]. Whether the antigen specific VM population serves to restrain, rather than enhance, immune reactivity has not been tested, and is especially relevant for their potential role in protective immunity against pathogens.

Here we study the functional traits of spontaneously arising VM CD8 T cells, and find that this population differs from both naïve and TM CD8 T cells. In vitro studies revealed that VM CD8 T cells manifest certain functions of TM CD8 T cells (e.g.

increased T-box transcription factors expression and advanced G1 cell cycle status), but also naïve-like properties, such as poor IFN-γ production after antigen stimulation. Moreover, VM CD8 T cells display qualitative and quantitative differences with naïve and TM counterparts during antigen specific immune response in vivo yet, importantly, VM provide potent antigen-specific protective immunity against LM infection, similar to antigen-primed memory CD8 T cells. Together our data suggest that, despite their distinct characteristics in comparison with conventional memory and naïve CD8 T cells, VM cells display enhanced functional properties that allow them to mount a more effective immune response during primary pathogen encounter.

Results

Although virtual memory (VM) cells constitute 5-20% of the foreign antigen specific CD8 T cell population in unprimed mice[26,27,42-44], the very low frequency of precursors for a given MHC/peptide ligand makes functional assessment of VM CD8 T cells challenging. To solve this problem, we utilized mice expressing the rearranged TCR β-chain of the OVA-specific OT-I TCR (henceforth called "Vβ5 Tg"). Pairing of this TCR chain with endogenously rearranged TCR α-chains generates a diverse, polyclonal repertoire, yet leads to an elevated precursor frequency (~1-2%) of CD8 T cells specific for Ova/K^b in unimmunized Vβ5 Tg mice[51,52] (Fig. 1A). Importantly, both total CD8 T cell numbers and the frequency of memory-phenotype (CD44hi, CD122hi, CXCR3hi, Ly6Chi) CD8 T cells are similar in Vβ5 Tg and normal B6 mice (Fig. 1B and D). Likewise, analysis of foreign antigen specific CD8 T cells (identified using peptide/MHC tetramers) in unprimed mice showed that the frequency and phenotype of Ova/K^b specific VM cells in Vβ5 Tg mice was similar to polyclonal VM cells in normal B6 mice (Fig. 1D)[27]. The expression of these markers on Ova/K^b tetramer-binding VM cells mirrored that of Ova/K^b specific TM cells (generated by LM-OVA priming of adoptively transferred Vβ5 Tg CD8 T cells) (Fig. 1D). However, while the TM population included both CD62L+ and CD62L- populations (i.e. Central and Effector memory phenotype cells, respectively), the antigen specific VM population was uniformly CD62L+ (Fig 1D). Furthermore, Vβ5 VM cells displayed low levels of α4 integrin (CD49d) when compared to antigen primed TM cells (Fig. 1C and D), in keeping with previous studies on phenotypic differences between polyclonal VM and TM

populations[27,45]. Hence, the phenotype of naïve and VM CD8 T cells within the Ova/K^b specific population of Vβ5 mice resembled that of normal mice, yet the elevated frequency of OVA-specific cells in Vβ5 mice provided an opportunity to compare the antigen-specific responses by naïve, VM and TM subsets.

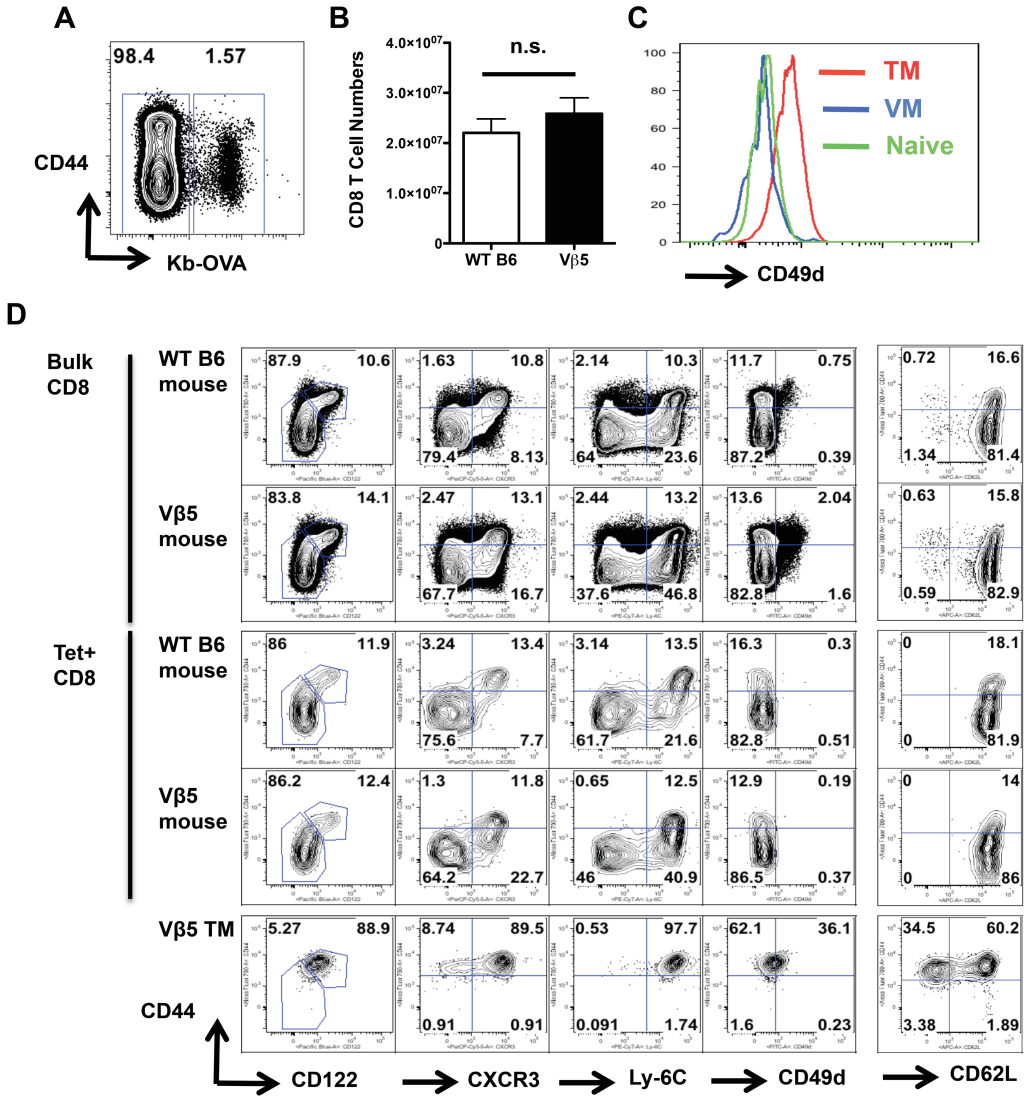

Figure 2-1. Analysis of CD8 T cell subsets derived from Vβ5 tg mice. (A) Representative data on the frequency and CD44 expression phenotype of OVA/K^b-specific CD8 T cells in unprimed Vβ5 tg mice. (B) Number of CD8 T cells in unprimed WT B6 mice and Vβ5 tg mice. Statistical significance between the number of CD8 T cells from WT B6 and Vβ5 mice is not significant ("n.s.", P >0.05, Student t test). (C) CD49d expression of Ova/Kb tetramer+ naïve, VM and TM Vβ5 CD8 T cells. (D) Comparison of cell surface marker expression (CD122, Ly-6C, CXCR3, CD49d and CD62L) between indicated populations of normal and Vβ5 CD8 T cells. Ova/K^b specific unprimed and TM Vβ5 CD8 T cells were detected by an appropriate combination of congenic markers and Ova/K^b tetramer staining. Tetramer+ve CD8 T cells from wild type B6 mouse were stained with a cocktail of tetramers (Ova/K^b, B8R/K^b, HSVgB/K^b) and enriched by tetramer pull-down assay. All the data is representative of more than 3 experiments.

VM CD8 T cells share some in vitro functional traits with "true" memory CD8 T cells.

Previous studies suggest that antigen-driven TM CD8 T cells display changes in gene expression, cytokine production and cell cycle regulation, all of which are thought to enhance the capacity of these cells to rapidly enter an immune response[23,53]. Hence we investigated whether VM share these features with TM.

The T-box transcription factors, T-bet and Eomes, serve as critical regulators of effector functions and differentiation of memory CD8 T cells, and both factors are upregulated in TM cells[54-56]. Expression of both T-bet and Eomes were significantly increased on both VM and TM populations, compared to naïve Ova/K^b tetramer+ Vβ5 Tg CD8 T cells, although we observed reciprocal differences between the memory populations in the extent of T-bet and Eomes upregulation (Fig. 2A). RT-PCR analysis confirmed these expression patterns at the transcriptional level (Fig. 2B). Hence, these data indicate that VM cells express not only memory phenotypic markers (Fig. 1D), but also key transcription factors characteristic of TM CD8 T cells.

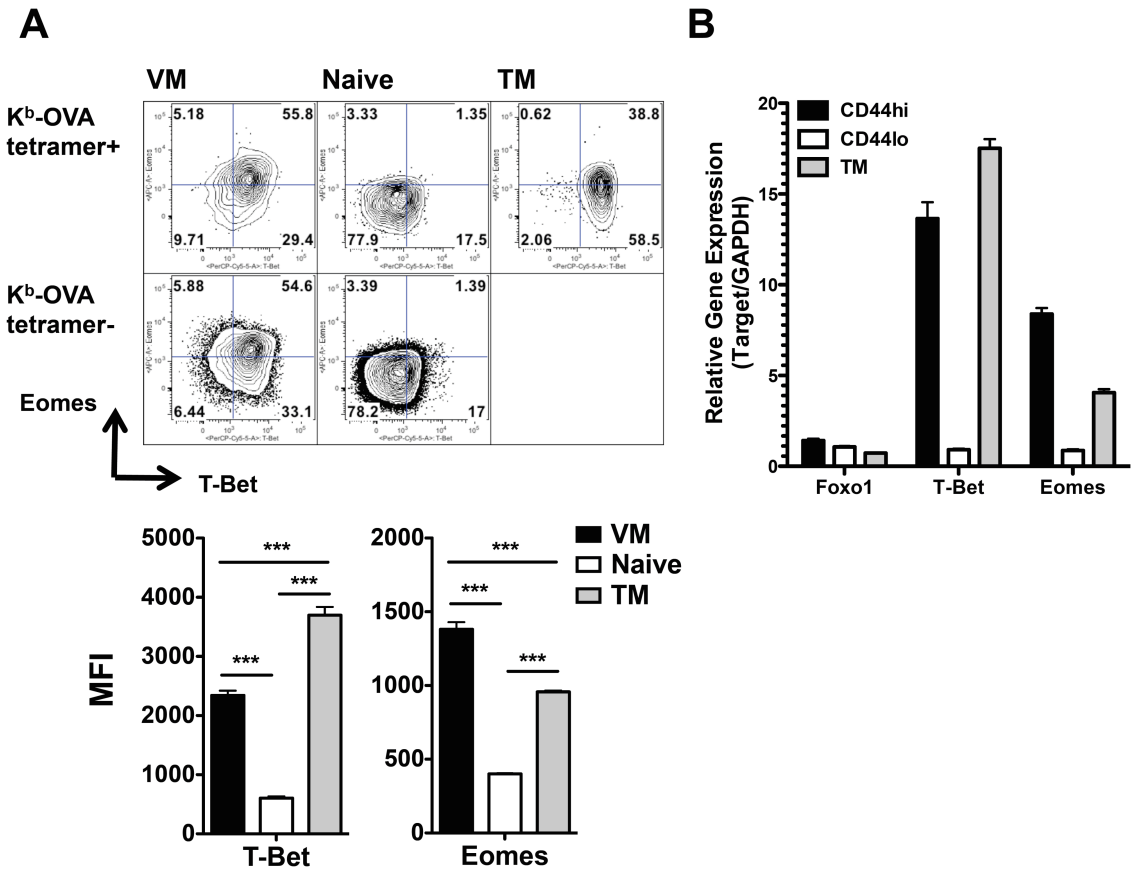

Figure 2-2. Expression of T box transcription factors on naïve, VM and TM CD8 T cells. (A) Expression of T-bet and Eomes on Ova/K^b specific VM, naïve and TM Vβ5 CD8 T cells were determined by FACS. Data are representative of at least 3 independent experiments. (B) qRT-PCR analysis of indicated genes on sort purified CD44high and CD44low Vβ5 CD8 T cells from unprimed mice, in comparison with TM Vβ5 CD8 T cells (from immunized mice). Relative gene expression levels were normalized by GAPDH, and the levels in CD44low Vβ5 CD8 T cells were chosen as the baseline for comparison. Data are compiled from 3 independent experiments using independently generated cDNAs (n=3) and graphs show mean +/- SD.

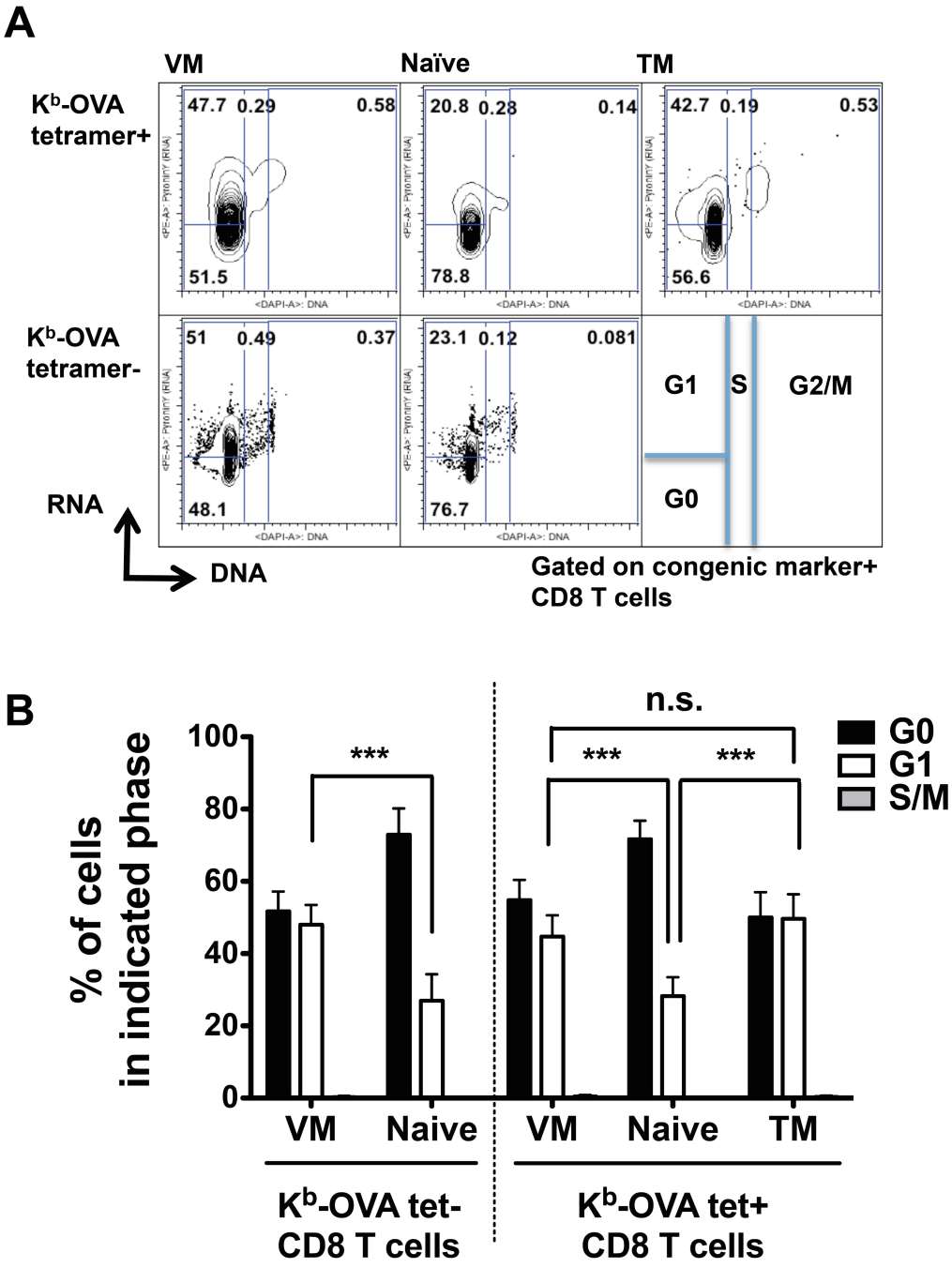

Figure 2-3. Comparison of cell cycle status between naïve, VM and TM CD8 T cells. Cell-cycle analysis of indicated Vβ5 CD8 T cell populations. (A) Represented FACS plot showing amount of intracellular DNA and RNA that indicate cell cycle status of cells. Numbers in boxed areas indicate percentage of cells in each. (B) Analysis of cell cycle status on indicated populations. Data are compiled from at least 3 experiments and bars show the mean +/- SD. Statistical significance is indicated (***, $p<0.001$, "n.s." ("not significant") is used to denote P-values >0.05, Student t test).

Previous studies showed that most TM are maintained in G1 phase of the cell cycle, which has been proposed to allow them to progress to proliferation more quickly than naïve CD8 T cells[57,58]. Hence we analyzed intracellular RNA and DNA levels[58] to investigate the cell cycle status of VM, TM and naïve CD8 T cell populations (Fig. 3A). As expected, very few (<1%) cells of any type showed signs of active progression through cell cycle (i.e. S/G2/M phases) at steady state (Fig. 3A), but the VM and TM populations were significantly enriched in cells at G1 phase, compared to the naïve pool (Fig. 3A, B). Furthermore, gene expression of cell cycle regulators associated with G1 phase (CDK6 and CyclinD3)[57,59] showed significantly elevated expression in both memory populations (Fig. 4).

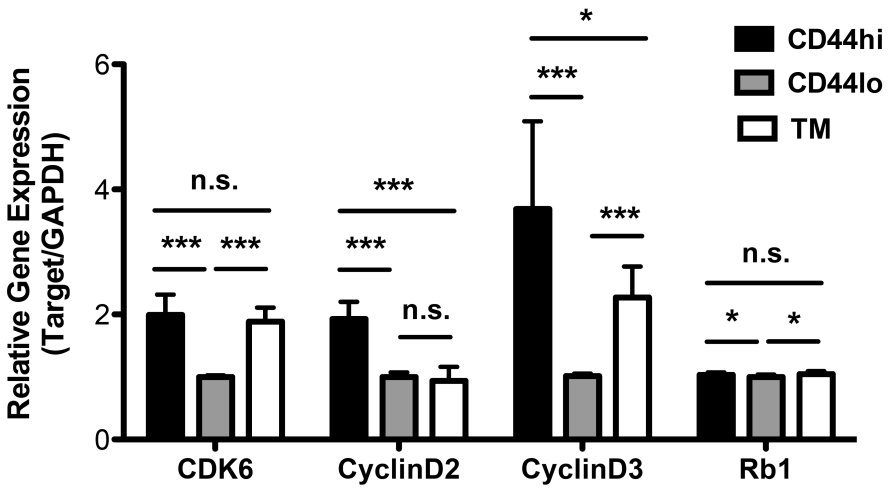

Figure 2-4. G1 cell cycle regulatory gene expression in naïve, VM and TM CD8 T cells. qRT-PCR analysis of cell cycle regulatory genes on sort purified CD44high and CD44low Vβ5 CD8 T cells from unprimed mice, in comparison with TM Vβ5 CD8 T cells (from immunized mice). Relative gene expression levels were normalized by GAPDH, and the levels in CD44low Vβ5 CD8 T cells were chosen as the baseline for comparison. Data are compiled from 3 independent experiments using independently generated cDNAs (n=3). Graphs show mean +/- SD and statistical significance is indicated (***, $p<0.001$; *, $p<0.05$, while "n.s." ("not significant") is used to denote P-values >0.05, Student t test)

Memory CD8 T cells are characterized by basal proliferation, which maintains their numbers long-term[60,61]. Our data showed that both TM and VM populations have advanced cell cycle status in G1 phase (Fig. 3, 4), suggesting VM may undergo the memory like basal proliferation. However, it is not clear whether a similar process occurs for the VM population. To explore this issue, we measured BrdU incorporation during a 2 weeks labeling period in adult B6 mice. At the end of the labeling period, BrdU labeling was measured in naive and memory-phenotype CD8 T cells in the bulk population as well as cells isolated using a mixture of peptide/MHC tetramers (comprised of B8R/K^b, M57/K^b, and HSVgB/K^b). As was expected based on previous studies[62], a fraction of bulk naive CD8 T cells incorporated a low level of BrdU (Fig. 5A), which has been ascribed to labeling during thymic development[62]. A larger cohort of bulk memory-phenotype CD8 T cells showed BrdU incorporation, and BrdU staining was of greater intensity, suggestive of active proliferation during the labeling period. Importantly, similar patterns of BrdU incorporation were observed for the tetramer-staining cells isolated by tetramer enrichment (Fig. 5), suggesting that VM cells undergo basal proliferation, albeit at a slightly lower rate than observed in the bulk memory-phenotype CD8 T cell pool (Fig. 5B). Overall, these data suggest VM cells, similar to conventional TM CD8 T cells, are advanced in their cell cycle status and capable of long-term maintenance (involving basal proliferation).

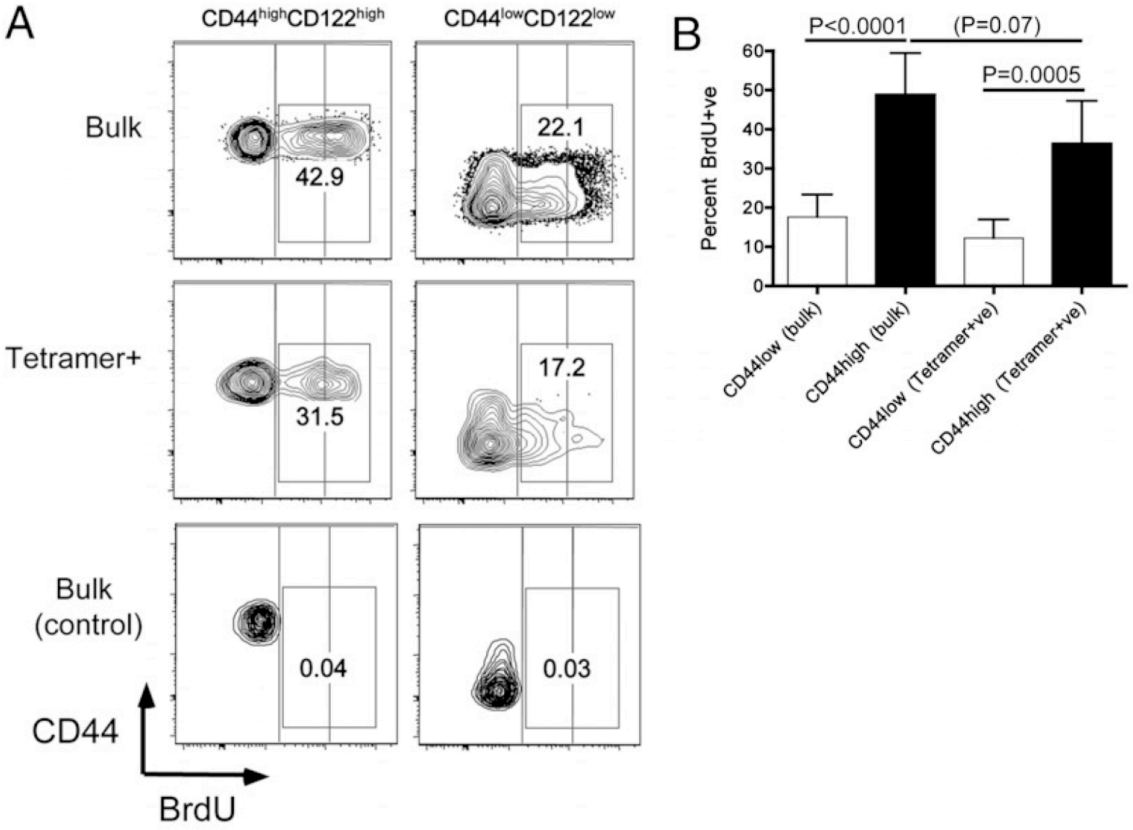

Figure 2-5. Basal proliferation of VM cells at steady state. Normal adult B6 mice were labeled with BrdU for 14–16 d, or were maintained in parallel without BrdU exposure (control). Spleen and lymph node cells were isolated and stained for cell surface markers and intracellular BrdU (for the bulk population), or were first subjected to tetramer enrichment (using a mixture of B8R/K^b, M57/K^b, and HSVgB/K^b tetramers) prior to surface and intracellular staining with Abs. Events were gated on bulk or tetramer+ve naive and memory-phenotype CD8 T cells, as indicated. (A) Representative data. Vertical blocks are overlaid on the contour plots to highlight the different levels of BrdU staining on naive and memory T cells. The numbers on the plots indicate the percentage of total BrdU+ve cells (regardless of staining intensity). (B) Compiled data on the percentage of BrdU+ve cells among the naive and memory-phenotype cells among bulk and tetramer+ve CD8 T cells. Data are from three experiments deriving from two independent BrdU-labeling cohorts.

VM CD8 T cells display differential cytokine producing capacity to "true" memory CD8 T cells.

T-box transcription factors are known to serve as positive regulators of IFN-γ production[54,55,63]. Therefore, we next examined IFN-γ production by naïve, VM and TM populations from Vβ5 mice, following peptide/MHC (Ova peptide) stimulation in vitro for 2 or 5 hours. Since TCR engagement induces production of TNF-α in both naïve and memory CD8 T cells[32,64], we gated on TNF-α+ cells to identify the antigen responsive population: At 5 hours, this population represented around 80% of tetramer-binding cells (Fig. 6A, allowing us to accurately assess whether TNF-α producing cells also synthesized IFN-γ). As expected[32,54,55], few responding naïve phenotype CD8 T cells made IFN-γ by 5 hours, while nearly all TM cells produced this cytokine at 2 hours (Fig. 6B, C). Significantly, IFN-γ production by the VM CD8 T cell population was much weaker than that of TM cells at either time point, and was only marginally increased over induction in the naïve population at limiting antigen doses (Fig. 6B, C). Furthermore, production of TNF-α at 2h of stimulation was significantly greater in the TM pool compared to either VM or naïve cells (Fig. 6A). On the other hand, overall dose sensitivity was unchanged in these populations, arguing against differences in functional avidity. Such results extend and confirm our earlier in vivo studies[27] and suggest that the VM pool, despite expressing high levels of relevant T-box factors (Fig 2A, B), is less competent for rapid IFN-γ production, compared to TM cells.

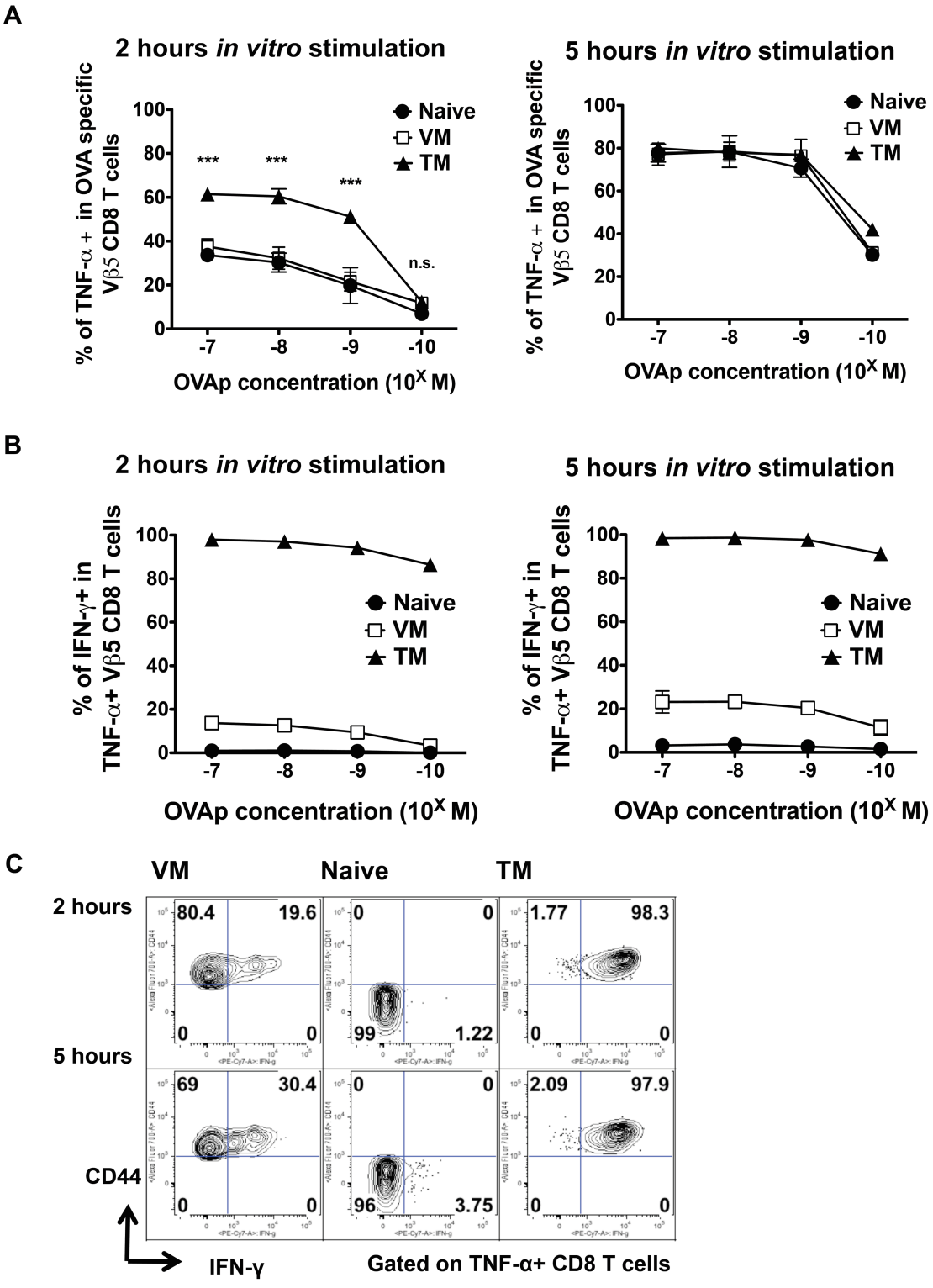
A
2 hours *in vitro* stimulation
5 hours *in vitro* stimulation
% of TNF-α + in OVA specific Vβ5 CD8 T cells
Naive
VM
TM
***
***
***
n.s.
OVAp concentration (10X M)
B
2 hours *in vitro* stimulation
5 hours *in vitro* stimulation
% of IFN-γ+ in TNF-α+ Vβ5 CD8 T cells
OVAp concentration (10X M)
C
VM
Naive
TM
2 hours
5 hours
80.4
19.6
0
0
0
0
99
1.22
1.77
98.3
0
0
69
30.4
0
0
96
3.75
2.09
97.9
0
0
CD44
IFN-γ
Gated on TNF-α+ CD8 T cells

Figure 2-6. Proinflammatory cytokine production in VM, naïve and TM Vβ5 CD8 T cells upon in vitro stimulation with OVA peptide. (A) Percentage of TNF-α producing cells among Ova peptide specific Vβ5 CD8 T cells upon in vitro stimulation of OVA peptide (10^{-7}M - 10^{-10}M) for 2 or 5 hours, corrected for the frequency of Ova/K^b tetramer+ cells in an unstimulated sample (i.e. % of TNF-α producing CD8 T cells ÷ % of Ova/K^b tetramer positive CD8 T cells). (B) IFN-γ production in VM, naïve and TM Vβ5 CD8 T cells upon in vitro stimulation with OVA peptide. Data show the frequency of TNF-α+, IFN- γ+ cells within the total responsive (TNF-α+) pool. The response was measure at 2 or 5 hours after simulation with titrated OVA peptide doses (10^{-7}M - 10^{-10}M). (C) IFN-γ production evaluated at 2 and 5 hours after 10^{-7}M OVA peptide treatment, and shown in comparison with CD44 expression levels. The graph shows compiled data from 4 independent experiments and lines show mean +/- SD. Statistical significance between VM and TM is indicated (***, $p<0.001$; **, $p<0.01$; while "n.s." ("not significant") is used to denote P-values >0.05, Student t test)

Taken together, these data support the concept that the VM population is similar to antigen-primed memory (TM) cells in some characteristics (elevated T-box factor expression, cell cycle position and long-term maintenance) yet not others (rapid, efficient IFN-γ production).

VM CD8 T cells preferentially expand during the effector phase of primary immune response compared to naïve CD8 T cells.

Previous studies showed that lymphopenia-induced memory cells expanded more quickly than naïve T cells during an antigen specific immune response[32,40]. However, such studies have not been reported for the naturally occurring VM population -- due in large part to the scarcity of VM cells specific for a given antigen in normal polyclonal mice. Use of the Vβ5 system allowed us to directly compare naïve and VM cell responses to cognate antigen. Specifically, we used a dual adoptive transfer system (Fig. 7), permitting characterization of each population responding in an identical environment throughout the immune response. To avoid TCR stimulation, transferred cells were not stained with OVA/K^b-tetramer (although an aliquot from each sorted sample was assessed for tetramer binding, to determine the antigen-specific precursor frequency). During early stage of the infection (0, 5 hours and 3 days post infection), we performed Ova/K^b tetramer enrichment, to track the rare antigen specific donor CD8 T cells.

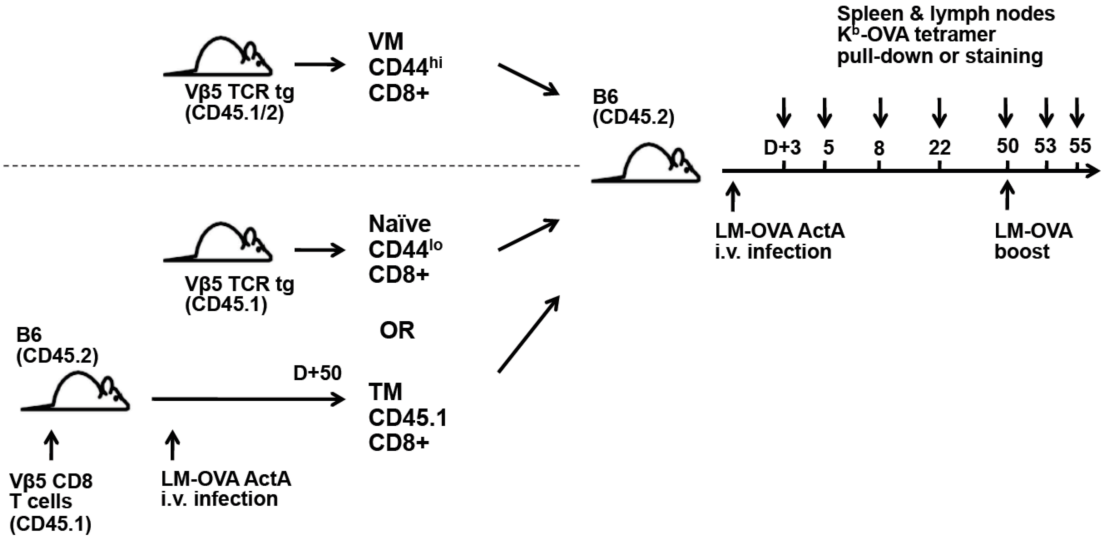

Figure 2-7. In vivo adoptive transfer of Vβ5 VM CD8 T cells with Naïve or TM. Experimental schematics. To directly compare VM to Naïve or TM during the cognate antigen specific immune response in vivo, congenically distinct VM (CD44high) and Naïve (CD44low) CD8 T cells were sorted from unprimed Vβ5 tg mice. Vβ5 TM CD8 T cells were generated in wild type B6 recipients by adoptive transfer of unprimed total Vβ5 CD8 T cells and subsequent infection of attenuated (ActA) LM-OVA for at least 50days, and sorted with congenic marker (CD45.1). Then, number of Ova/K^b specific CD8 T cells was determined by Ova/K^b-tetramer staining, and VM CD8 T cells were co-transferred with Naïve or TM CD8 T cells in 1:1 ratio (include 300-500 Ova/K^b specific CD8 T cells in each population) into recipients, which were subsequently infected with LM-OVA ActA. Ova/K^b-tetramer and relevant congenic markers determined the Ova antigen specific cells within each population. For inducing the secondary immune response, mice were infected with virulent LM-OVA at day 50 post primary infection.

Initial engraftment of both donor populations was similar (Fig. 8A), but by day 3 of LM-OVA infection, VM CD8 T cells had undergone significant expansion while the naïve pool had not increased in number, such that the VM-derived population outcompeted their naïve counterparts by more than 10-fold (Fig. 8A). The magnitude of this competitive advantage was rapidly lost however, as the response progressed through days 5 and 8 post-infection (Fig. 8A), and at memory time points both VM- and naïve-derived populations were observed in similar numbers. Hence, these data suggest a dramatic advantage for the VM population early in the immune response to infection, while naïve cells "catch up" by the peak of expansion. To analyze very early antigen encounter, we examined CD69 upregulation at 5 hours post infection. Notably, the Ova/Kb tetramer staining VM population exhibited significantly greater CD69 induction than naïve cells of the same specificity (Fig. 8B). Weaker CD69 upregulation was observed on tetramer-negative VM cells, though whether this represents low-grade non-specific activation or the response to other LM epitopes is unclear (Fig. 8B). We also examined the secondary response of cells derived from VM and naïve precursors (stimulated by infection with virulent LM-OVA at day 50) (Fig. 7). In contrast to the primary response, no numerical advantage of the VM-derived population was observed at day 3 or 5 of the recall response, which showed characteristically rapid kinetics (Fig. 8C). Such findings suggest that differences in the initial response of VM versus naïve CD8 T precursors are not carried forward into the memory pool they produce after antigen encounter.

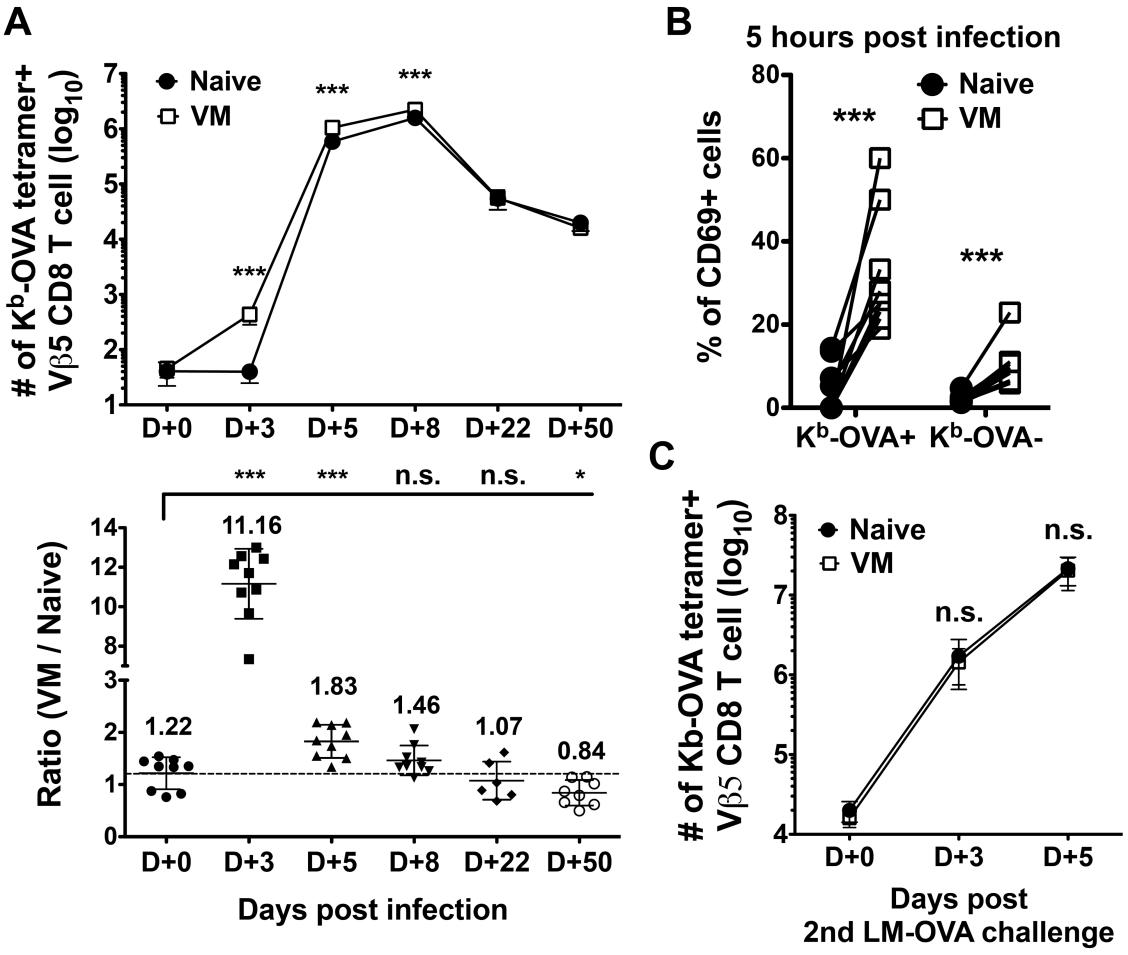

Figure 2-8. VM CD8 T cells out-compete their naïve counterparts during the expansion phase of the primary immune response. (A) At the indicated time points following LM-OVA infection, Ova/K^b tetramer+ve cells derived from VM and naïve Vβ5 donors in the spleen and superficial lymph nodes were enumerated. Data are shown as absolute numbers or ratio between VM and naïve derived cells. (B) The frequency of CD69 expressing Ova/Kb-tetramer + or Ova/K^b-tetramer – Vβ5 CD8 T cells was determined 5 hours after LM-OVA infection. Data show CD69 expression by paired samples of naïve and VM cells in the same recipients. (C) Number of Ova/K^b specific VM and naïve Vβ5 CD8 T cells during secondary immune respond against LM-OVA. For all experiments, the data are compiled from 3 independent experiments except day 22 p.i. (panels A) which were derived from 2 independent experiment (6 mice total). Line graphs show mean +/- SD and statistical significance is indicated (***, $p<0.001$; *, $p<0.05$, while "n.s." ("not significant") is used to denote P-values >0.05, Student t test).

This early proliferative advantage of VM cells could potentially be an artifact of the Vβ5 system, or specific to LM infections. Hence, we tested distinct model systems in which dual adoptive transfers were performed using naïve and VM populations from normal, polyclonal B6 CD8 T cells (Fig. 9A). In order to compensate for the low precursor frequency for specific antigens, we explored the response to multiple K^b-restricted epitopes during a response to LM, or examined the response to an immunodominant epitope (B8R) following infection with vaccinia virus (Fig. 9A). Similar to our findings with Vβ5 CD8 T cells, antigen specific cells derived from polyclonal VM population were present at elevated numbers compared to those derived from the naïve subset (Fig. 9B, C). These data suggest that VM CD8 T cells activate more rapidly and expand more quickly than naïve CD8 T cells of the same specificity, leading to an initial (but transient) advantage of the VM pool, during the primary immune response.

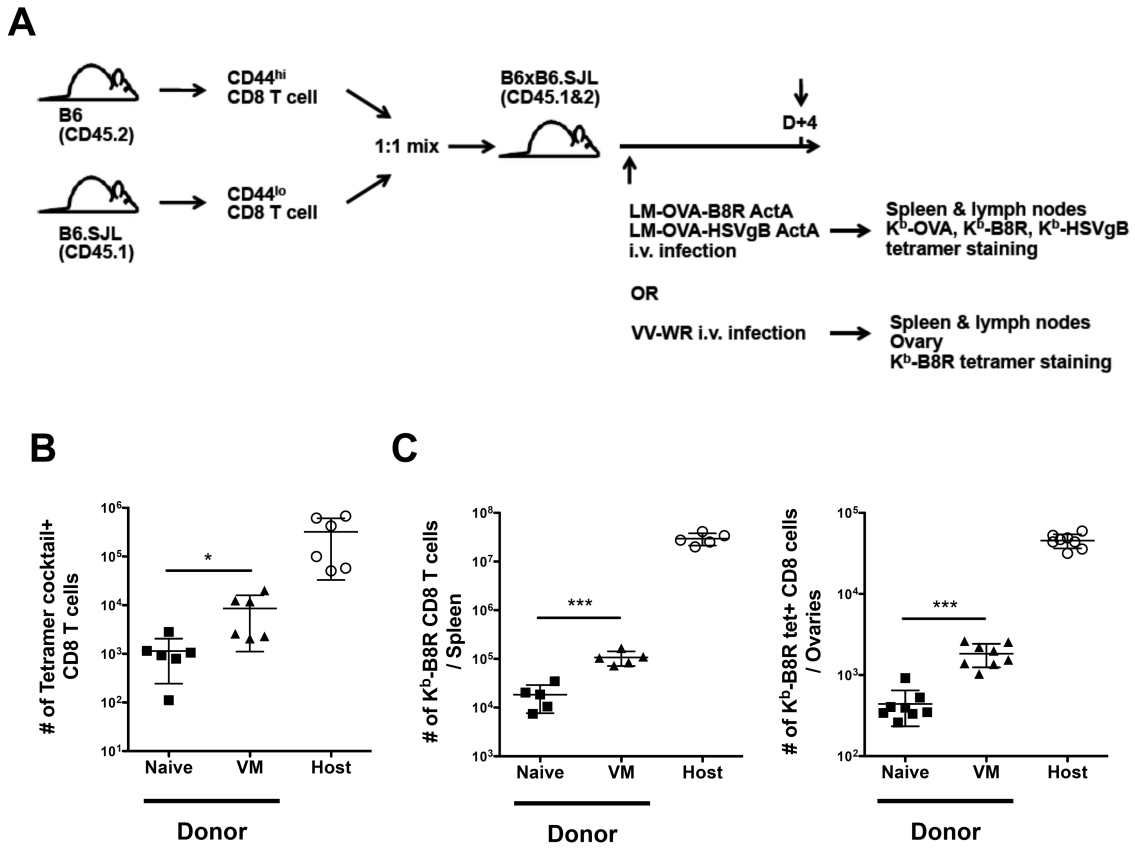

Figure 2-9. VM CD8 T cells out-compete naïve counterparts for acute phase of immune response. (A) Experimental schematic. Congenically distinct polyclonal CD44high and CD44low CD8 T cells ($2x10^6$ cells of each population) from unprimed mice were co-transferred in 1:1 ratio into congenic wild type host, which were subsequently immunized with attenuated LM strains (LM-OVA-B8R and LM-OVA-HSVgB) (B) or Vaccinia virus (VV-WR) (C). (B) shows the number of tetramer cocktail (K^b-OVA/K^b-B8R/K^b-HSVgB) positive CD8 T cells within each donor population (and host cells) in the spleen 4 days post infection after LM-OVA ActA infection. Data are compiled from 2 independent experiments (3 mice for each infection) (C) The numbers of donor and host K^b-B8R tetramer+ cells in the spleen and ovary of day 4 VV-WR infected recipients are shown. Data are compiled from 3 independent experiments and lines show mean +/- SD.

VM CD8 T cells preferentially differentiate into short-lived effector phenotype cells and Central Memory cells following priming.

At the effector stage, naïve- and VM-derived cells showed similar capacity for cytokine production and upregulation of T-bet and Eomes (Fig. 10A, B), suggesting similar acquisition of effector functions and characteristics. However, the finding that initial expansion advantage of VM cells is not sustained (Fig. 8A) might suggest that a greater fraction of these cells become "short-lived effector cells" (SLEC), and hence succumb to apoptotic death as the expansion phase ends[65]. Indeed, we observed a modest but significant elevation in the frequency of KLRG1+ CD127lo SLEC phenotype cells among VM-derived cells at the effector stage (Fig. 11A), while cells derived from the naïve donor population showed a reciprocal enrichment for KLRG1- CD127hi memory phenotype cells in the late effector and memory phases (Fig. 11B). Once again, these differences between VM and naïve responder cells were only detected following priming: in the recall response, progeny of both donors gave rise to phenotypically similar secondary effector populations (Fig. 10C, D).

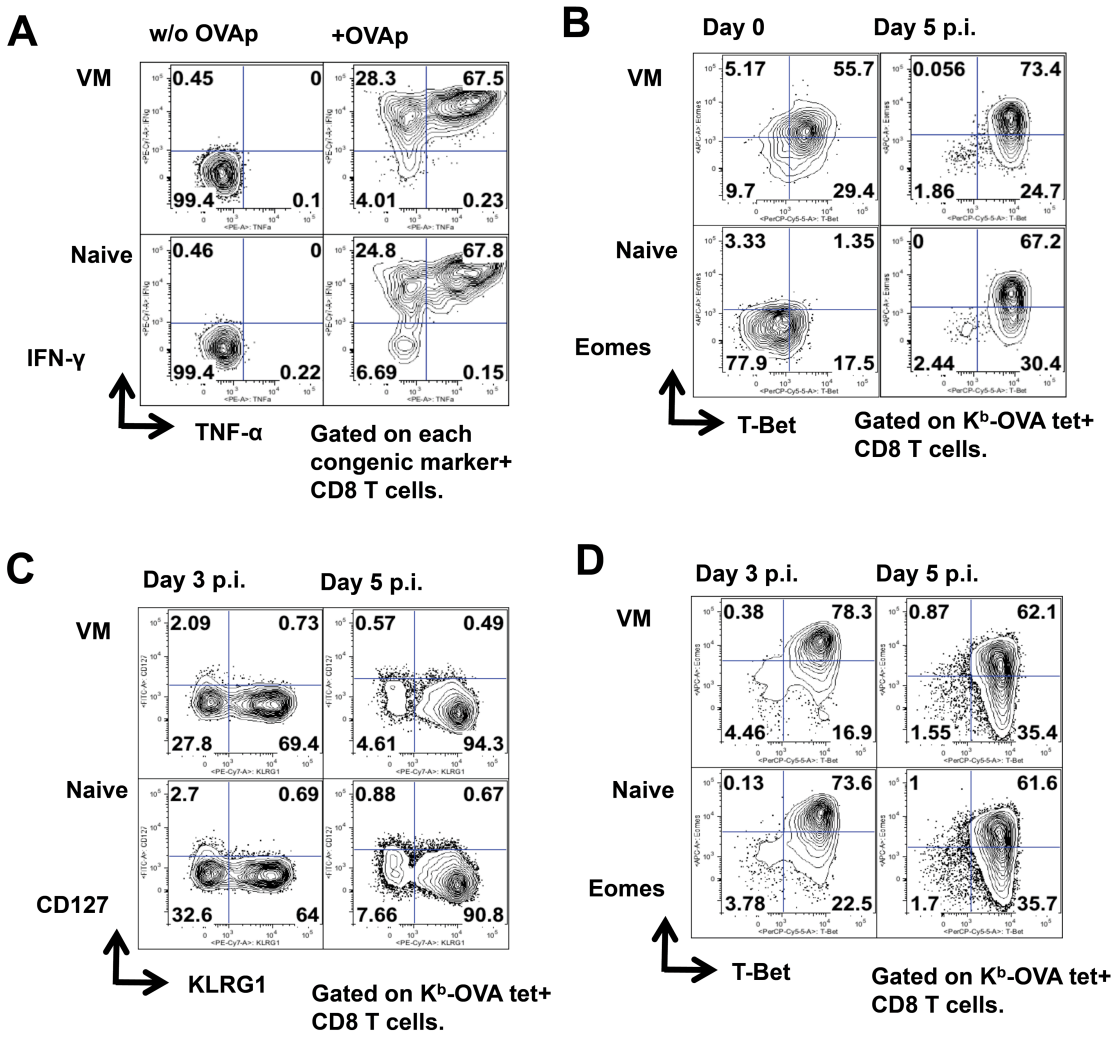

Figure 2-10. Phenotypic and functional comparison between VM and naïve CD8 T cells during primary and secondary LM infection. (A,B) Responder cells derived from co-transferred naïve and VM Vβ5 CD8 T cells were assayed at day 5 following primary LM-OVA infection. Pro-inflammatory cytokine (IFN-γ and TNF-α) production was determined for donor populations (identified by congenic markers) (B), and expression of T-box transcription factors (T-bet and Eomes) was determined for OVA/Kb tetramer+ donor (C). Data are representative of 2 experiments (6 mice total). (C,D) Phenotype of VM- and naïve- derived Vβ5 CD8 T cells at the indicated times during a recall response, induced by virulent LM-OVA infection. Data are representative of 3 independent experiments.

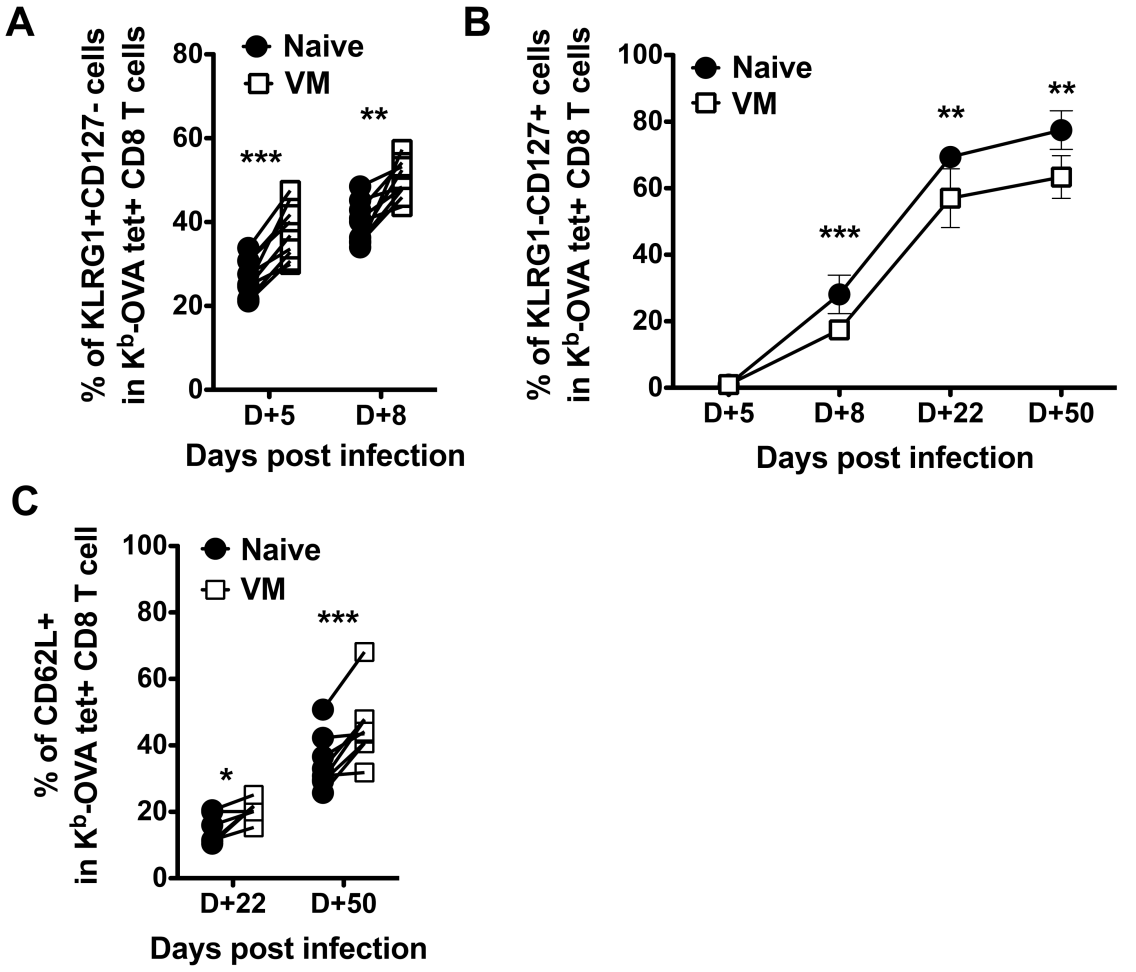

Figure 2-11. Comparisons of phenotype and peripheral residency between VM and naïve CD8 T cells during primary LM infection. (A,B) Short-lived effector (KLRG1+ CD127lo) and memory precursor (KLRG1- CD127hi) phenotype of responding VM and naïve CD8 T cells, during effector and memory phase of LM infection. Frequencies of phenotypic subsets were determined on Ova/K^b-tetramer+ donor Vβ5 CD8 T cells at the indicated times post infection. Line graphs show mean +/- SD. (C) Central memory (CD62L+ve) differentiation of responding VM and naïve donor Vβ5 CD8 T cells. The frequency of CD62L+ve cells in cotransfered naïve and VM populations is shown. For all experiments, data were compiled from 3 independent experiments, except day 22 p.i. (2 independent experiment; 6 mice total). Statistical significance between groups is indicated (***, $p<0.001$; **, $p<0.01$; *, $p<0.05$, while "n.s." ("not significant") is used to denote P-values >0.05, Student t test).

We also investigated whether the VM population might also be skewed in their memory subset distribution. Two prominent memory sub-populations are CD62L+ "Central memory" (Tcm) and CD62L- "Effector memory" (Tem) groups[66,67]. While T_{CM} typically recirculate through lymphoid sites, TEM are associated with trafficking and residency in non-lymphoid tissues. Hence, we analyzed naïve- and VM-derived cells at the memory phase (days 22 and 50) to determine their phenotype and patterns of tissue distribution. Interestingly, VM-derived cells showed a significant enrichment for Tcm phenotype cells compared to naïve-derived cells (Fig. 11C). Consistent with this, the progeny of naive responder cells were significantly over-represented in non-lymphoid tissues (salivary gland and kidney), sites where Tem are typically enriched (Fig. 12).

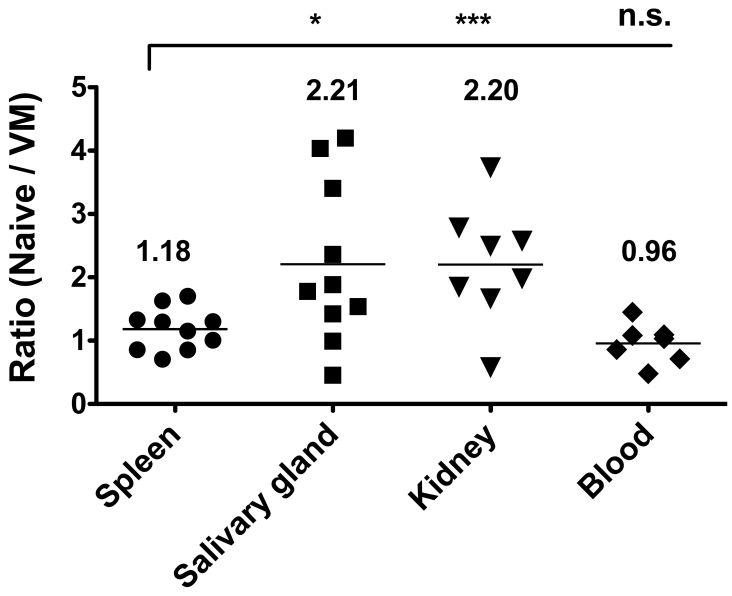

Figure 2-12. Peripheral tissue distribution of VM CD8 T cells in memory stage. Ratio between Ova/K^b-tetramer specific VM and naïve Vβ5 CD8 T cells in indicated tissues and blood at 50-60 days post-LM infection. (Blood contamination in each tissue was excluded as described in SI Materials and Methods). Data were compiled from 3 independent experiments. Statistical significance between groups is indicated (***, $p<0.001$; *, $p<0.05$, while "n.s." ("not significant") is used to denote P-values >0.05, Student t test).

These data argue that, during a primary immune response, VM cells differ from naïve cells not only in their response kinetics but by qualitative changes in the generation of effector and memory subsets.

VM and TM CD8 T cells show similar response kinetics, but qualitative differences in effector differentiation.

To this point, our studies had focused on comparing the immune response of VM cells to naïve counterparts. However, studies using lymphopenia-driven memory CD8 T cells showed that they are outcompeted by TM cells during an immune response[32,41]. To investigate this in our studies of spontaneously generated VM CD8 T cells, we again performed dual adoptive transfer experiments: as before, congenically distinct Vβ5 TM (generated by adoptive transfer of bulk Vβ5 CD8 T cells into congenic recipients, and subsequent LM-OVA infection) and VM cells were sorted and co-transferred into recipients, which were then infected with LM-OVA (Fig. 7). Adoptive transfer efficiencies were similar for VM and TM populations (data not shown).

At the level of kinetics and magnitude of the response, we observed no significant differences between TM and VM populations until the memory phase – at which point the TM pool had a slight (but significant) advantage over the VM pool (Fig. 13A). In contrast to these mild effects, substantial differences were observed in the differentiation of TM and VM-derived cells. Previous studies have shown that secondary immune responses (of "true" memory CD8 T cells) generate a population of effector-like CD8 T cells that are sustained into the memory phase, and a corresponding underrepresentation

of Tcm cells[23,68,69]. Indeed, we observed high frequencies of KLRG-1+ CD127lo cells, and a corresponding deficit in production of KLRG-1- CD127hi memory cells, for the population generated from the TM pool (Fig. 13B, C). In contrast, the responder cells derived from the VM pool showed much more efficient production of KLRG-1- CD127hi memory-phenotype cells. Furthermore, while responding TM cells showed inefficient production of CD62L+ (i.e. Tem) phenotype memory cells, the VM-derived pool produced a significantly larger CD62Lhi subset (Fig. 13D), echoing similar studies using lymphopenia-induced memory OT-I CD8 T cells[41]. It is important to note, however, that the bias of VM-derived cells toward the TCM phenotype did not result in their more efficient maintenance, compared to the TM-derived pool (Fig. 13A). Overall, our findings suggest that VM CD8 T cells expand similarly to "true" memory CD8 T cells, yet display substantially altered differentiation characteristics.

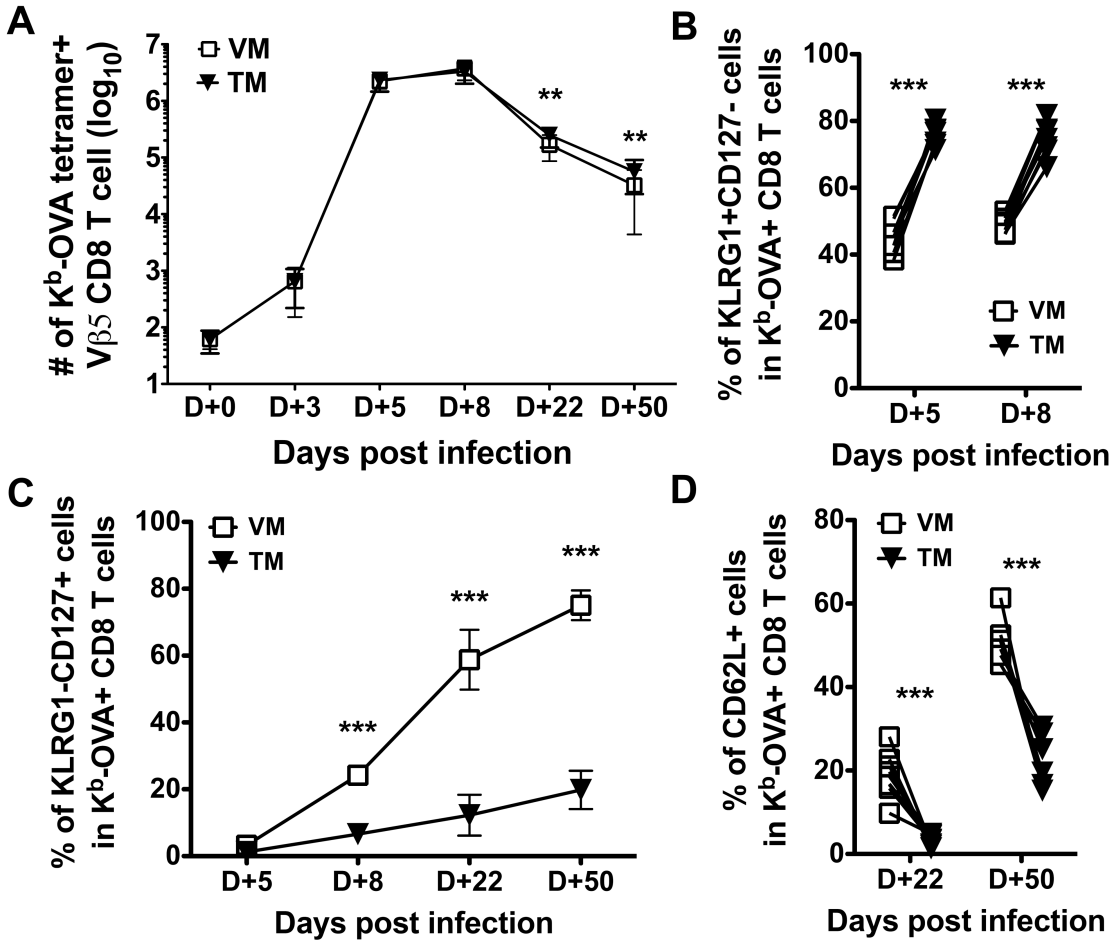

Figure 2-13. VM and TM CD8 T cells show similar kinetics in proliferation, but differential effector differentiation. (A) Graphs show the number of co-transferred Ova/Kb specific VM and TM Vβ5 CD8 T cells in the spleen and superficial lymph nodes at the indicated times post LM-OVA infection. (B,C,D) Phenotypic comparison between responding VM and TM CD8 T cells, gated on OVA/Kb tetramer+ donor cells at the indicated days post LM-OVA infection. Graphs show compiled data from 3 independent experiments and lines show mean +/- SD. Statistical significance between groups is indicated (***, $p<0.001$; **, $p<0.01$, while "n.s." ("not significant") is used to denote P-values >0.05, Student t test).

VM cells provide potent antigen-specific protective immunity against LM infection.

Our findings indicate that VM cells display only some characteristics of true memory cells. This raised the question of whether VM cells would be capable of mediating protective responses against infection. Our previous studies showed that lymphopenia-induced homeostatic memory OT-I CD8+ T cells were capable of Listeria monocytogenes control[32,33], and a recent report showed similar potent protection by the VM population that arises spontaneously in intact OT-I mice[45]. However, it was not clear whether these findings would correspond to the polyclonal Vβ5 CD8 T cells studied here. In particular, the poor induction of IFN-γ following TCR stimulation of Vβ5 VM (Fig. 6B, C) was noteworthy, since this factor is critical in control of several pathogens, including Listeria[70]. Furthermore, several studies have suggested that memory-phenotype CD8 T cells from unimmunized mice have regulatory functions[46-50,71]: hence, the VM population might inhibit, not elicit pathogen control. To explore this issue, we performed studies to compare VM, naïve and TM CD8 T cells for protection against virulent LM-OVA infection. Cells were isolated and sorted as before, but populations were transferred into separate hosts, and were designed to include ~$2x10^4$ Ova/K^b tetramer+ cells. Host mice were subsequently challenged with a LD50 dose of virulent LM-OVA (or wild type LM) and on day 5 after infection, CFU in the spleen and liver were measured, and the expansion of donor CD8 T cells was assayed as in previous reports.

Similar to other studies using OT-I TCR transgenic CD8 T cells[32,33,45], naïve Vβ5 CD8 T cells offered little protection against LM-OVA infection, while antigen-primed

TM cells induced significantly greater bacterial control, in both spleen and liver (Fig. 14A). Remarkably, the VM population was at least as potent as TM cells in mediating LM-OVA clearance (Fig. 14A), suggesting that spontaneously arising VM cells can provide efficient protective immunity. Given the low number of donor cells transferred ($2x10^4$ cells, corresponding to ~$2x10^3$ cells with a calculated 10% take), these data suggest that, like the TM population, VM cells exhibit potent and efficient protective capacity. Since we could not purify Ova/K^b specific VM cells prior to transfer (which would necessarily have involved staining with peptide/MHC tetramers, possibly affecting functional responses), it was possible that bacterial control by the polyclonal VM population involved responses to other LM epitopes and/or non TCR specific responses. For example, we previously showed that VM cells (like TM) elaborate IFN-γ when stimulated with IL-12 and IL-18, in the absence of TCR engagement[27,72-74]. In order to test whether protection in our studies was antigen specific we conducted parallel experiments using non-recombinant (WT) LM infection. In this situation, none of the transferred Vβ5 populations provided protection in the spleen, and LM control in the liver was insubstantial (Fig. 14A).

All the transferred populations underwent vigorous expansion after LM-OVA infection, with both memory cell populations reaching ~1,000 fold increase in number and significantly out-expanding naive CD8 T cells (Fig. 14B). In our earlier studies using attenuated LM-OVA, there was little difference between expansion of naïve and VM cells at this time point (day 5), hence these findings may relate to use of virulent LM-OVA for the protection assays. In keeping with our other findings, we found that the

frequency of KLRG1+CD127lo effector cells was significantly different for each donor population, following the hierarchy TM > VM > naïve (Fig. 14C). Hence, these phenotypic characteristics of each responsive pool were preserved during the response to virulent LM-OVA.

These data suggest that, despite their distinct characteristics in comparison with both TM and naïve CD8 T cells, the VM pool can provide potent and antigen-specific protective immunity against pathogen infection.

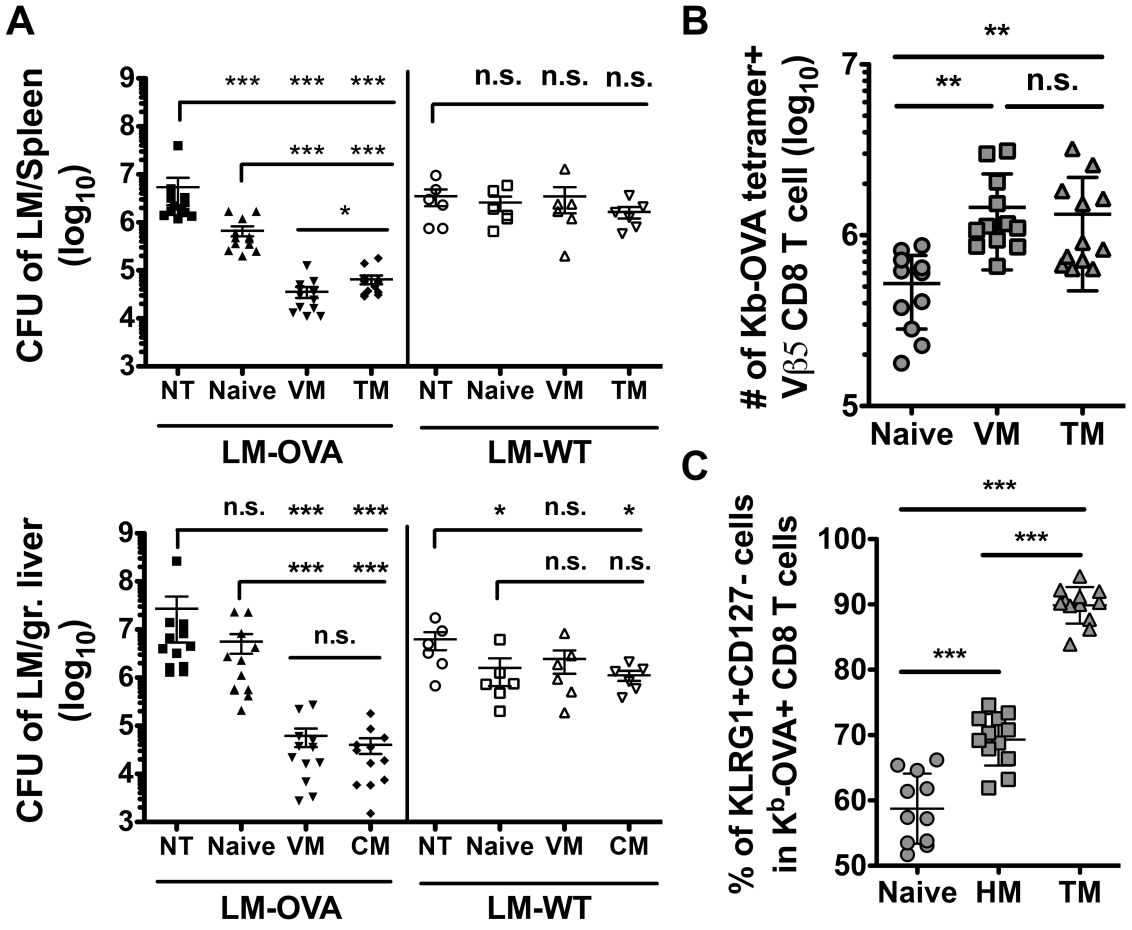

Figure 2-14. VM cells provide potent antigen-specific protective immunity against LM infection. Naïve, VM and TM Vβ5 CD8 T cells were sorted and approximately 2 x 10^4 Ova/K^b specific cells were singly transferred into unprimed recipients. Host mice were infected the next day with virulent LM-OVA or wild type LM (LM-WT). (A) CFU of indicated LM strains in the spleens and livers of the recipient mice 5 days after infection. (B) Number of Ova/K^b specific CD8 T cells and (C) Frequency of KLRG1+CD127- CD8 T cells in the spleens of recipient mice at day 5 post LM-OVA infection. Graphs show compiled data from 4 independent experiments for LM-OVA infection and 2 independent experiments for LM-WT infection and lines show mean +/- SD. Statistical significance between groups is indicated (***, $p<0.001$; **, $p<0.01$; *, $p<0.05$, while "n.s." ("not significant") is used to denote P-values >0.05, Student t test).

Discussion

Studies over the last dozen years have shown that memory T cells are not exclusively generated through encounter with foreign antigen, but can also be induced through homeostatic pathways[12,24,28-31]. Furthermore, we and others reported that a population of memory-like cells arise spontaneously in unimmunized mice, and that such cells constitute a small but significant fraction of the precursors specific for a given foreign antigen, prior to priming[26,27]. Data in this report suggest that the functional properties of these "virtual memory" cells lies in between those of naïve and "true" memory cells. The VM pool differed from naïve cells (and resembled TM) in their early in vivo expansion, elevated expression of T-box factors and position in G1 stage of the cell cycle. Perhaps most importantly, VM cells resembled true memory cells in highly efficient, antigen-specific control of the pathogen Listeria monocytogenes. On the other hand, we found that the VM pool differed markedly from TM cells in their preferential differentiation toward the Tcm phenotype following antigen encounter in vivo, and that VM cells were much less efficient at rapid production of IFN-γ following TCR stimulation. The latter findings differ slightly from our initial study, which had concluded that VM cells behaved like naïve cells in their slow induction of IFN-γ following TCR stimulation[27]. Since VM cells show strong expression of both T-box factors (T-bet and Eomes), and evidence of Tc1 differentiation (e.g. robust CXCR3 expression), their inefficient production of IFN-γ is unexpected and intriguing. Although T-bet clearly requires other factors (such as the Jmjd3 histone demethylase for chromatin remodeling of target loci)[75], such studies show good concordance for multiple T-bet

targets, including CXCR3 and IFN-γ. It is possible that this trait reflects altered T-bet/Eomes expression levels (Fig. 2A), although both T-box factors are reported to be capable of promoting IFN-γ expression. Hence the selective deficiency in IFN-γ induction appears unique to VM cells.

Taken together, these data suggest homeostatic pathways only partially substitute for antigen encounter in programming full memory differentiation (although, significantly, this includes the capacity to mediate protective immunity against some infections). Interestingly, our results differ from previous studies on the properties of homeostatic memory cells generated in severely lymphopenic hosts. We and others found that such cells rapidly produce IFN-γ after TCR stimulation at levels similar to true memory cells[32,40], while our current data show that the VM pool is substantially compromised in this response (Fig. 6B, C). On the other hand, using OT-I T cells, Cheung et al reported that true memory cells exerted a substantial numerical advantage over lymphopenia-induced homeostatic memory cells during a competitive in vivo responses to LM-OVA infection[41]: In contrast, we found minimal differences in numbers of TM and naturally occurring VM during a similar response (Fig 13A). These discrepancies may reflect the distinct pathways for homeostatic memory generation entailing different intensities or mechanisms of response[13,24]. The naturally occurring VM pool arises slowly over the weeks following birth (as the T cell compartment is filling)[26], in a process involving IL-15 presentation by CD8α+ dendritic cells[45]. In contrast, acute lymphopenia provides a stronger and more sustained homeostatic signal, potentially leading to altered differentiation. Regardless, our current report suggests that

the functional properties of naturally arising VM cells are not accurately reflected in studies (including our own)[32] on homeostatic memory cells artificially produced in severely lymphopenic hosts.

Interestingly, VM CD8 T cells preferentially differentiated toward Tcm phenotype after antigen priming. This was especially notable in the comparison between TM and VM – since, as expected, restimulated TM cells showed a strong bias toward Tem differentiation. Similar findings were reported in comparison of true and lymphopenia-induced memory OT-I cells[41]. However, this bias toward Tcm differentiation was detected even when VM were compared to naïve precursors, which was unexpected. While the basis for this focused differentiation is unclear, a consequence is that VM cells would contribute disproportionately to the Tcm pool. Since recent studies have suggested that Tcm cells are especially important for control of chronic viral infections[76], these findings may suggest a particular relevance of VM in mounting rapid, effective responses against such pathogens.

	T Box TF	Cell cycle	Migration	IFN-γ	IL10	LM protection	Immuno-pathology
Naïve	-	Arrested in G0	Delayed	Delayed	+++	+	Moderate
Virtual Memory	+++	Advanced in G1	Rapid	Delayed	+++	+++	Moderate
True Memory	+++	Advanced in G1	Rapid	Accute	+	+++	Severe

Figure 2-15. Comparison of immunologic caracters among Naïve, VM and TM CD8 T cells.

Materials and methods

Mice

Female C57BL/6 (CD45.2/Thy1.2), B6.SJL (CD45.1/Thy1.2) and B6.PL (CD45.2/Thy1.1) mice (6-7 weeks old) were purchased from the Jackson laboratory and the National Cancer Institute. Female B6.SJL mice were bred with male B6.PL to generate B6.PL.SJL (CD45.1/CD45.2/Thy1.1/Thy1.2) mice. Vβ5 TCR transgenic mice were maintained on a B6.SJL background, or bred with C57BL/6 mice to generate Vβ5/B6xB6.SJL (CD45.1/CD45.2). All mice were maintained in specific pathogen-free conditions. All experimental procedures were approved through the University of Minnesota IACUC.

In vivo generation of "true" memory Vβ5 CD8 T cells

CD45.1 Vβ5 CD8 T cells (1×10^6) were negatively enriched from spleen and superficial lymph nodes, using a CD8α+ isolation kit (Miltenyi Biotec) and injected intravenously (i.v.) into CD45.2 congenic C57BL/6 mice. Mice were immunized 24 hours later by i.v. injection of 3×10^6 colony-forming units (CFU) of L. monocytogenes strain expressing OVA (LM-OVA ActA attenuated) (a kind gift of Hao Shen, University of Pennsylvania School of Medicine). In vivo generated memory T cells were detected with fluorescent–labeled anti-CD45.1 (eBioscience) 30–60 days after priming.

Adoptive transfer and Immunization

Combinations of CD45 and CD90 alleles were chosen to allow discrimination of co-transferred naïve, VM and TM populations. For Vβ5 CD8 T cell experiments, spleen and superficial lymph nodes were harvested from unprimed Vβ5 tg mouse strains (CD45.1 or CD45.1/CD45.2), and/or mice carrying primed, memory Vβ5 CD8 T cells (as a source of TM cells). Collagenase digestion was performed on tissues, and CD8 T cells were negatively enriched by CD8α+ isolation kit (Miltenyi Biotec). To avoid pre TCR stimulation, cells were sorted by CD8, CD44 and relevant congenic marker antibodies without Ova/Kb-tetramer staining using a FACSAria (BD Biosciences). After the sorting, the number of antigen specific cells within each population was determined using Ova/K^b-tetramer staining of an aliquot from the sorted samples. Next, 300-500 Ova/K^b-tetramer positive cells of the indicated phenotype were mixed 1:1 and co-transferred (i.v.) into naïve C57BL/6 (CD45.2/Thy1.2) hosts, which were infected with 3 x 106 CFU LM-OVA ActA one day later. To induce recall immune response, mice were infected with 1 x 10^5 CFU of virulent LM-OVA. For polyclonal CD8 T cell transfer, VM and naïve CD8 T cells were sorted from unprimed C57BL/6 (CD45.2/Thy1.1) and B6.SJL (CD45.1/Thy1.2) mice (as described above), and 2 x 10^6 cells of each population were mixed 1:1 and co-transferred (i.v.) into naïve (B6.PL x B6.SJL)F1 hosts (CD45.1/CD45.2/Thy1.1/Thy1.2). The recipient mice were infected with 2x10^6 PFU of Vaccinia virus (VV-WR) or a cocktail of attenuated recombinant LM strains (LM-OVA-B8R, LM-OVA-HSVgB) one day later. Attenuated LM-OVA-B8R and LM-OVA-

HSVgB strains were provided from Dr. Ross M. Kedl (University of Colorado) and Dr. SingSing Way (University of Minnesota) respectively.

Flow cytometry

For determining surface phenotype, cells were isolated from spleen and superficial lymph nodes, and stained with the antibodies specific for following molecules: CD3e (145-2C11), CD4 (GK1.5), CD8 (53-6.7), CD44 (IM7), CD69 (H1.2F3), KLRG1 (2F1), CD62L (MEL-14), CD122 (TMb1), CD127 (A7R34), CD45.1 (A20), CD45.2 (104), Thy1.1 (HIS51), Ly-6C (HK1.4), CD49d (R1-2) and CXCR3 (CXCR3-173). For detecting foreign antigen specific CD8 T cells, fluorochrome (PE or APC) labeled Ova/K^b (SIINFEKL), B8R/K^b (TSYKFESV) and HSVgB/K^b (SSIEFARL) tetramers were generated as previously described[77,78] and used to stain cells (30 minutes at 4°C), simultaneously with other surface markers. In some experiments tetramer binding cells were enriched by a MACS based pull-down assay, as previously described in detail[27]. For intracellular transcription factor staining, stained cells with surface antibodies were fixed and permeabilized with Foxp3 Fixation/Permeabilization solution (eBioscience), and stained with antibodies to T-bet (4B10) and Eomesodermin (Dan11mag) for 1 hour at 4°C in Permeabilization Solution. Flow cytometry was performed on LSRII or Fortessa instruments (BD), and analyzed using FlowJo analysis software.

In vitro stimulation and IFN-γ production assay

Naïve and memory Vβ5 tg splenocytes were incubated with various doses (10^{-6}-10^{-10}M) of OVA peptide (SIINFEKL), and Golgi Plug (BD Biosciences) for 2-5 hours. Cells were then surface stained, fixed and permeabilized with BD Cytofix/Cytoperm (BD Biosciences), and intracellularly stained for IFN-γ (XMG1.2) and TNF-α (MP6-XT2.2) in BD Perm Wash Buffer (BD Biosciences), similarly to our previous studies[32].

Cell cycle analysis

Cell cycle analysis was performed using staining for DNA and RNA with DAPI and pyronin Y, respectively. Negatively enriched CD8+ T cells were obtained using a CD8α+ T Cell Isolation Kit II, mouse (Miltenyi Biotec) from unprimed mice (for naïve and VM populations) and immunized animals (for TM cells). Cells were surface stained and then fixed/permeabilized with FoxP3/Transcription Factor Staining Buffer (eBioscience) overnight. The cells were then incubated with 5 μg/ml DAPI in 200 μl FACS buffer (2% FCS, 0.1% NaN3) for 1 hour and, without further washing, an equal volume of 3 μg/ml pyronin Y diluted FACS buffer was added to each sample 5 minutes before flow cytometric analysis.

Quantitative real-time PCR

CD44high memory phenotype, CD44low naïve phenotype and TM Vβ5 CD8 T cells were sorted on a FACSAria (BD bioscience), as described above. RNA was isolated by RNeasy microkit (Qiagen), and cDNA was generated using SuperScript III

Reverse Transcriptase (Life technologies). Real-time RT-PCR was performed using the ABI 7700 sequence detection system, with SYBR Green PCR Master Mix (Applied Biosystems). Primer sequences are available upon request.

Resident memory CD8 T cell (Trm) determination

To exclude blood circulating CD8 T cells from tissue parenchymal Trm populations, we performed intravascular staining method with fluorescently labeled anti-CD8 antibodies as previously described[79]. Briefly, mice were injected i.v. with fluorescently labeled anti-CD8α antibody on 50~60 days post primary infection of LM-OVA. Then, the mice were bled and sacrificed 3 minutes later and perfused for remove residual blood. Spleen, kidney, salivary glands were harvested, and single cell suspensions were prepared by collagenase treatment. Tissue parenchymal CD8 T cells were stained by using a distinct fluorochrome conjugated CD8α antibody that allows distinguish CD8β stained blood circulating CD8 T cells.

Listeria monocytogenes protection assays

To assess protective immune function of VM, naïve, and TM Vβ5 CD8 T cells, each population was sorted as described above and an inoculum containing ~2 x 10^4 Ova/K^b specific cells (determined by staining an aliquot of sorted cells with Ova/K^b tetramer) was adoptively transferred into unprimed C57BL/6 host. In these experiments, populations were transferred singly, not co-transferred. One day later, mice were infected with 8 x 10^4 CFU of virulent LM-OVA or 1 x 10^4 CFU of virulent wild type LM

(the ~LD50 of each strain). On day 5 after infection, CFU of LM in the spleen and liver were measured as previously described[32,33]. For determining antigen specific expansion of host and transferred CD8 T cells, splenocytes from the infected mice were counted and stained with K^b-OVA tetramer.

BrdU incorporation assays

Mice were injected i.p. with 1 mg BrdU (in PBS), and then maintained on BrdU-laced drinking water (0.8 mg/ml, with 2% sucrose to offset bitterness) for 14–16 d. For bulk analysis, thymocytes and pooled spleen and lymph node cells were prepared and stained for surface markers, followed by fixation, permeabilization, and intracellular staining for BrdU following manufacturer's instructions (BD Biosciences). In parallel, the remaining spleen and lymph node sample was subject to tetramer pulldown (using a mixture of PE-labeled B8R/K^b, M57/K^b, and HSVgB/K^b tetramers) prior to staining for surface markers and BrdU.

Statistics

A two-tailed, paired or unpaired, Student's t-test was performed using Prism (GraphPad Software Inc.). In some figures, plotted data represent means ± SD, and P-values are represented as follows: ***, $p<0.001$; **, $p<0.01$; *, $p<0.05$, while "n.s." ("not significant") is used to denote P-values >0.05.

Chapter 3

Role of KLF2 in effector CD4+ T cell lineage commitment

Germinal center follicular helper T cells (GC-Tfh) are essential for efficient B cell responses, yet the factors that regulate differentiation of this CD4+ T cell subset are incompletely understood. We show that the KLF2 transcription factor serves to restrain GC-Tfh generation. Downregulation of the trafficking molecule S1PR1 (a KLF2 target) is required for GC-Tfh establishment. In addition, KLF2 drives expression of Blimp-1, which represses Bcl-6 and thereby impairs GC-Tfh differentiation. KLF2 also promotes expression of T-bet and Gata-3 and can enhance Th1 differentiation. Hence, our data indicate KLF2 is pivotal for coordinating CD4+ T cell differentiation through two distinct and complementary mechanisms: via control of T cell localization, and by regulation of lineage-defining transcription factors.

Introduction

During the immune response toward foreign antigens, the germinal center (GC) reaction represents a central mechanism for generating high affinity antibodies of diverse isotypes[80]. Fundamental in this process is the activity of follicular helper CD4 T cells (Tfh), which coordinate generation of the germinal center, initiate help for antigen specific B cells, and promote selection of germinal center B cell clones that have developed enhanced antigen recognition through somatic hypermutation[80-83]. Characteristic features of Tfh include expression of ICOS, PD-1, the chemokine receptor CXCR5 and the cytokine IL-21, and these molecules are key for Tfh generation and function[80-83]. Cells with a Tfh phenotype accumulate around and enter B cell follicles, while cells that localize within GC (i.e. GC-Tfh) are characterized by high levels of CXCR5, PD-1 and Bcl-6[80-83]. Migration and retention of GC-Tfh in the GC depends on CXCR5 and the sphingosine-1-phosphate receptor S1PR2[84]. Downregulation of CCR7 is also critical for Tfh accumulation in the follicle and normal GC responses[85], however other factors that negatively regulate Tfh trafficking are not well defined.

Multiple transcription factors, including c-Maf, Batf, Irf4, STAT1, STAT3 and Ascl2 are involved in development and function of Tfh[81,83,86], but maintenance and differentiation of Tfh to the fully mature GC-Tfh stage critically requires expression of Bcl-6[81-83]. The Tfh differentiation pathway is opposed by other factors, the best studied of which is Blimp-1. Bcl-6 and Blimp-1 are mutually antagonistic, making the balance in expression of these two factors a critical element in determining helper T cell fate. IL-2R signaling impairs Tfh generation in a mechanism involving Blimp-1 and STAT5[87-90].

Furthermore, the factors Foxo1 and Foxp1 both restrain Tfh generation, although the mechanisms involved are not fully defined[91-93]. Activated CD4+ T cells that do not mature into Tfh may join one of several alternative "non-Tfh" subsets (including Th1, Th2, Th17 and Treg) that are thought to not localize into the germinal center. Key transcription factors for several of these alternative fates are blocked by Bcl-6[81,83,94], further establishing this factor as central to reinforcing Tfh differentiation.

Hence, in order to effectively participate in the germinal center response, Tfh must a) migrate into the B cell follicle and reside in the GC; b) acquire specific functional properties needed for effective B cell help; and c) exclude alternative differentiation fates. It is unclear, however, whether these three aspects are coordinately regulated, and if so what transcription factors are involved in that control.

The transcription factor KLF2 is critical for regulating naïve T cell trafficking, in part through promoting expression of CD62L (L-selectin) and S1PR1 – which are critical for lymphocyte entry and egress, respectively, from secondary lymphoid tissues[7,8,95,96]. More recently, we reported that reduced KLF2 expression was a prerequisite for effective generation of "Resident Memory" CD8+ T cells (Trm) – a population that is prominent in non-lymphoid tissues and does not appear to exchange with other sites through recirculation via the blood and lymph[20]. We found that KLF2 induction of S1PR1 was a key aspect of this regulation, since forced expression of either KLF2 or S1PR1 served to impede generation of Trm[20]. Those studies suggested that T lymphocyte residence and recirculation were characterized by low and high expression of KLF2, respectively. Similarly, in order to function in sustained B cell help, GC-Tfh must become a resident

population, within the active germinal center. Hence, in this report we explore whether KLF2 impacts the capacity of activated CD4+ T cells to become GC-Tfh cells.

Results

GC-Tfh exhibit a KLF2low phenotype

We initially studied KLF2 expression in antigen specific CD4+ and CD8+ T cells responding to lymphocytic choriomeningitis virus (LCMV), using a previously described KLF2-GFP reporter mouse strain[20,97]. In keeping with our earlier findings[20], the vast majority of effector CD8+ T cells in lymphoid tissues express KLF2 (Fig. 1A), yet we noted that KLF2 expression in effector CD4+ T cells was bimodal, with some cells expressing KLF2 to similar levels as observed in the CD8+ T cell population, while other cells exhibited substantially reduced KLF2 expression (Fig. 1A). We have reported that KLF2 downregulation characterized tissue-resident, non-recirculating CD8+ T cells[20] and the B-cell helper function of Tfh cells obliges them to be retained within the priming lymphoid tissue[80,81]. Hence we investigated whether KLF2 levels correlated with the Tfh populations. Indeed, we found that the KLF2lo subset was highly enriched for cells expressing GC-Tfh phenotype (CXCR5hi, PD-1hi and Bcl-6hi) (Fig. 1B). Further analysis confirmed that GC-Tfh phenotype cells were KLF2lo, while both Tfh and non-Tfh populations expressed significantly higher KLF2 levels (Fig. 1C, D). This expression pattern was not limited to CD4+ T cells responding to LCMV, since we observed similar profiles for polyclonal CD4+ T cells responding to distinct epitopes during acute infection with the bacteria Listeria monocytogenes (Fig. 1D). Our findings are consistent with gene expression studies that suggested that GC-Tfh populations express lower levels of Klf2 and S1pr1 transcripts than non-Tfh[92], although those reports did not explore the significance of these changes.

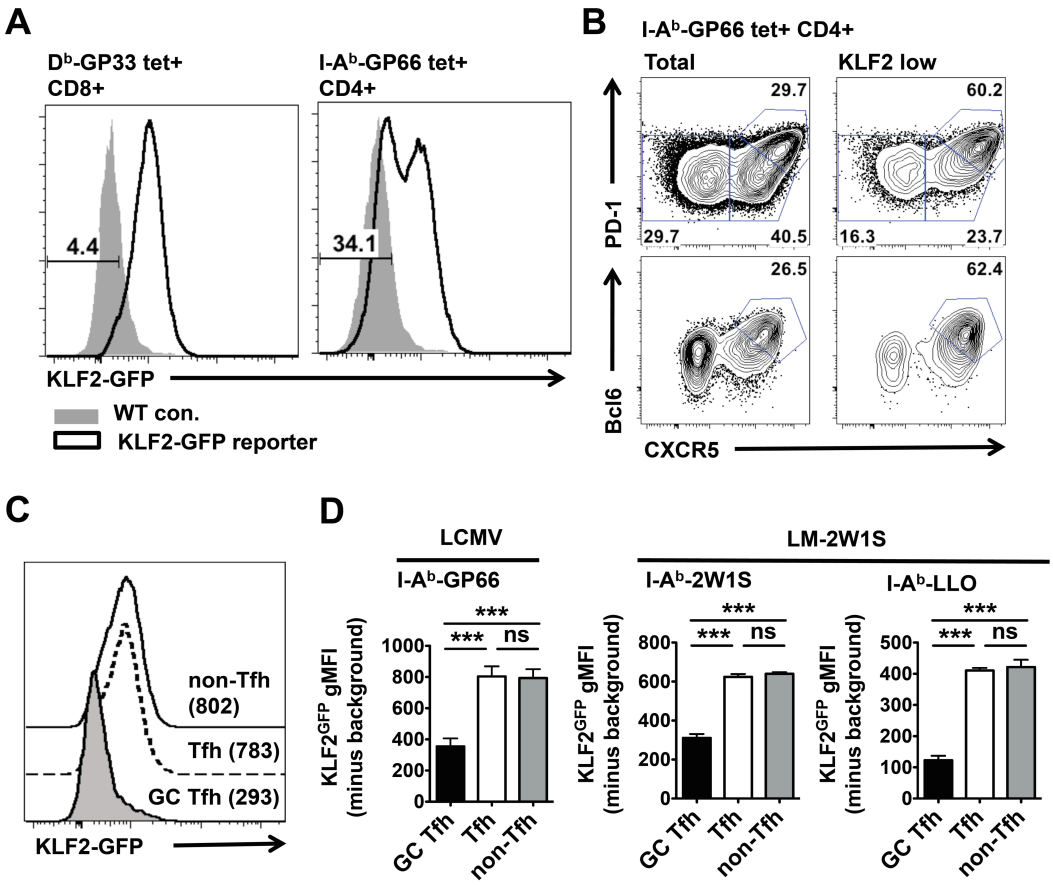

Figure 3-1. KLF2 is down-regulated in GC-Tfh. KLF2-GFP reporter mice were infected with LCMV (A-C) or recombinant Listeria monocytogenes expressing the 2W1S epitope (LM-2W1S)(B), and analyzed 7 days later. (A) Antigen-specific splenic CD8+ and CD4+ T cells were enriched using D^b-GP33 and I-A^b-GP66 tetramers, respectively, and monitored for KLF2-GFP expression. Shadow area shows background level of GFP signal in non-transgenic wild-type (WT) controls. (B) CXCR5, PD-1 and Bcl-6 expression is shown for total or KLF2-GFP low LCMV specific CD4+ T cells. (C) KLF2-GFP expression by GC-Tfh (CXCR5highPD-1+), Tfh (CXCR5intPD-1-) and non-Tfh (CXCR5-PD-1-) phenotype cells in I-Ab-GP66 tetramer+ CD4+ T cells from LCMV infected mice. Numbers indicate geometric mean fluorescence intensity (gMFI) of KLF2-GFP expressed in each population. In (D), KLF2-GFP expression levels are shown for GC-Tfh, Tfh and non-Tfh phenotype cells in the LCMV specific CD4+ T cells (left), and in I-A^b-2W1S tetramer+ and I-A^b-LLO tetramer+ CD4+ T cells LM-2W1S infected mice (right). Data are shown as gMFI minus background gMFI of WT CD4+ T cells. Data are from at least three independent experiments with a total of 13 (A, B, C for LCMV infection) or 8 (D for LM-2W1S infection) KLF2-GFP reporter mice, and are representative of (A, B, C) or accumulated (D) from the independent experiments as mean ±s.e.m. Statistical significance was determined using two-tailed t-test: ns, not significant ($P > 0.05$); and ***, $P < 0.001$.

To extend these findings and visualize differences in KLF2 expression in the context of lymphoid tissue architecture, we used immunohistochemistry to determine KLF2-GFP expression in situ in the draining lymph node following immunization with the protein Phycoerythrin (Fig 2). Interestingly, CD4+ T cells that were physically localized to the germinal center had significantly lower KLF2 expression than CD4+ T cells located in the T cell zone (Fig. 3A, B). Indeed, GFP expression was clearly lower in the GC as a whole indicating that both CD4+ T cells and B cells in this zone were KLF2lo (Fig. 3B, C). Collectively, these data suggested that the reduced KLF2 expression is a signature feature of the GC-Tfh population.

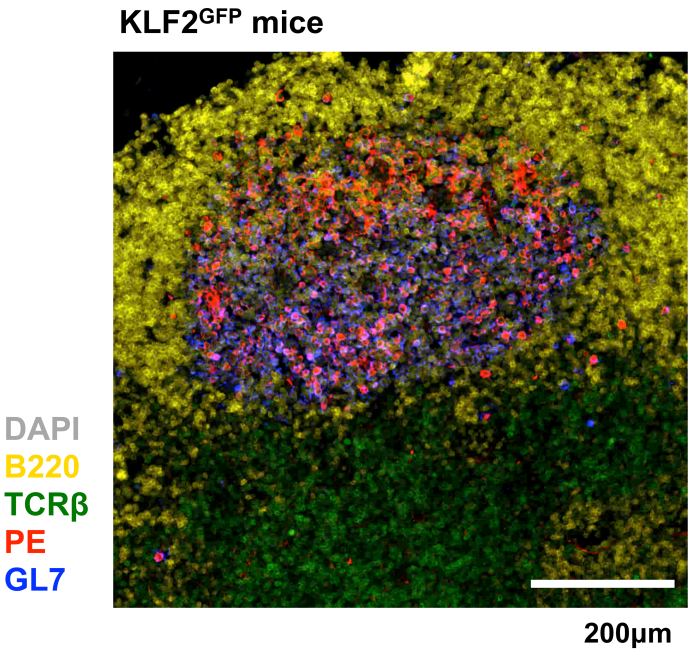

Figure 3-2. Immunohistochemistry analysis of KLF2-GFP expression in PE specific germinal centers. PE specific GCs were determined by GL7+B220+PE+TCRβ- area in dLNs (inguinal and lumbar LNs) from mice immunized subcutaneously with PE (15μg)/CFA at day 14 post immunization. See Figure 2 for more details. Gray, DAPI; Yellow, B220; Green, TCRβ; Red, PE; Blue, GL7; scale bar, 200μm. The image is representative of the staining pattern from three independent experiments.

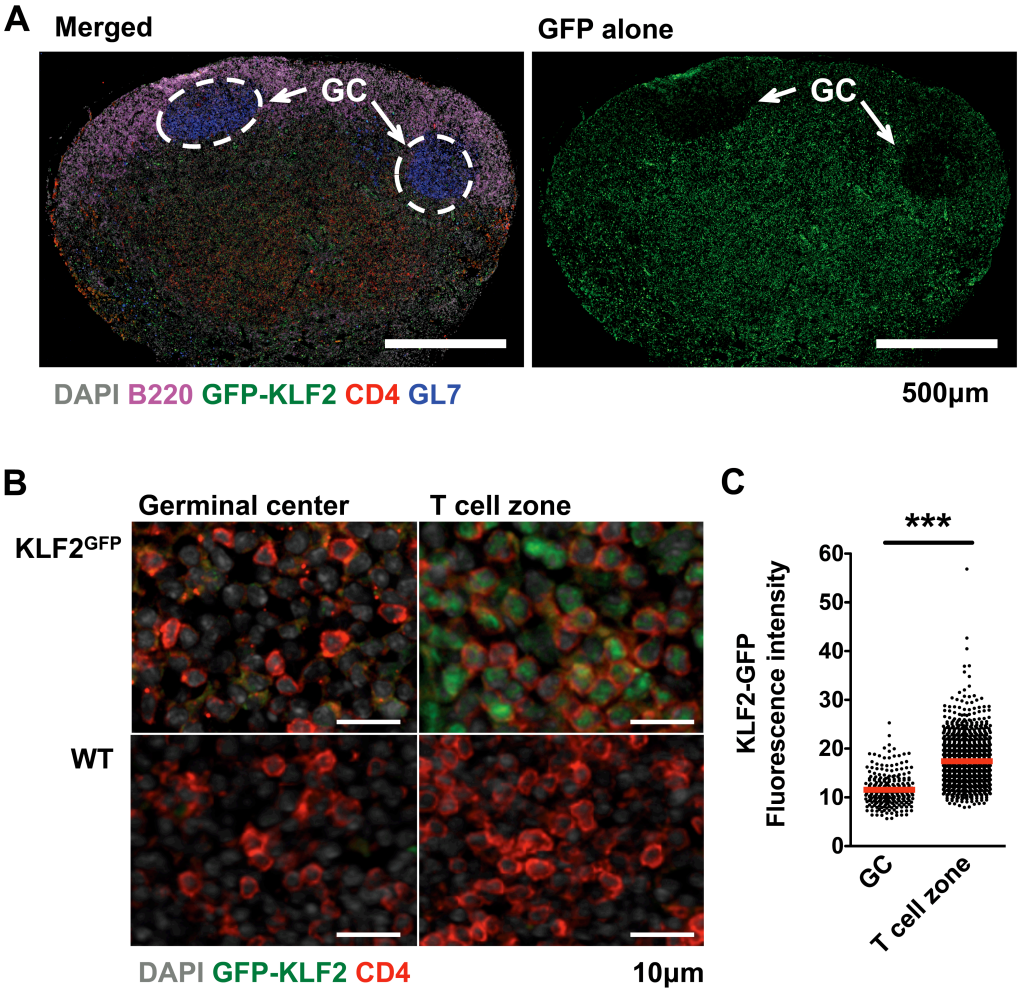

Figure 3-3. Reduced expression of KLF2 by CD4+ T cells in the germinal center compared to T cell zone. Immunohistochemistry analysis of a draining lymph node (dLN) from KLF2-GFP reporter mice immunized subcutaneously with Phycoerythrin (PE) 14 days earlier. (A) In the left image, the indicated stains were used to identify B cell follicles (B220+) and T cell zone (B220-, CD4+), while germinal centers (GCs) were identified by GL7 staining (and confirmed by PE co-staining: data not shown). Two GCs are indicated by white arrows. The right image is the same section, but only the KLF2-GFP staining signal is shown. (B) The panels show the staining for KLF2-GFP (green) and CD4+ (red) for cells in the GC or T cell zone as indicated. The upper two panels are from immunized KLF2-GFP mice, while the lower two panels are from immunized WT B6 mice. Gray, DAPI; Purple, B220; Green, KLF2-GFP; Red, CD4; Blue, GL7. The scale bars for the images are shown. (C) shows the KLF2-GFP fluorescence intensity of CD4+ T cells in the GC or T cell zone (using the criteria defined in a,b). Each dot represents a single CD4+ T cell and the red bar indicate average fluorescence intensity of each group. All experiments were repeated three times with similar results. Graphs show accumulated data from three independent experiments as mean ±s.e.m., two-tailed t-test. ***, $P < 0.001$.

KLF2 and S1PR1 expression throughout the CD4+ T cell response

To further investigate the regulation and function of KLF2 during CD4+ T cell lineage commitment, we developed an adoptive transfer system using TCR transgenic CD4+ T cells (TEa), specific for Eα/I-A^{b} [98]. To enhance antigen-specific B cell interactions and optimize GC-Tfh cell differentiation[80,81], we co-transferred MD4 BCR transgenic B cells specific for hen/duck egg lysozyme (HEL/DEL)[99], and immunized the recipient mice with a conjugate antigen (Eα-DEL) bearing antigens for both TEa and MD4 cells (Fig. 4A, B, C).

With this system, we first defined the detailed kinetics of KLF2 and S1PR1 expression in vivo, through adoptive transfer of KLF2-GFP[20,97] or S1PR1-GFP reporter[100] TEa CD4+ T cells. At an early activation stage (day 2), primed TEa cells uniformly reduced KLF2 and S1PR1 reporter expression in secondary lymphoid organs (Fig. 5A, B), in keeping with previous data on KLF2 and S1PR1 downregulation following TCR engagement[20,35,100]. From day 5 of the response, however, non-Tfh phenotype cells showed sustained KLF2 re-expression, whereas GC-Tfh phenotype cells maintained low KLF2 reporter expression well into the memory phase (day 30). CXCR5int, PD-1lo Tfh cells showed intermediate patterns of KLF2 expression (Fig. 5A, B). These findings contrast somewhat with the KLF2hi phenotype observed for polyclonal Tfh T cells in the response to LCMV or LM (Fig. 1), which may relate to the immunization approaches, differences in the frequency of available antigen-specific B cells or idiosyncrasies of TEa TCR transgenic T cells[101].

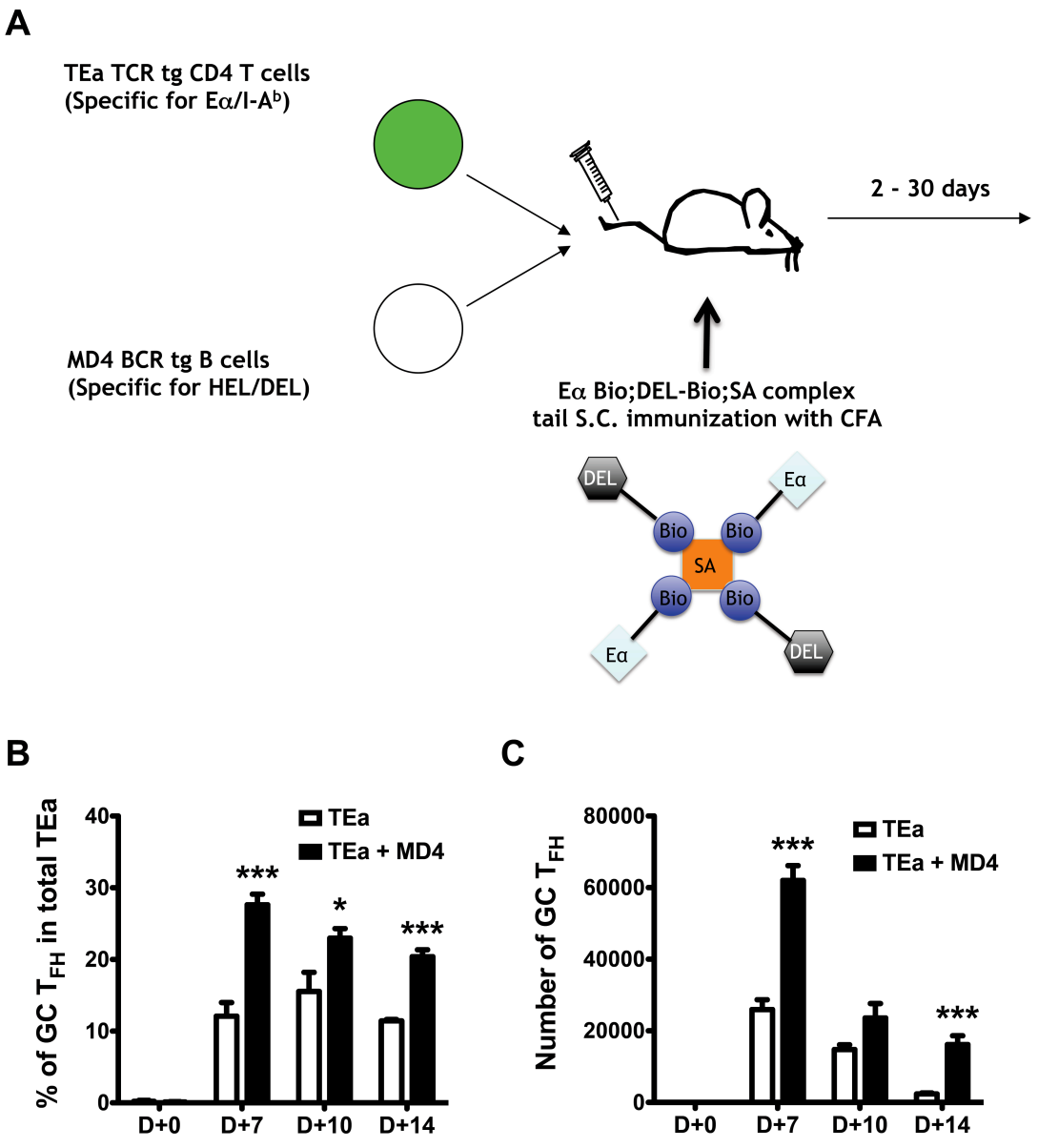

Figure 3-4. TEa adoptive transfer system. (A) Experimental scheme. To enhance antigen-specific B cell help (required for optimal GC-Tfh cell differentiation), TEa TCR transgenic CD4+ T cells, specific for an Eα-derived peptide (amino acid residues 52–68) in the context of MHC class II molecule I-A^b, were co-transferred with BCR transgenic B cells (MD4) specific for hen/duck egg lysozyme (HEL/DEL), and the recipient mice were immunized with a conjugate antigen bearing antigens for both TEa and MD4 cells (Eα-SA-DEL) in CFA. (B, C) Quantification of GC-Tfh differentiation in donor TEa populations at various time points with/without MD4 cells. Graphs show accumulated data from 3 individual recipients at each time point, represented as mean ±s.e.m., two-tailed t-test. *, $P < 0.05$; and ***, $P < 0.001$.

Regardless, S1PR1 reporter expression was markedly lower in GC-Tfh cells than the other subsets (Fig. 5A, B), consistent with the very low KLF2 expression by that population. CD69 was expressed at significantly higher levels in GC-Tfh than Tfh or non-Tfh effector populations (Fig. 5C): It has been proposed that this phenotype indicates TCR stimulation of the GC-Tfh population[102], since CD69 is an activation marker. However, CD69 has been shown to compete with S1PR1 for cell surface expression, and loss of S1PR1 expression can result in elevated basal CD69 levels[20,36,103], complicating interpretation of this phenotype. Hence we also monitored evidence for recent TCR signaling using the Nur77-GFP reporter transgenic system[104]. This analysis revealed that TCR stimulation was similar in GC-Tfh, Tfh and non-Tfh cells at day 7 of the response (Fig. 5D), consistent with the increased CD69 surface expression by GC-Tfh at that time being a consequence of lower S1PR1 expression. By day 14 of the response, we saw evidence for sustained TCR signaling in the GC-Tfh pool (consistent with the conclusions of previous studies)[101,102], while Nur77-GFP levels were declining in Tfh and non-Tfh phenotype cells.

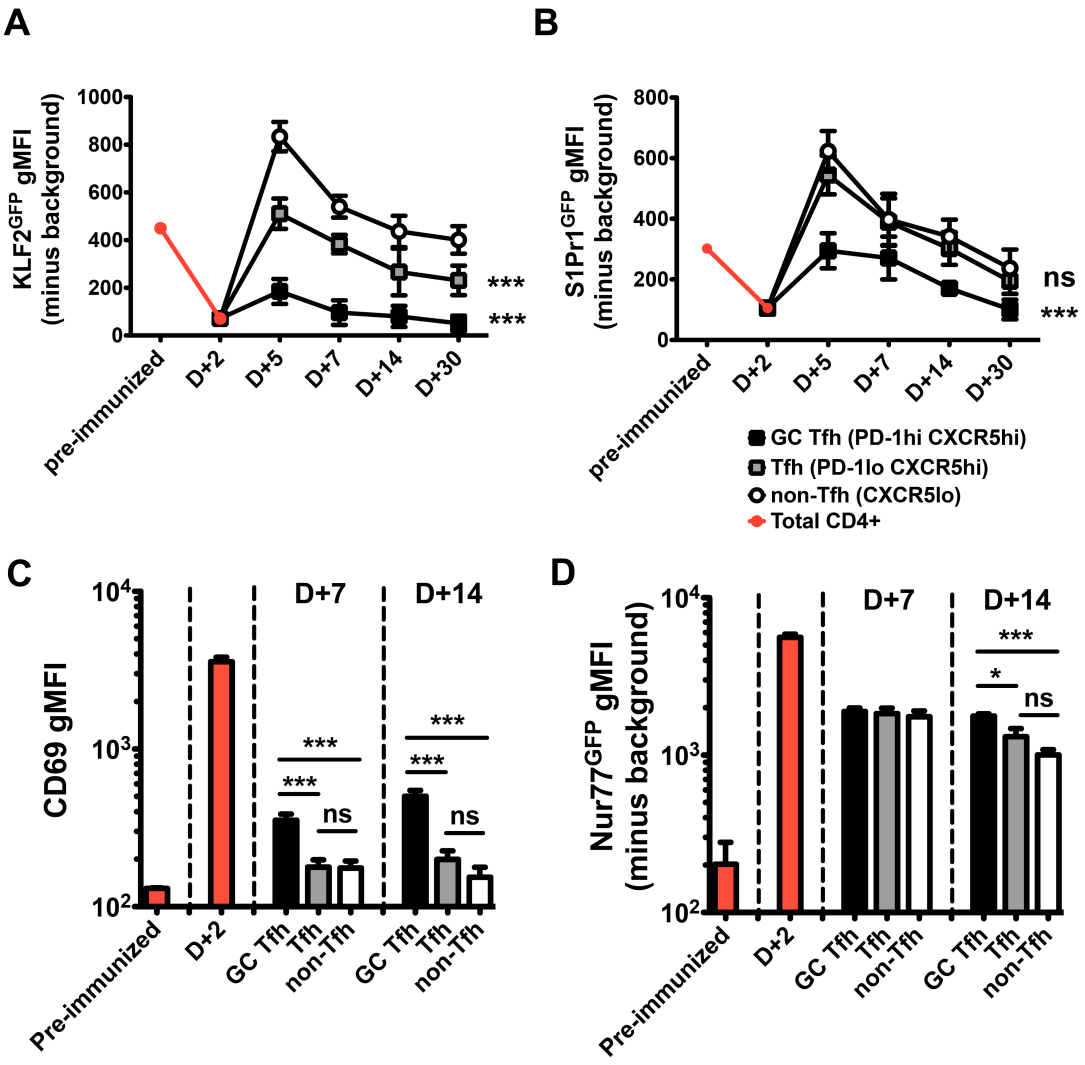

Figure 3-5. Sustained downregulation of KLF2 and S1PR1 expression in GC-Tfh. (A, B) Expression levels of KLF2-GFP (top) or S1PR1-GFP (bottom) by TEa CD4+ T cells at indicated time points following Eα-SA-DEL/CFA immunization. TEa cells were co-transferred with MD4 B cells into WT B6 recipients prior to priming. Data are presented as gMFI minus background gMFI of co-transferred non-transgenic TEa CD4+ T cells, after gating on the indicated phenotypic subsets (defined in Figure 1). Statistical significance was calculated relative to the non-Tfh population. (C) Cell surface expression of CD69 on GC-Tfh, Tfh and non-Tfh TEa CD4+ T cells at days 2, 7 and 14 post Eα-SA-DEL/CFA immunization, presented as gMFI. (D) Expression of Nur77-GFP (a reporter for TCR signaling) by GC-Tfh, Tfh and non-Tfh TEa CD4+ T cells (shown as gMFI, calculated as above). Data are from three independent experiments with a total of 9 recipient mice at each time points. Graphs show accumulated data from the independent experiments as mean ±s.d., two-tailed t-test. ns, not significant ($P > 0.05$); *, $P < 0.05$; **, $P < 0.01$; and ***, $P < 0.001$.

Loss of KLF2 enhances GC-Tfh generation and the GC B cell response

While these results indicate that GC-Tfh characteristically display reduced KLF2 and S1PR1 levels, the functional relevance of this expression pattern was unclear. Hence, we examined the consequences of dysregulated KLF2 expression. Analysis of KLF2 deficient naïve T cells is compromised by their altered trafficking[7,95], hence we utilized an inducible knockout approach in which tamoxifen administration stimulates ERT2-Cre to mediate Klf2 ablation (monitored through a Cre-induced YFP reporter: Fig. 6A, B)[86,93]. Klf2 gene deletion in TEa T CD4+ T cells was initiated at day 2 of the response (when KLF2 expression level is already low – Fig. 6A, 5A). Ablation of Klf2 led to a striking increase in the frequency (Fig. 6C) and number (data not shown) of GC-Tfh (and Tfh) phenotype CD4+ T cells compared to controls, consistent with the hypothesis that KLF2 acts to restrain GC-Tfh differentiation.

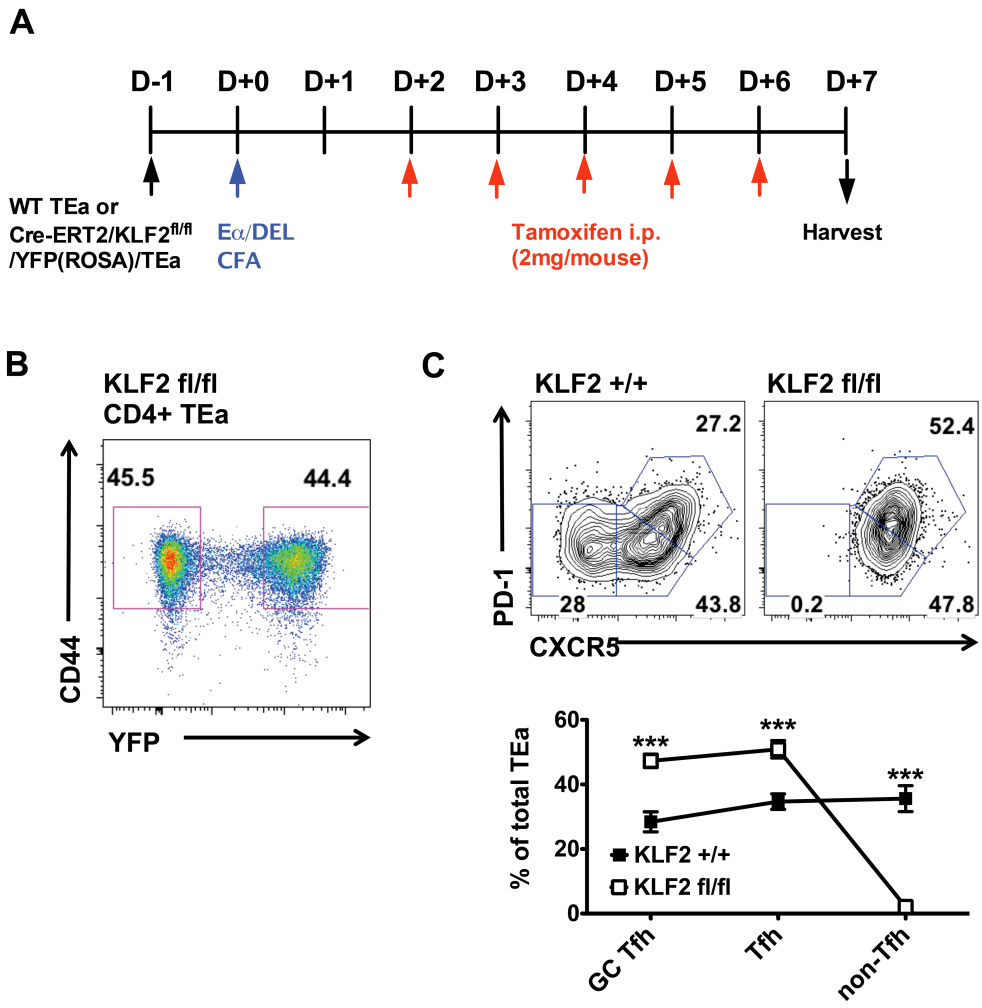

Figure 3-6 Inducible deletion of KLF2 in peripheral CD4+ T cells enhances generation of GC-Tfh. (A) Experimental scheme. WT KLF2 TEa cells (KLF2+/+; Cre-ERT2 / TEa) or KLF2 inducible KO TEa cells (KLF2 fl/fl; KLF2fl/fl / Cre-ERT2 / Rosa-YFP / TEa) were transferred into WT B6 (with MD4 B cells) or TCRα-/- (without MD4 B cells) recipients and primed by subcutaneous immunization of Eα-SA-DEL/CFA. Tamoxifen was administered via intra-peritoneal injection daily from days 2 to 6 post-immunization. At day 7 after immunization, pooled spleen and LN cells from each recipient were stained with APC conjugated anti-CD45.1 (congenic marker specific for transferred TEa CD4+ T cells) antibody, and TEa CD4+ T cells enriched by anti-APC magnetic beads pull-down. (b), Representative data on the frequency of YFP induction of donor KLF2 inducible KO TEa cells from tamoxifen treated animals at day 7 post immunization. (C) Analysis of Tfh differentiation upon tamoxifen-induced (Cre-ERT2) KLF2 deletion. Data are from three independent experiments with a total of 9 WT B6 recipient mice. Graphs show accumulated data from the independent experiments as mean ±s.e.m., two-tailed t-test. ***, $P < 0.001$.

To test whether KLF2-deficient CD4+ T cells were functional as GC-Tfh, we tested their capacity to mediate antigen specific B cell priming and the GC reaction. Klf2-inducible knockout TEa T cells were transferred into TCRα-deficient recipients and primed with Eα-SA-DEL. In this way, the antigen-specific response of endogenous polyclonal B cells can be monitored, while T cell help is limited to the donor population. As we observed before, Klf2 deletion in the TCRα-deficient recipients also increased the frequency and number of GC-Tfh and Tfh phenotype CD4+ T cells compared to controls (Fig. 7A). Serum anti-Eα-SA-DEL IgM, IgG1, IgG2a, IgG2c, IgG3 as well as IgE titers were increased within 5 days of induced KLF2-knockout (Fig. 7B). Moreover, inducible KLF2 deletion in donor TEa cells increased the number of both plasma cells (Fig. 9A) and GC B cells (Fig. 9B) within the Eα-SA specific polyclonal B cell population (Fig. 8A, B). Taken together, these results showed that deletion of KLF2 in early activated CD4+ T cells promoted polarization toward Tfh and GC-Tfh cells, and that those T cell populations were functional in providing help for robust antigen specific B cell priming and GC dependent isotype switching.

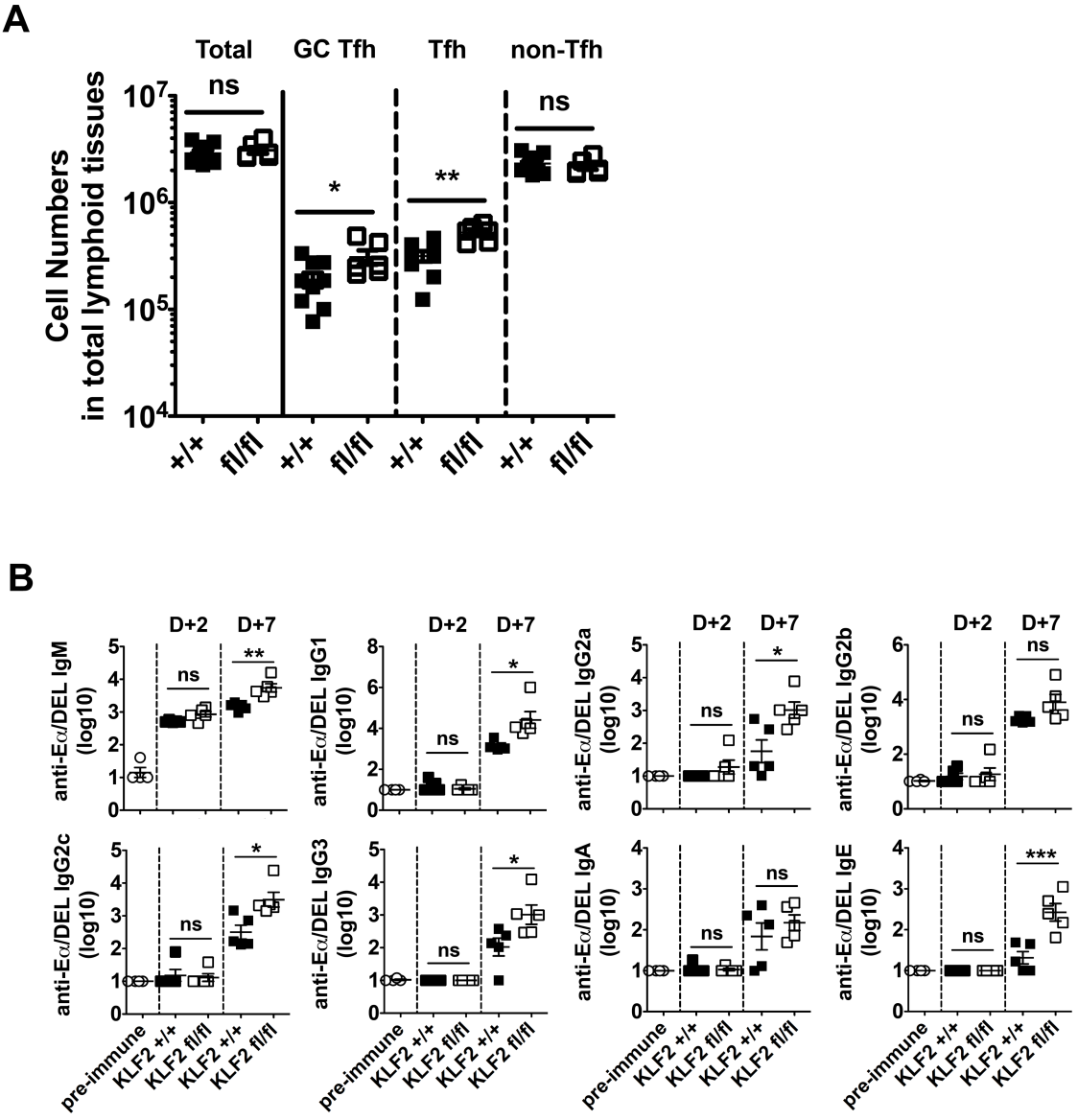

Figure 3-7. Inducible deletion of KLF2 in peripheral CD4+ T cells enhances Tfh differentiation and the germinal center B cell response. (A) Absolute numbers of donor TEa CD4+ T cells recovered from TCRα KO mice that received KLF2+/+ or KLF2 inducible KO TEa cells, determined 7 days after immunization and 5 days after tamoxifen treatment. (B) Titers of Eα-SA-DEL specific antibodies in serum from mice receiving KLF2+/+ (n=5) or KLF2 fl/fl (n=5) TEa T cells. Serum samples were collected at the day of immunization (pre-immune), beginning of tamoxifen treatment (day 2 after immunization: "D+2") and 5 days of tamoxifen treatment (day 7 after immunization: "D+7"). Graphs show accumulated data from the independent experiments as mean ±s.e.m., two-tailed t-test. ns, not significant ($P > 0.05$); *, $P < 0.05$; **, $P < 0.01$; and ***, $P < 0.001$.

A

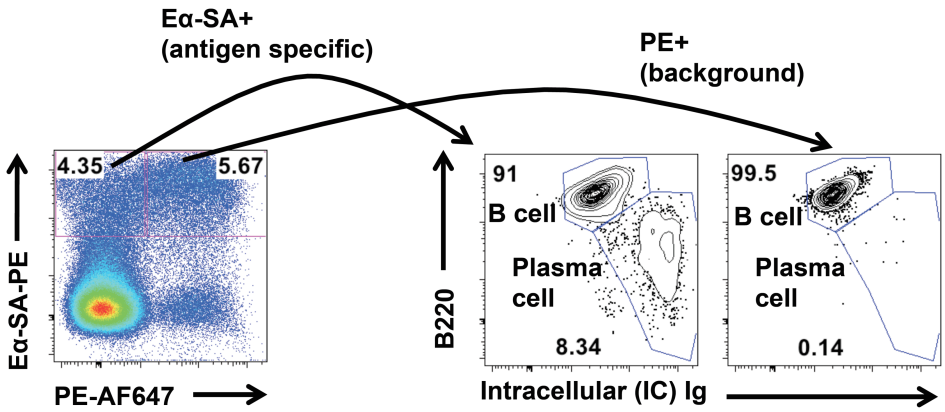

Prior gating: Live cells, and "dump" (CD90, F4/80, Gr-1, NK1.1) negative.

B

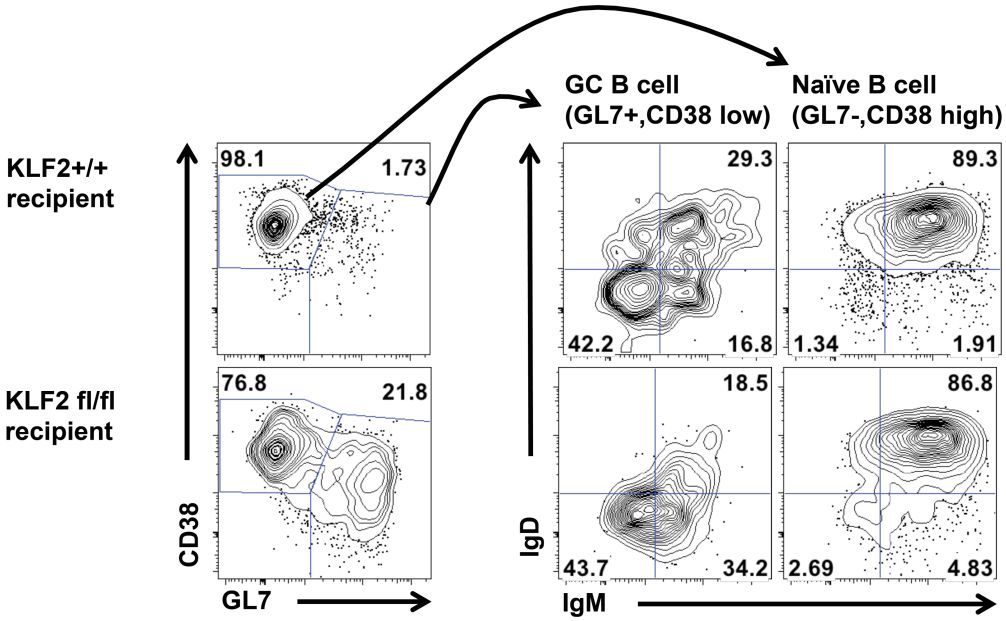

Prior gating:
Antigen specific (Eα-SA-PE+ve, PE-AF647-ve), B220 high, IC Ig low.

Figure 3-8. Identification of antigen specific germinal center response. At day 7 after immunization, pooled spleen and LN cells from each recipient were stained with Eα-SA-PE tetramer, and cells enriched by anti-PE magnetic beads pull-down. Host antigen specific B cells were identified based on the following criteria: Eα-SA-PE tetramer+ PE-AF647- Thy1- Gr-1- CD11c- NK1.1- and F4/80-. Plasma blast/cells were determined as IC-Ighigh/B220low, and GC B cells were determined as C-Ighigh/B220low/GL7high. GC B cells were further validated by surface expression of IgD and IgM. (A) After enrichment, B cells were gated as negative for non-B cell lineage markers ("dump": Thy1, Gr-1, CD11c, NK1.1 and F4/80), and the antigen specific B cells were determined by PE positive gating (Eα-SA-PE tetramer bound fraction). In order to exclude B cells specific for PE (which was not a component of the immunogen) cells were also stained with PE-AF647: Cells stained with Eα-SA-PE but not PE-AF647 were designated as Eα-SA "antigen" specific. Indeed, plasma cells - B220lo, intracellular immunoglobulin (IC-Ig)hi - were found in the Eα-SA specific but not PE specific ("Background") population, as expected. (B) Enriched cells were gated as indicated and analyzed for expression of CD38, GL7, IgM and IgD. The designation of the populations as GC B cells or naïve B cells is indicated. Data are from three independent experiments with a total of 9 (KLF2+/+) or 6 (KLF2 fl/fl) TCRα KO recipient mice.

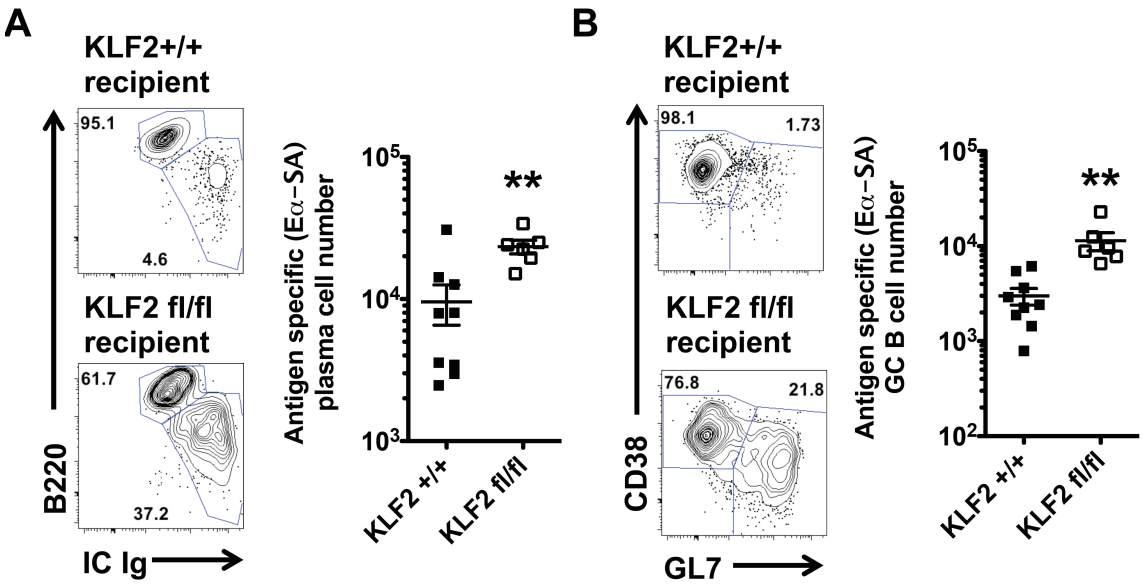

Figure 3-9. Inducible deletion of KLF2 in peripheral CD4+ T cells enhances plasma cell and germinal center (GC) B cell differentiaion. Quantification of endogenous Eα-SA specific (A) plasma cells (intracellular immunoglobulin (Ig)^{high}, B220^{low}; left) and (B) GC B cells (B220high, GL7high; right). Each symbol represents an individual mouse and small horizontal lines indicate the mean. Data are from three independent experiments with a total of 9 (KLF2+/+) or 6 (KLF2 fl/fl) TCRα KO recipient mice. Graphs show accumulated data from the independent experiments as mean ±s.e.m., two-tailed t-test. **, $P < 0.01$.

Forced expression of KLF2 or S1PR1 in CD4+ T cells impairs generation of GC-Tfh

As a complementary approach, we next assessed the impact of increased KLF2 expression on GC Tfh differentiation in vivo, using a retroviral overexpression system[20]. At day 7 p.i., forced expression of KLF2 in TEa CD4+ T cells resulted in a dramatic inhibition of Tfh and GC-Tfh cell differentiation (compared to non-transduced and "empty" retroviral transduced controls) (Fig. 10), supporting the proposal that KLF2 played a dominant negative regulatory role in Tfh and GC-Tfh differentiation. KLF2 is required for S1PR1 expression in T cells, and previous studies have suggested that induction of S1PR1 is sufficient to substitute for KLF2 in control of thymocyte egress[105] and establishment of CD8 T cell resident memory[20]. Hence, we tested whether the effects of forced KLF2 expression were mimicked by S1PR1, using a similar retroviral transduction approach. Indeed, ectopic expression of S1PR1, like KLF2, significantly decreased generation of Tfh and GC-Tfh CD4+ T cells (Fig. 10). These results suggest that downregulation of KLF2 and its target S1PR1 are obligatory steps in the production of GC-Tfh CD4+ T cells.

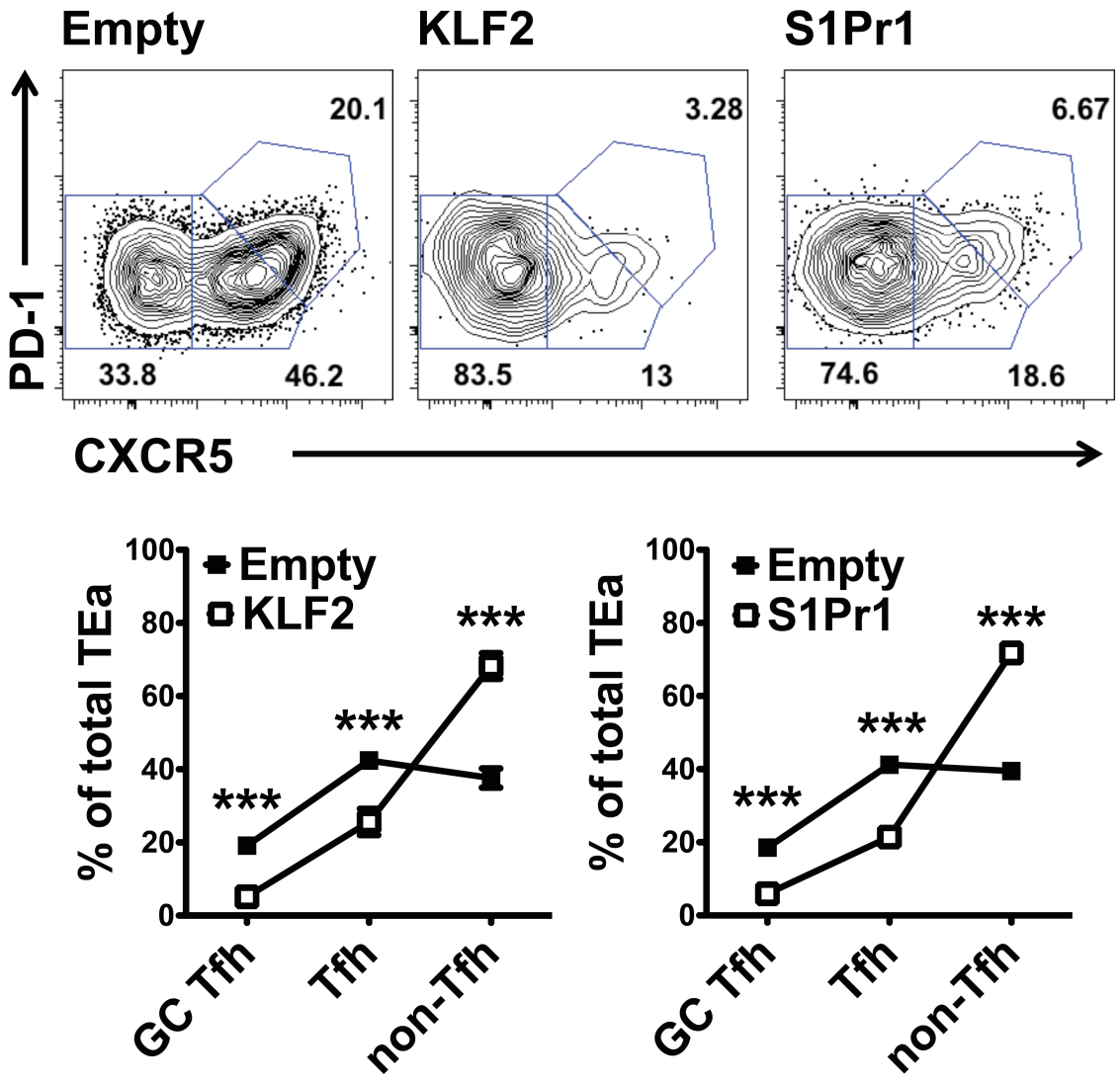

Figure 3-10. Forced expression of KLF2 or S1PR1 inhibits Tfh differentiation. (a) TEa CD4+ T cells were in vitro activated and transduced with MiT-based retroviruses encoding KLF2, S1Pr1 or no insert (empty) and adoptively transferred (with naïve MD4 B cells) in recipient mice that were immunized with Eα-SA-DEL in CFA. At day 7 of the response, transduced TEa cells (identified by the Thy-1.1 marker) were analyzed for phenotypic markers (defined in Figure 1). Data are from at least three independent experiments with a total of 11 recipient mice, and graphs show accumulated data from the independent experiments as mean ±s.e.m., two-tailed t-test. ***, $P < 0.001$.

KLF2 influences GC-Tfh production independent of S1PR1 regulation

These findings might suggest that the critical function of KLF2 in controlling Tfh production is mediated by control of S1PR1 expression. In order to test this directly, we utilized the opportunity to neutralize S1PR1 functional activity with the drug FTY720[35]. As before, S1PR1 overexpression led to reduced generation of Tfh and GC-Tfh, but this effect was substantially reversed by treatment with FTY720 (Fig. 11), consistent with the hypothesis that S1PR1 expression blocks Tfh and GC-Tfh generation. Surprisingly, however, FTY720 treatment had no effect on the skewed Tfh/GC-Tfh differentiation induced by forced KLF2 expression (Fig. 11). This implied that the effects of forced KLF2 expression were not limited to induction of S1PR1. Furthermore, FTY720 treatment did not impact CD4+ T cell differentiation in the control-transduced population (Fig. 11), suggesting that S1PR1 function alone was not regulating Tfh/GC-Tfh subset in normal cells. Taken together, these studies indicate that S1PR1 expression is a critical component, but not the dominant regulatory mechanism though which KLF2 regulates GC-Tfh differentiation.

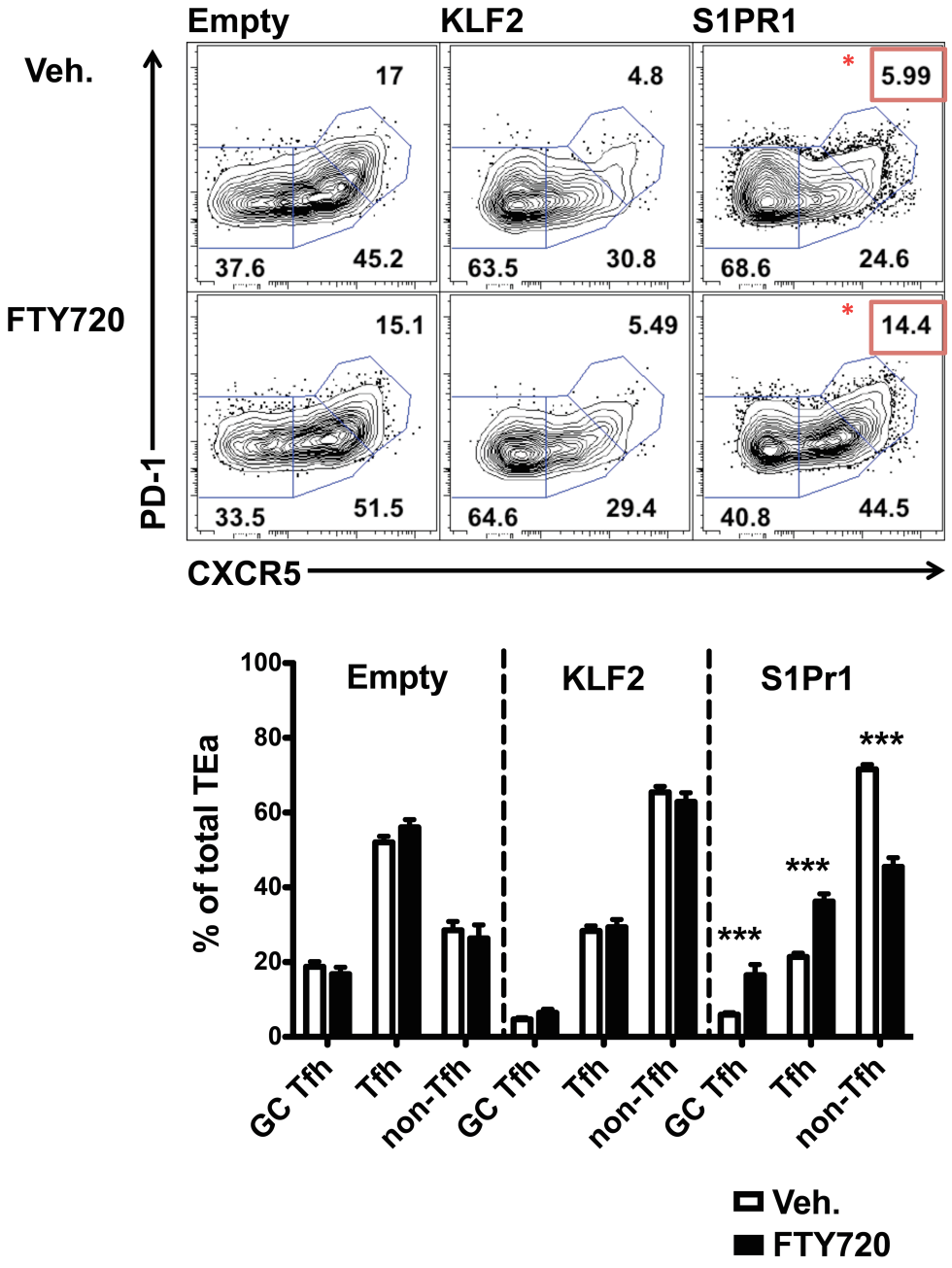

Figure 3-11. Effect of FTY720 treatment (S1PR1 blocking) on representation of GC-Tfh, Tfh and non-Tfh populations within the retrovirally transduced TEa T cells in vivo. FTY720 or vehicle control ("Veh.") was administrated by intra-peritoneal injection at day 2, 4, and 6 post immunization, and the phenotype of donor cells were analyzed at day 7 after the immunization. Data are from at least three independent experiments with a total of 11(a) or 9(b) recipient mice, and graphs show accumulated data from the independent experiments as mean ±s.e.m., two-tailed t-test. ***, $P < 0.001$.

KLF2 induces Blimp-1 and affects the balance of Blimp-1/Bcl-6 expression

Thus, we hypothesized KLF2 would have other downstream targets that affect GC-Tfh generation. To address this we tested whether KLF2 regulates expression of known factors in the GC-Tfh differentiation pathway. We assessed the impact of KLF2 overexpression and induced deletion of in vitro stimulated CD4+ T cells, maintained in non-polarizing culture conditions (Fig. 12A, B).

Quantitative RT-PCR data showed KLF2 deletion led to significant induction of Bcl6 and reduced expression of the Prdm1 gene (encoding Blimp-1) (Fig. 13A). In contrast, over-expression of KLF2 significantly decreased bcl6 gene expression, but increased Blimp-1 gene (Fig. 13B) and protein (Fig. 13C). Bcl-6 promotes generation of GC-Tfh, while Blimp-1 represses Bcl-6 expression[81,88,106], hence these findings reveal that KLF2 influences the balance in expression of key transcription factors that regulate GC-Tfh differentiation. In contrast, we did not observe effects of KLF2 manipulation on mRNA expression of Ascl2, CXCR5, ICOS or IL-21, in these in vitro cultured cells (Fig. 13A, B and data not shown). Also, forced expression of S1PR1 had no effect on Blimp-1 or Bcl-6 expression (Fig. 13B, C). Although these data showed that KLF2 impacts the balance of Blimp-1 and Bcl-6 expression, the transcriptional antagonism between these factors complicates defining how KLF2 regulates this expression profile.

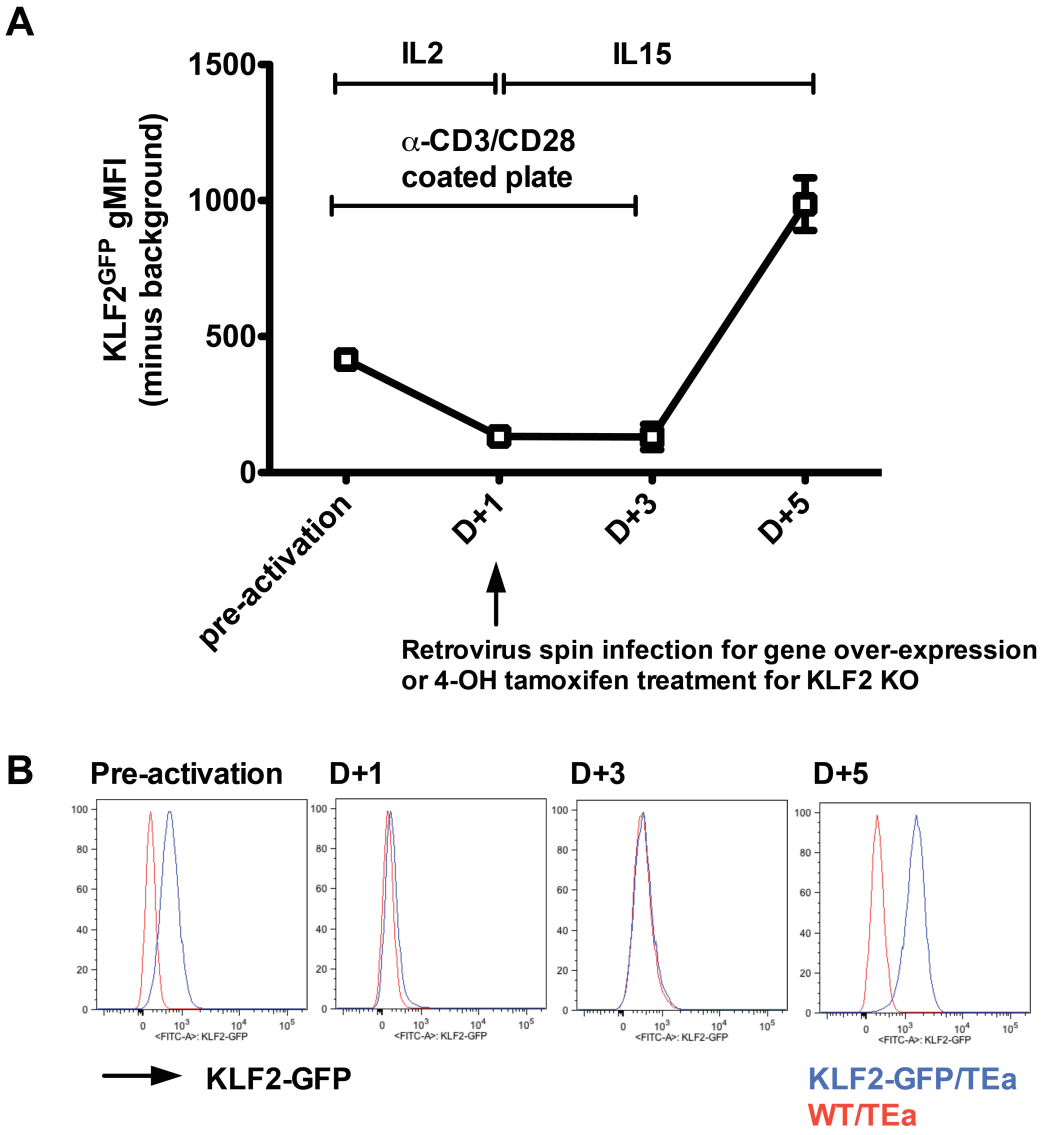

Figure 3-12. In vitro cell culture conditions and resulting KLF2-GFP expression pattern. For in vitro culture studies, isolated KLF2-GFP CD4+ T cells were initially primed with IL-2 (20ng/ml) for 24 hours and further cultured with IL-15 (20ng/ml) for 48 hours in anti-CD3/CD28 coated plates. Cells were then transferred to non-coated plates and cultured to recover KLF2-GFP expression for an additional 48 hours. The timing for retroviral transduction and 4-OH tamoxifen (100nM) treatment (for KLF2fl/fl inducible knockout) is indicated. Graph (A) and FACS plots (B) show expression of KLF2-GFP in KLF2GFP reporter TEa CD4+ T cells (blue) during in vitro culture, presented as experimental gMFI minus background gMFI of co-cultured non-transgenic TEa CD4+ T cells (red). This in vitro culture experiment was repeated three times with similar results. All data are representative of at least three independent experiments. Graphs show accumulated data from the independent experiments as mean ±s.e.m..

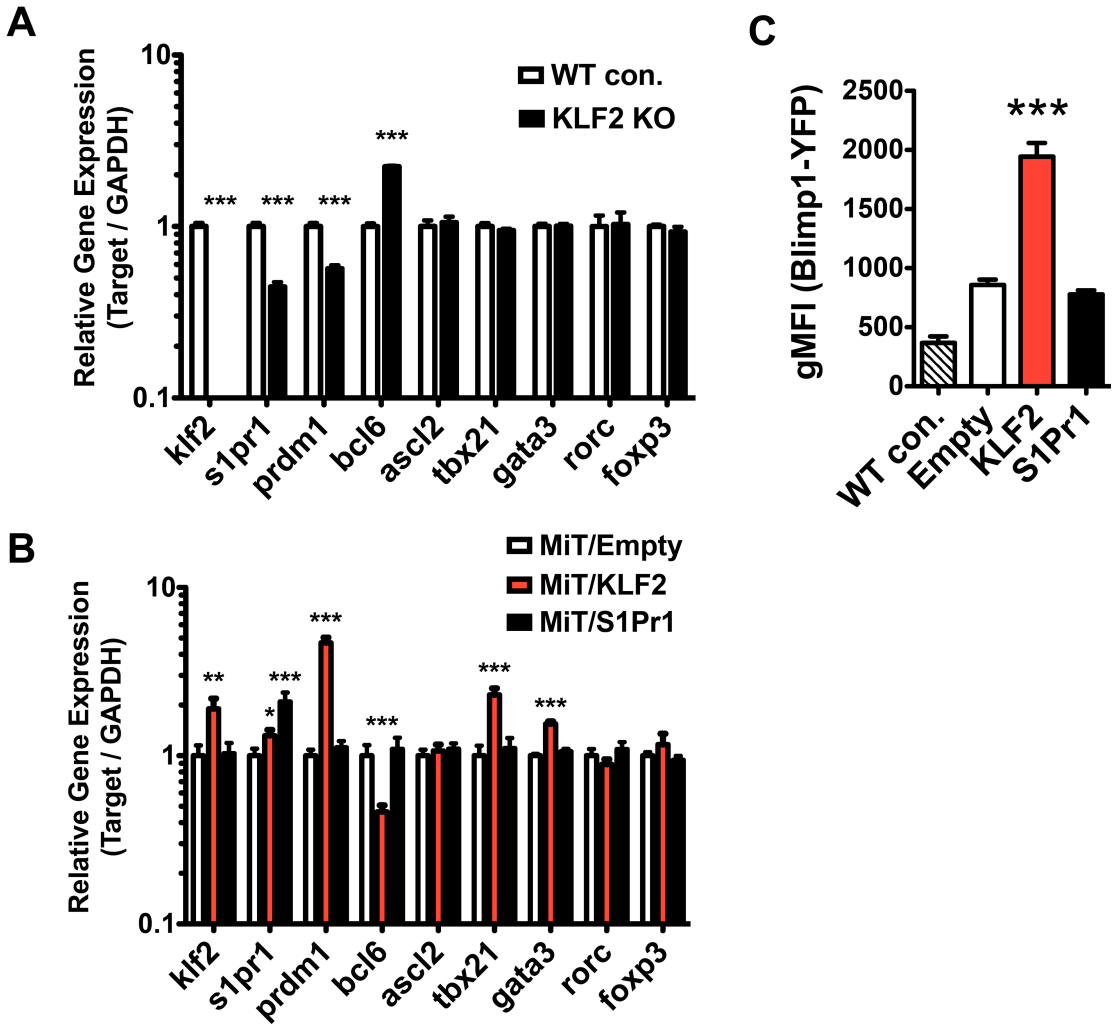

Figure 3-13. Transcriptional regulation of KLF2 in expression of CD4+ T cell lineage defining factors. (A, B) RT-PCR analysis of various genes (horizontal axis) for in vitro cultured KLF2 KO (A) or retrovirus-transduced (B) TEa CD4+ T cells after sorting based on expression of Cre-reporter signal (for KLF2 KO; YFP+) or retro-transduction marker (Thy1.1). (Detailed in vitro culture conditions are described in Fig. 12). (C) FACS analysis of transcription factor expression in retrovirally-transduced TEa cells (identified by Thy1.1+ expression). Induction of Blimp-1 in the retrovirus-infected Blimp-1-YFP reporter CD4+ T cells in vitro. All experiments repeated at least three times with similar results. Graphs show accumulated data from the independent experiments as mean ±s.e.m., two-tailed t-test. **, $P < 0.01$; and ***, $P < 0.001$.

To test whether KLF2 directly binds to promoters for these genes, we performed chromatin immunoprecipitation (ChIP) assays for KLF2-GFP on both naïve and activated CD4 T cells. As expected, KLF2 was found at the promoter of S1pr1 in naïve and activated CD4+ T cells (Fig. 14). In addition, we found that KLF2 bound the promoter region of the gene encoding Blimp-1 (Prdm1) following T cell activation, but we did not observe a significant ChIP signal for KLF2 at the Bcl6 promoter (Fig. 14). These findings are consistent with changes in Bcl6 mRNA expression (Fig. 13A, B) being secondary to KLF2 induction of the repressor Blimp-1.

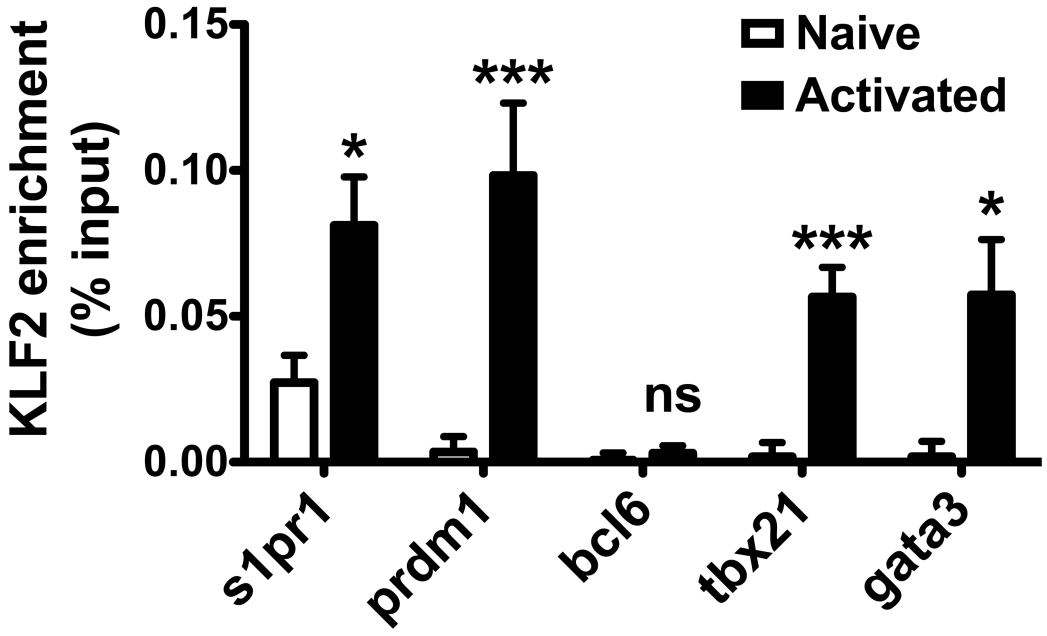

Figure 3-14. KLF2 chromatin immunoprecipitation (ChIP). ChIP analysis of naïve or in vitro activated KLF2GFP-reporter TEa CD4+ T cells, followed by chromatin immunoprecipitation using rabbit IgG (control) or anti-GFP and quantitative PCR analysis of binding at the promotor regions of each gene (horizontal axis) (primers are listed in Materials and Methods). Results were normalized to those of a standardized aliquot of input chromatin, followed by subtraction of the signal obtained with IgG (nonspecific background). All experiments repeated at least three times with similar results. Graphs show accumulated data from the independent experiments as mean ±s.e.m., two-tailed t-test. ns, not significant ($P > 0.05$); *, $P < 0.05$; and ***, $P < 0.001$.

KLF2 promotes expression of T-bet and Gata3 and Th1 generation

To broaden our analysis, we also explored how expression of transcription factors that define other T helper (Th) subsets is affected by KLF2 manipulation. Intriguingly, over-expression of KLF2 also led to substantially increased expression of T-Bet (Tbx21) and Gata3 genes and proteins, but did not affect expression of the genes for Rorγt (Rorc) or Foxp3 (Fig. 13B, 15A and data not shown). Furthermore, ChIP assays revealed that KLF2 occupies the regulatory regions of the genes for T-Bet (Tbx21) and GATA3 (Gata3) following T cell activation (Fig. 14). It is important to note, however, that induced KLF2 deficiency did not lead to reduced expression of Tbx21 or Gata3, in contrast with the decline in Prdm1 expression, suggesting KLF2 is not required for Tbx21 or Gata3 expression (Fig. 13A). Nevertheless, enforced KLF2 expression led to a significant increase in the frequency of CD4 T cells with the canonical Th1 function of IFN-γ production (Fig. 15B, C), in keeping with strong enhancement of T-bet expression.

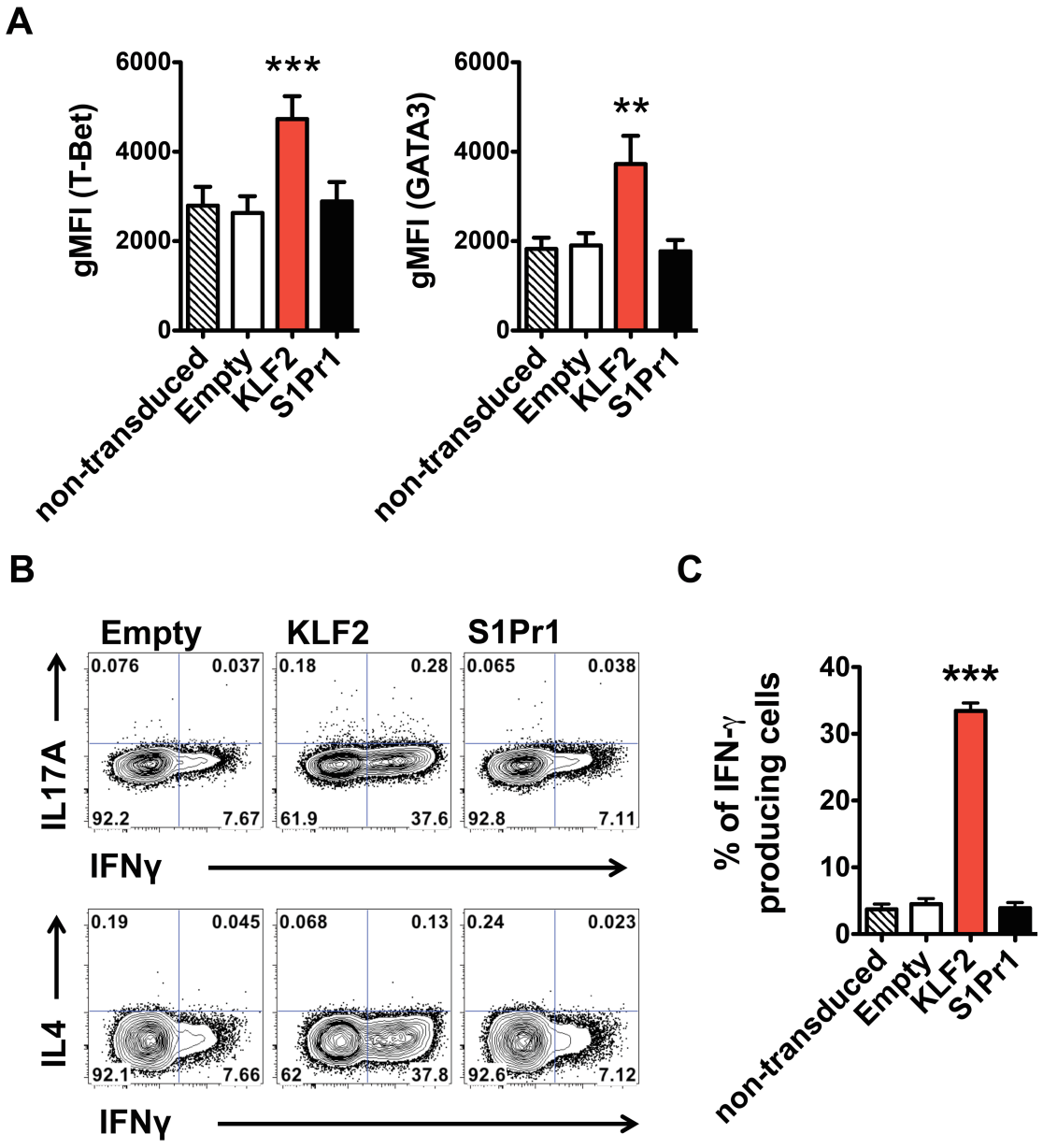

Figure 3-15. KLF2 promotes T-Bet and GATA3 expression in activated CD4+ T cells and dictates Th1 lineage differentiation. (A) T-Bet and GATA3 expression in the retrovirus-infected TEa CD4+ T cells in vitro. (B, C) Percentage of IFN-γ producing population upon PMA/Ionomycin stimulation for 3 hours in the retrovirus-infected TEa CD4+ T cells in vitro. All experiments repeated at least three times with similar results. Graphs show accumulated data from the independent experiments as mean ±s.e.m., two-tailed t-test. **, $P < 0.01$; and ***, $P < 0.001$.

We next extended these studies to explore how KLF2 expression influenced Th subset-defining transcription factor expression in vivo. To assess this, we analyzed expression of key transcription factors in responding CD4 T (using a sequential gating strategy - Fig. 16A). Consistent with the studies discussed above, forced expression of either KLF2 or S1PR1 led to a decrease in the frequency of CD4 T cells that predominantly expressed Bcl-6, while ectopic KLF2 (but not S1PR1) led to a substantial increase in frequencies of cells expressing T-bet and a proportional decrease in the fraction of cells expressing RORγt (Fig. 16B, C). Forced KLF2 expression induced a modest (although significant) increase in the frequency of T-bet-/Gata3+ cells (Fig. 16B, C). Unexpectedly, we found that the increased frequency of T-bet+ cells induced by KLF2 transduction was predominantly a population that co-expressed both Gata3 and T-Bet (Fig. 16C, D).

KLF2 over-expression might induce non-physiological gene expression patterns. Hence we also evaluated whether endogenous KLF2 expression levels correlated with expression of lineage-defining transcription factors in differentiating TEa CD4+ T cells. KLF2 levels were lowest in the Bcl-6hi pool, corresponding to GC-Tfh (Fig. 17A, B). On the other hand, TEa CD4+ T cells co-expressing T-Bet and GATA3 were characterized by substantially higher expression levels of endogenous KLF2 (Fig. 17A, B). Other transcription-factor defined subsets showed intermediate levels of endogenous KLF2 (Fig. 17B). These data support the hypothesis that physiological KLF2 expression levels correspond with expression of the Th lineage-defining transcription factors that are direct targets of KLF2.

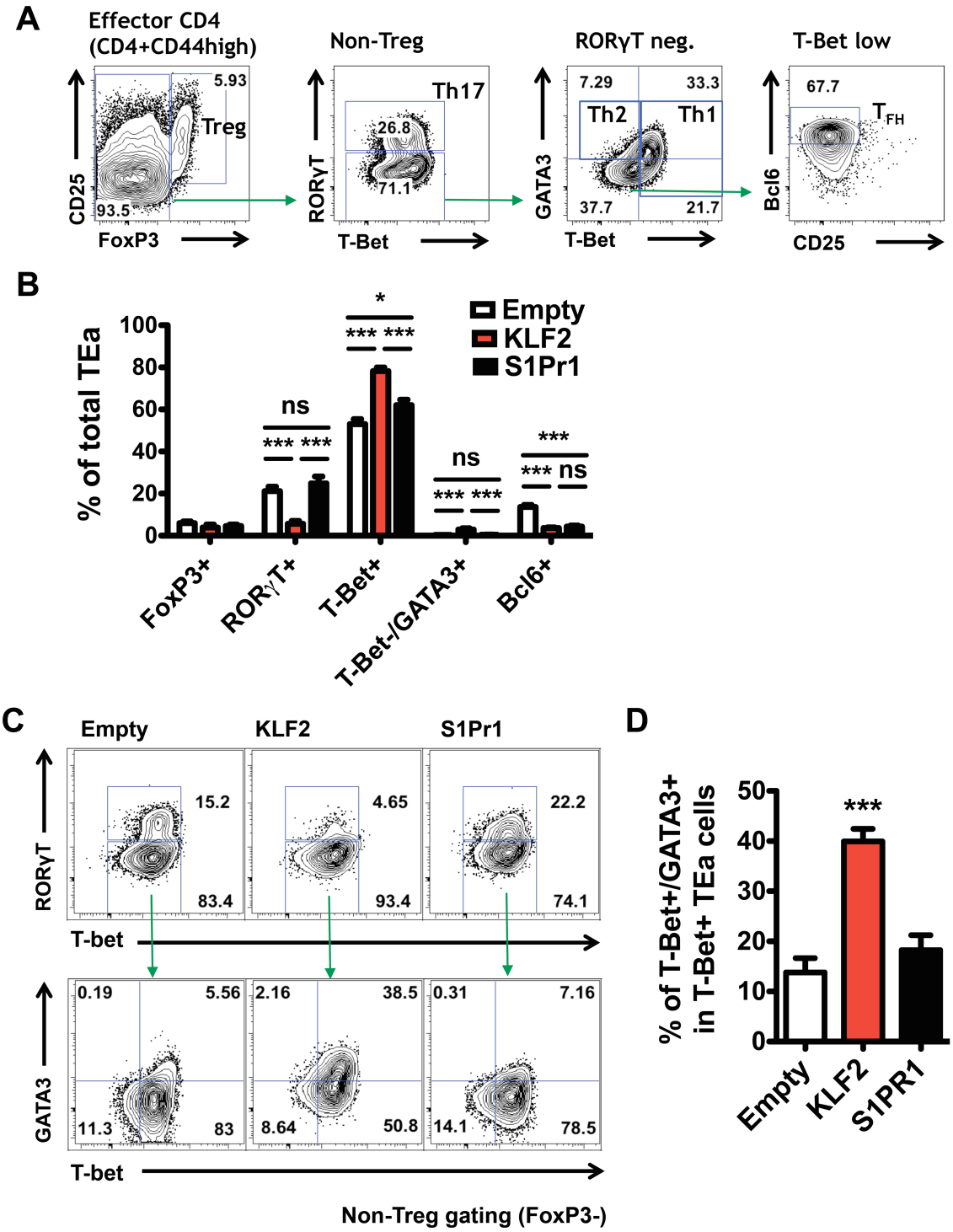
A
Effector CD4
(CD4+CD44high)
5.93
Treg
93.5
CD25
FoxP3
Non-Treg
Th17
26.8
71.1
RORγT
T-Bet
RORγT neg.
7.29
33.3
Th2
Th1
37.7
21.7
GATA3
T-Bet
T-Bet low
67.7
T_FH
Bcl6
CD25
B
% of total TEa
100
80
60
40
20
0
Empty
KLF2
S1Pr1
*
*** ***
ns
*** ***
ns
*** ***
***
*** ns
FoxP3+
RORγT+
T-Bet+
T-Bet-/GATA3+
Bcl6+
C
Empty
KLF2
S1Pr1
RORγT
15.2
83.4
4.65
93.4
22.2
74.1
T-bet
GATA3
0.19
5.56
11.3
83
2.16
38.5
8.64
50.8
0.31
7.16
14.1
78.5
T-bet
Non-Treg gating (FoxP3-)
D
% of T-Bet+/GATA3+
in T-Bet+ TEa cells
50
40
30
20
10
0
***
Empty
KLF2
S1PR1

Figure 3-16. KLF2 induces T-bet and GATA3 expression during CD4 T cell lineage commitment in vivo. Analysis of in vivo derived Th subsets. (A) The gating strategy of CD4+ helper T cell lineages. At day 7 after subcutaneous immunization of Eα-SA-DEL/CFA, donor CD4+ TEa cells were enriched and analyzed for lineage specific transcription factor expression. First, the Treg population was identified by FoxP3 and CD25 expression. FoxP3- (non-Treg) cells were characterized for RORγT+ expression (identifying presumed Th17 cells). Next, the RORγT- population was further sub-populated into T-bet+ and GATA3+/T-bet- populations. Finally, the Bcl6+/CD25- Tfh cells were identified within the T-betlow/GATA3- population. (B) Analysis of TEa CD4+ T cells for expression of lineage-defining transcription factors following transduction with indicated retroviruses at day 7 post immunization in vivo. (C, B) Analysis of T-bet and GATA3 double positive TEa CD4+ T cells in T-bet+ population (Th1; T-bet+FoxP3-RORγT-). Data are from at least three independent experiments with a total of 15, and graphs show accumulated data from the independent experiments as mean ±s.e.m., two-tailed t-test. ns, not significant ($P > 0.05$); *, $P < 0.05$; and ***, $P < 0.001$.

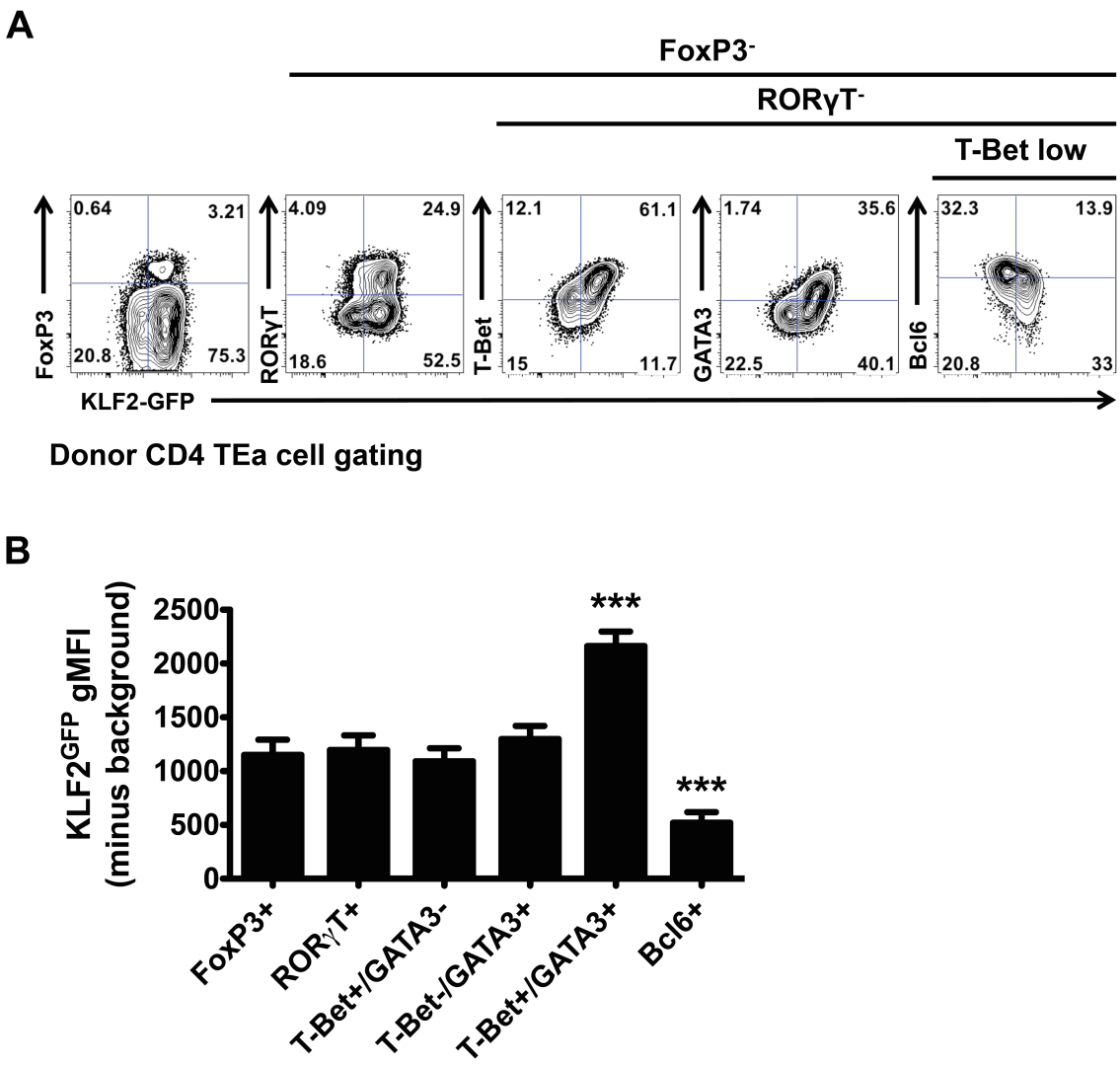

Figure 3-17. KLF2 expression is corelated with T-Bet/GATA3 and inversly corelated with Bcl6 in effector CD4+ T cells in vivo. (A, B) KLF2-GFP expression level (gMFI) within TEa CD4+ T cells expressing the indicated transcription factors at day 7 post immunization. Data are from at least three independent experiments with a total of 9 KLF2-GFP reporter mice, and graphs show accumulated data from the independent experiments as mean ±s.e.m., two-tailed t-test. ***, $P < 0.001$.

Discussion

The factors that determine both Tfh differentiation and localization within the germinal center are still being defined. In particular, whether and how those features are coordinately regulated by individual factors is unclear. In this report, we show that one transcription factor, KLF2, influences both activated CD4+ T cell trafficking (through regulation of S1PR1) and Th subset differentiation (through control of Blimp-1, T-bet and Gata3), such that KLF2 expression directs differentiating CD4+ T cells away from the Tfh fate. However, KLF2 does not simply act as a block for Tfh differentiation: rather, the regulation of multiple key transcription factors suggests KLF2 serves to shape alternative Th differentiation choices. Indeed, we find that the physiological KLF2 expression levels correlate with expression of lineage-defining transcription factors, suggesting that KLF2 levels can serve to tune the Th-subset differentiation fate.

We and others reported that KLF2 regulates expression of the S1PR1, which is critical for lymphocyte recirculation[7,20,34,95]. Indeed, for certain functions – such as the substituted by expression of S1PR1[34,105]. Furthermore, in recent studies we showed that ectopic expression of either KLF2 or S1PR1 was sufficient to impede establishment of resident memory CD8+ T cells[20]. Similarly we found that forced expression of S1PR1 in activated CD4+ T cells led to a dramatic reduction in generation of Tfh. This effect correlated with functional activity and/or expression of S1PR1 on the cell surface, since treatment with FTY720 substantially reversed the effects of S1PR1 overexpression. One interpretation of these findings is that S1PR1 expression opposes the migration of activated T cells into the follicle, thereby blunting the reinforcing signals that normally

drive continued Tfh differentiation as CD4+ T cells migrate into the B cell follicle. S1PR1 signals over-ride migration induced by CXCR5 in MZ B cells[107], and counteract responses through a related chemokine receptor CCR7 in T cells[35,36]. In addition, S1PR2 has recently been shown to cooperate with CXCR5 for efficient GC-Tfh generation[84] – since S1PR1 and S1PR2 signal through distinct G-protein complexes, they can have opposing effects on cell migration[35]. Encounter with B cells and continued antigen stimulation is needed for sustained expression of Bcl-6 and expansion of the Tfh population[81,101] - hence denying activated CD4+ T cells access to the B cell follicle could explain the deficit in CXCR5-expressing cells following forced S1PR1 expression.

Nevertheless, our data indicate that S1PR1 regulation is not sufficient to explain the effects of KLF2 expression on Tfh differentiation. FTY720 treatment did not reverse the paucity in Tfh and GC-Tfh generation that followed transduction with a KLF2-encoding retrovirus. This suggested that blocking the S1PR1-mediated changes in cell trafficking was insufficient to compensate for dysregulated KLF2 expression. It is unlikely that this difference is a consequence of the dose of FTY720 being too low to affect the KLF2 transduced cells, since mRNA expression for S1PR1 was lower in KLF2 transduced compared to S1PR1 transduced CD4+ T cells (Fig. 13b). It is also noteworthy that FTY720 treatment did not impact the ratios of non-Tfh, Tfh and GC-Tfh for control TEa cells – this implies that there is not a cohort of normal activated CD4+ T cells that are prevented from Tfh differentiation due to expression of S1PR1 alone. So, while S1PR1 downregulation is clearly necessary for effective Tfh generation and/or maintenance, this does not fully account for the significance of KLF2 downregulation.

Our further studies showed that KLF2 had an unexpected impact on a series of T cell lineage-defining transcription factors. Overexpression of KLF2 led to increased expression of Blimp-1, while induced ablation of the klf2 gene led to the opposite outcome. Bcl-6 expression changed in the reciprocal direction, as expected from the known mutual repression exerted between Bcl-6 and Blimp-1[81,88,106]. Given this expression pattern, KLF2 could potentially regulate either (or both) Bcl-6 and Blimp-1, however, our data from ChIP suggested that Blimp-1 was a direct target for KLF2 binding. Previous studies on CD8+ T cells showed that forced KLF2 led to elevated Blimp-1 expression[38,39], consistent with this result – but the impact on Bcl-6 expression, and impact of KLF2 deletion on Blimp-1/Bcl-6 expression has not been reported. We did not note gene expression changes in Ascl-2, CXCR5, ICOS or IL-21 when KLF2 levels were manipulated, but it is possible that our in vitro studies would not reveal those changes, and further analysis of KLF2 binding to other genes involved in Tfh differentiation and migration will be important. Nevertheless, our data on the impact of KLF2 on the balance between Blimp-1 and Bcl-6 expression levels provides a ready explanation for KLF2's ability to derail the Tfh differentiation pathway.

Surprisingly, we also observed that elevated KLF2 expression could induce the T-bet and Gata3 transcription factors, and ChIP assays suggested KLF2 directly bound to the regulatory regions for the genes encoding these factors. Our data suggest this regulation is not simply an artifact of overexpression studies, since analysis of normal TEa cells responding in vivo showed that the populations expressing T-bet and Gata3 had significantly higher levels of endogenous KLF2. T-bet and Gata3 are frequently co-

expressed in human Th1 cells[108], but analysis in mouse T cells suggest these two factors are normally differentially expressed (with Th1 cells expressing T-bet and Th2 cells expressing Gata3)[109]. While there have been studies suggesting that restimulating Th1 cells in Th2 conditions can provoke T-bet+/Gata3+ cells with hybrid Th1/Th2 properties[110], our studies found that KLF2 overexpressing CD4 T cells are potentiated for production of the Th1 cytokine IFN-γ, but did not exhibit detectable production of the Th2 cytokine IL-4. Studies comparing the gene expression characteristics of T-bet/Gata3 co-expressing cells suggest that T-bet typically co-opts Gata3 to support induction of genes characteristic of the Th1 lineage[111], in keeping with our findings. Others have reported that Blimp-1 acts to directly repress expression of T-bet and IFN-γ in activated CD4+ T cells[112], while our studies indicate that, when induced by KLF2, Blimp-1 and T-bet can be co-expressed. Though the significance of KLF2hi cells expressing T-bet and Gata3 will require further study, these findings suggest that KLF2 expression does not simply present a barrier to Tfh differentiation, but can foster the differentiation into other Th lineages (Th1 and potentially Th2). Hence these data suggest KLF2 acts as a critical pivot in regulating which Th subset developmental pathway a CD4 T cell will follow.

Kruppel-like factors play diverse roles in multiple tissues, often related to late differentiation steps[8,20]. We and others showed that KLF2 regulates B cell subset differentiation[8,113]. The studies reported here demonstrate a novel and significant impact of KLF2 expression on helper CD4 T cell subset differentiation in two separable ways: Through trafficking (via S1PR1) and through regulation of three lineage-defining

transcription factors (Blimp-1, T-bet and GATA3). Hence KLF2 serves a hitherto unsuspected function in dictating the lineage fate of CD4 T cells.

Materials and methods

Mice

C57BL/6 (B6) and B6.SJL mice were purchased from the National Cancer Institute, and ETR2-Cre, Blimp1-YFP and Tcra−/− mice were obtained from Jackson Laboratories. TEa TCR transgenic mice (specific for a peptide from the I-Eα MHC II molecule (pEα) bound to I-Ab), and MD4 BCR transgenic mice (specific for hen/duck egg lysozyme (HEL/DEL)) were maintained at the University of Minnesota. The S1PR1 reporter strain was a kind gift of Dr. Hugh Rosen (Research Institute of the Scripps Clinic) – this and the KLF2-GFP, Nur77-GFP and KLF2 fl/fl mice have been previously described[20,97,100,104,114] and were crossed to TEa mice at the University of Minnesota. KLF2fl/fl/TEa mice were further bred with ETR2-Cre and Rosa26-YFP mice to generate KLF2fl/fl/ETR2-Cre/Rosa26-YFP/TEa (KLF2 fl/fl) and KLF2+/+/ETR2-Cre/TEa (KLF2 +/+) control mice. For adoptive co-transfer studies, combinations of CD45.2+, CD45.1+ and CD45.1+CD45.2+ mice were used as donor and host strains to allow discrimination between each donor population and the host cells. Six to eight week old mice were used for all experiments. Animals were maintained under specific pathogen free conditions at the University of Minnesota. All experimental procedures were approved by the Institutional Animal Care and Use Committee at the University of Minnesota.

Infections and MHC II-tetramer based cell enrichment

Mice were injected intravenously with 1×10^7 colony-forming units of ActA-deficient LM-2W1S bacteria or intraperitoneally (i.p.) with 2×10^5 plaque-forming units

of the LCMV Armstrong strain. Tetramers composed of I-A^b and either 2W1S, LLO190-201, or LCMV glycoprotein (GP) 66-77 peptides were made as described previously[101,115]. Single cell suspensions of spleen and LN cells were stained for 1 hour at room temperature with the PE or APC-conjugated tetramers and 2 μg of CXCR5-BV421 antibody (2G8; BD bioscience). Samples were then enriched and enumerated as described previously[101,115]. For identification of surface markers, the sample was stained on ice with antibodies specific for MHCII (M5/114.15.2), F4/80 (BM8), B220 (RA3-6B2), CD11c (N418), CD8α (53-6.7), PD-1 (J43), CD4+ (RM4-5), CD3ε (145-2C11), CD44 (IM7), CD45.1 (A20), CD45.2 (104) and CD69 (H1.2F3). Intracellular staining for T-bet (4B10, BioLegend), GATA3 (TWAJ), RORγT (Q31-378, BD bioscience), FoxP3 (FJK-16s) and Bcl-6 (K112-91, BD bioscience) was performed as described previously[101,116]. For determining reporter signal in CD4+ T cell lineage subpopulations, intracellular staining for anti-GFP antibody (rabbit, Life technologies) followed by AlexaFluor488 goat anti-rabbit IgG antibody (Life technologies) was performed. All antibodies were from eBioscience (San Diego) unless otherwise noted. Cells were then analyzed on an LSR II or Fortessa (Becton Dickinson) flow cytometer. Data were analyzed with FlowJo (TreeStar).

Adoptive transfer and Eα-SA-DEL immunization

For adoptive transfer experiments, $1x10^5$ TEa CD4+ T cells were typically co-transferred with $5x10^4$ MD4 B cells into WT B6, B6.SJL, or Tcra−/− mice depending on the CD45 congenic marker expression of the donor cells. Naive CD4+ T cells from

various TEa strains mice were isolated by using mouse CD4+ T Cell Isolation Kit (Miltenyi Biotec), and MD4 B cells were isolated by using mouse B Cell Isolation Kit (Miltenyi Biotec). For reporter studies, background reporter signal was evaluated by mixing reporter and congenic WT TEa CD4+ T-cells at a ratio of 1:1, and 5×10^4 of each TEa CD4+ T cells were transferred into congenic recipient mice. After 12 hours, the recipients were immunized subcutaneously (7μM in 50 μl per mouse) with a conjugate antigen bearing antigens for both TEa and MD4 cells (Eα-SA-DEL) emulsified in CFA (0.5 mg/ ml). On the day of harvest, TEa CD4+ T cells were enriched based on CD45 expression as described previously[20].

To generate the conjugated antigen (Eα-SA-DEL), biotinylated Eα peptide (Eα-Bio) and Streptavidin (SA) were purchased from New England Peptide and ProZyme respectively. Purified duck egg lysozyme (DEL) was obtained by special order from Worthington Biochemical Corporation, and biotinylated using an EZ-link Sulfo-NHS-LC Biotinylation kit (Thermo Fisher Scientific) using a 1:1 ratio of biotin to protein. After removal of free biotin by use of desalting columns (GE Healthcare), the molar amount of biotinylated DEL (DEL-Bio) was measured by Western blot, as previously described[117]. The prepared Eα-Bio and DEL-Bio were then conjugated by incubation with SA (Eα-Bio:DEL-Bio:SA= 2:2:1 ratio) at room temperature for 30 minutes.

Inducible KLF2 deletion and B cell germinal center reaction

In vivo KLF2 deletion of KLF2 fl/fl (KLF2fl/fl/ETR2-Cre/Rosa26-YFP/TEa) cells in WT B6.SJL or Tcra-/- recipient mice was achieved by administering tamoxifen

(10 mg/ml) in sunflower seed oil i.p. for 5 consecutive days from day 2 post-immunization. At day 7 post-immunization, the spleen and inguinal, axillary, brachial, cervical and mesenteric LNs were harvested and analyzed. KLF2 fl/fl or KLF2 +/+ control cells were enriched through their congenic markers, and KLF2 KO populations were identified by YFP expression (Rosa26-YFP reporter). For in vitro KLF2 deletion, primed KLF2 fl/fl cells (cultured with recombinant IL-2 (20ng/ml), anti-CD3 (8 μg/ml per well; 145-2C11; BioXCell), and anti-CD28 (8 μg/ml per well; 37.51; BioXCell) coated plate for 24 hours) were cultured with 4-OH tamoxifen (100nM) and IL-15 (20ng/ml) for 48 hours in anti-CD3/CD28 coated wells, followed by 48 hours of additional culture in IL-15 in non-coated plates.

Antigen specific B cells were identified and enriched using Eα-SA-PE tetramer. Eα-SA-PE tetramer was prepared by incubation of Eα-Bio and SA-PE (4:1 ratio) at room temperature for 30 minutes. Antigen specific endogenous B cells from pooled spleen and LNs of the Tcra-/- recipients were stained with Eα-SA-PE tetramer, and enriched by anti-PE magnetic beads pull-down[118]. Sera from immunized mice were collected at day 0, 2 and 7 post immunization, and antigen-specific IgM, IgG1, IgG2a, IgG2b, IgG2c, IgG3, IgA and IgE antibodies were measured by ELISA as previously described10. Briefly, sera were titrated into ELISA plates that had been coated with Eα-SA-DEL (20μg/ml in PBS, overnight) then blocked with 1% BSA. HRP conjugated anti-mouse-antibody isotype antibodies (Southern Biotech) were applied and detected using ABTS Peroxidase Substrate (KPL). Titers were presented as the maximum serum dilution exceeding 1.5-fold above the average background.

Retroviral transduction approaches

All retrovirus constructs (Empty control, KLF2 and S1PR1) were cloned using MSCV-IRES-Thy1.1 (MiT) backbone vector as described previously[20]. The plasmid MiT-S1PR1, MiT-KLF2 or MiT (empty vector) was transfected together with the retroviral packaging vector pCL-Eco into 293T human embryonic kidney cells with Lipofectamine 2000 (Life Technology). Supernatants were collected at 48 h after transfection.

Naive CD4+ T cells from TEa or Blimp1-YFP mice were isolated and activated by plate-bound anti-CD3 and anti-CD28 with recombinant IL-2 (20ng/ml). 24 hours after activation, cells were spin-infected by retroviruses MiT-KLF2, MiT-S1PR1 or control empty vector (MiT-Empty) as described previously[20]. Some transduced cells were transferred with MD4 B cells into congenic recipients that were then immunized with Eα-SA-DEL/CFA. In some experiment, S1PR1 function was inhibited by i.p. injection (200ml) of FTY720 (20μg/mouse) or vehicle control (10% EtOH in PBS) at day 2, 4 and 6 post immunization. For in vitro over-expression of KLF2 or S1PR1, the retrovirally transduced CD4+ T cells were cultured with recombinant IL-15 (20ng/ml) in anti-CD3/CD28 coated plate for 2 days, and were further cultured with recombinant IL-15 (20ng/ml) in non-coated plate. To examine cytokine production in the KLF2 or S1PR1 over-expressing TEa cells, cells were re-stimulated with PMA (50ng/ml, SIGMA) and ionomycin (1.5μM, SIGMA) in the presence of Monensin for 5 h and intracellular staining for IFN-γ (XMG1.2), IL-4 (11B11) and IL-17 (eBio17B7) was performed.

Chromatin immuneprecipitation (ChIP)

ChIP was performed as previously described[119]. Briefly, approximately 10^7 naïve or in vitro activated KLF2-GFP TEa cells were cross-linked with 1% formaldehyde at room temperature for 10 min and neutralized with 0.125 M glycine for 10 minutes. Chromatin was fragmented using Bioruptor®. Subsequently, the soluble chromatin was incubated with 5 μg of anti-GFP (Life technologies) or control rabbit IgG antibodies at 4°C overnight. Immunoprecipitated complexes were collected using 30ul Dynabeads G (Invitrogen) per reaction. Final ChIP DNA was extracted and purified using QIAquick spin columns (Qiagen). Precipitated DNA and input DNA were assessed by quantitative real-time PCR with SYBR Green PCR Master Mix (Applied Biosystems). The sequences of the primer pairs used were as follows: for the prdm1 promoter region, forward, 5'-TTTTGTTGTCCCTGCCTCTC-3', and reverse, 5'-CCCCTTTTTAACTGGGAAGC-3'; for the s1pr1 promoter region, forward, 5'-ACCAGCTCACTCGCAAAGTT-3', and reverse, 5'-GCGCTCAGAGACTTCGTCTT-3'; for the bcl6 promoter region, forward, 5'-GGCAGCAACAGCAATAATCA-3', and reverse, 5'-CGAGAATTGAGCTCTGTTGA-3'; for the tbx21 promoter region, forward, 5'-CGTCCGAAGACCAATGAAAC-3', and reverse, 5'-TCATAAAGCCACAGCAAAGG-3'; and for the gata3 promoter region, forward, 5'-GGGTTTGGGTTGCAGTTTCCTTGT-3', and reverse, 5'-GCGACGCAACTTAAGGAGGTTCTA-3'.

Quantitative RT-PCR

After in vitro deletion of KLF2 or retroviral overexpression of KLF2 (S1PR1), cells were sorted on a FACSAria (Becton Dickinson) on the basis of the YFP (Rosa26-YFP Cre reporter) or Thy1.1 transduction markers respectively. In all cases, RNA was isolated with an RNeasy microkit (Qiagen), followed by reverse transcription (SuperScript® III Reverse Transcriptase, Life technologies). Gene expression was assessed (in triplicate for cultured cells) with an ABI 7700 sequence-detection system, and amplification was detected with SYBR Green PCR Master Mix (Applied Biosystems).

Cycling threshold values for the control target gene (Gapdh) were subtracted from cycle threshold values for the gene of interest. Next, the mean values (averaged across all repeated experiments) for gene expression of WT (KLF2 +/+) or non-overexpressing control (Empty) TEa cells were used for normalization between experiments. The sequences of the primer pairs used were as follows: klf2, forward, 5'-ACCAACTGCGGCAAGACCTA-3', and reverse, 5'-CATCCTTCCCAGTTGCAATGA-3'; s1pr1, forward, 5'-GTGTAGACCCAGAGTCCTGCG-3', and reverse, 5'-AGCTTTTCCTTGGCTGGAGAG-3'; prdm1, forward, 5'-GACGGGGGTACTTCTGTTCA-3', and reverse, 5'- GGCATTCTTGGGAACTGTGT-3'; bcl6, forward, 5'- CACACCCGTCCATCATTGAA-3', and reverse, 5'-TGTCCTCACGGTGCCTTTTT-3'; tbx21, forward, 5'-CAACAACCCCTTTGCCAAAG-3', and reverse, 5'- TCCCCCAAGCAGTTGACAGT-

3’; gata3, forward, 5’- AGAACCGGCCCCTTATGAA-3’, and reverse, 5’-AGTTCGCGCAGGATGTCC-3’; rorc, forward, 5’-GGAGGTGACCAGCTACCAGA-3’, and reverse, 5’-TGGCAAACTCCACCACATAC-3’; foxp3, forward, 5’-GGCCCTTCTCCAGGACAGA-3’, and reverse, 5’-GCTGATCATGGCTGGGTTGT-3’; ascl2, forward, 5’- CGCTGCCCAGACTCATGCCC-3’, and reverse, 5’-GCTTTACGCGGTTGCGCTCG-3’; CXCR5, forward, 5’-ACTCCTTACCACAGTGCACCTT-3’, and reverse, 5’-GGAAACGGGAGGTGAACCA-3’; GAPDH, forward, 5’-TGGCCTACATGGCCTCCA -3’, and reverse, 5’- TCCCTAGGCCCCTCCTGTTAT-3’;

Immunohistochemistry

KLF2-GFP or WT B6 mice were subcutaneously immunized with PE (15μg in CFA) at the base of the tail and were sacrificed after 14 days. Draining LNs were fixed with 4% PFA and incubated in 30% sucrose solution. Five micrometer sections were cut and stained with anti-GFP antibody (Life technology). GFP fluorescence intensities were quantified in GC (GL7 and B220 abundant) or T cell zone (CD4+ abundant and B220 negative) CD4+ T cells using ImageJ software according to histocytometric algorithms as previously described[120].

Statistical analysis

Data were analyzed with Prism software 4.0 (GraphPad). For standard data sets, an unpaired two-tailed Student's t-test was used. For values that differed by over tenfold,

the data was log10-transformed before t-test analysis. When data were normalized (by the appropriate control samples), normalization involved division of all values by the overall mean of the control values to avoid type I and II errors during calculation of significance through the t-test. Data sets (in Prism format) are available on request.

Chapter 4

Discussion

Immunological function of Virtual Memory CD8 T cells

In Chapter 2, our studies show naturally occurring VM cells constitute a bridge between the response of naïve and antigen-experienced memory CD8 T cells. Specifically, my initial work focused on characterizing functional properties of VM CD8 T cells. Previous studies suggested that antigen-driven TM CD8 T cells display changes in gene expression, cytokine production, and cell cycle regulation, all of which are thought to enhance the capacity of these cells to rapidly enter an immune response[23,53,55-58,63,121]. Hence we investigated whether VM share these features with TM, and found that the VM population resembled TM cells in their expression of the T-box transcription factors T-bet and Eomes, which serve as critical regulators of effector functions and differentiation of memory CD8 T cells. Also, VM populations were significantly enriched in cells at G1 phase and showed rapid expansion following in vivo priming, compared with the naïve pool. However, unlike TM CD8 T cells, the VM pool exhibited impaired capacity for rapid IFN-γ synthesis and preferentially differentiated into central memory population after in vivo priming. Importantly, although VM and TM displayed several differences in functional properties, VM resembled TM cells in their efficient control of Listeria monocytogenes infection, indicating that VM cells can contribute to rapid pathogen elimination during a primary immune response. Although the VM pool accounts for only a fraction (~10%) of antigen-specific precursors for a given foreign antigen, this may constitute a significant pool in the response to a complex pathogen. For example, elegant in vivo limiting dilution assays estimate that ~14,000 CD8 T cells (in an

unprimed C57BL/6 mouse) are responsive to vaccinia virus[122]: this would correspond, on average, to > 1000 vaccinia specific VM cells. Since we observed protective immunity against LM-OVA after adoptive transfer of a few thousand Ova/K^b specific cells (Fig .14), these calculations suggest that the naturally arising VM pool may serve a hitherto unappreciated role in "pre-immune" resistance to infection, at least in mice.

Currently, to further extend my initial study, I am investigating the immune-regulatory role of VM CD8 T cells during lung infection with influenza virus. Previous studies have connected the superior memory response of CD8 T cells with collateral lung damage and increased immunopathology during influenza virus infection[123-125]. However, interestingly, our recent data showed that the VM CD8 T cells preferentially produce the immunosuppressive cytokine IL-10 in the infected lung and preserve the tissue function in the IL-10 dependent manner. Importantly, VM CD8 T cells still displayed similar virus clearance ability compared to TM population (not included in this dissertation). These finding indicate that VM cells have additional unique functional properties that allow them to balance between effective immune response and immunopathology during primary pathogen encounter.

"Are VM cells present in human? If they are, do they provide similar pre-immune protection? Do they modulate immune balance during acute local infection in human, like in mice?" Our research in the mouse system raises the significance of these questions. Recently, studies on human T cells have shown that significant fraction of CD4 T cells specific for unexperienced foreign antigens (such as HIV specific CD4 T cells in sero-

negative individual) shows memory-like phenotype[126]. Although the authors of that study proposed that these memory-like CD4+ T cells were generated through cross-reaction with environmental microbes, these data are also compatible with the idea that the human immune system generates a VM population in the absence of foreign antigen exposure. However, because of the genetic heterogeneity and multiple pathogen exposers during lifetime, defining the origins of these memory populations in human is very difficult. Therefore, to further study the immune function of homeostatic-memory T cells in humans, genetic and epigenetic unique features of the population that separate them from antigen-exposed memory T cells should be identified.

Role of KLF2 in effector CD4+ T cell lineage commitment

In the second project, I studied the transcriptional regulation of KLF2 and its role in the cell fate determination of effector and memory T cells. My initial collaborative work with former graduate student of our lab, Dr. Cara Skon, focused on CD8 T cells showed that KLF2 and its transcriptional target S1PR1 provide a molecular switch determining whether CD8 T cells commit to recirculating or tissue-resident memory (Trm) populations (not included in this dissertation)[20]. The data suggest that induced down-regulation of KLF2 or S1PR1 could be used as a method to enhance the formation of Trm during vaccination. Trm may also contribute to pathological conditions, such as fixed drug eruptions in the skin. Hence, our studies indicate potential therapeutic targets through which generation of resident memory CD8 T cells can be promoted or reversed.

Next, to extend our finding in CD8 T cells, I investigated whether CD4 T cells also have heterogeneity in terms of KLF2 and its target gene expression during antigen-specific immune response. I observed that KLF2 levels are drastically reduced on follicular helper CD4 T cells (Tfh) compared to non-Tfh populations of CD4 T cells. My data show that, similar to our findings with resident memory CD8 T cells, loss of the KLF2 target S1PR1 is critical for establishment of Tfh. S1PR1 serves to oppose migration induced by Gαi-chemokine receptor such as CCR7[36,85], during regulation of T cell recirculation through lymphoid tissues, and it is possible that S1PR1 expression also impairs activated CD4 T cell entry into the B cell follicle. However, I also find that KLF2 plays an additional role in regulating the balance of Blimp-1 and Bcl-6 expression during activated CD4 T cell differentiation, providing a second mechanism through which KLF2 controls the Tfh cell fate. These data suggest that KLF2 has crucial roles not only in proper cellular positioning (by regulating expression of S1PR1 and, incidentally, CD62L), but also in regulating lineage commitment of primed T cells during peripheral immune response. Surprisingly and unexpectedly, I also found that KLF2 promote T-bet and GATA3 expression, critical regulator for Th1 and Th2 differentiation respectively[15,16], suggesting that KLF2 may serve a hitherto unsuspected function in dictating the lineage fate of CD4 T-cells.

The factors regulating KLF2 expression during Th subset differentiation are currently unclear. KLF2 expression is downregulated with TCR activation, and it is notable that, through analysis of the Nur77-GFP mice, I find evidence that TCR engagement is sustained in cells of GC-Tfh phenotype, while this signal declines in non-

Tfh cells. This correlates with data indicating that TCR engagement is required for sustaining Tfh proliferation and maintenance[127]. However, this finding does not exclude the potential action of other factors. Signals that provoke strong PI3K/Akt activation can lead to loss of KLF2 expression[20], at least in part due to degradation of the transcription factor Foxo1 (which promotes KLF2 expression)[20,91,128-130]. Foxo1 ablation leads to substantially enhanced Tfh differentiation[91,92], and recent studies indicate that degradation of Foxo1 through action of the E3 ubiquitin ligase Itch was important for Tfh differentiation, and that Itch deficiency led to elevated expression of Foxo1 target genes (including KLF2)[92,95,130]. Studies with CD8+ T cells have shown that various cytokines - including TGF-β, IL-33, IL-12, IFN-I and TNF – can act individually or cooperatively to impair KLF2 expression[20,95,130]. Hence the specific cytokine milieu surrounding an activated CD4 T cell may dictate its KLF2 expression pattern. It is also worth noting that ICOS signaling, which is critical for Tfh differentiation, is mediated at least in part through PI3K[81,131] and hence signals induced by ICOS-ICOSL interactions may inhibit KLF2 expression.

Bibliography

1 Murphy, K., Travers, P., Walport, M. & Janeway, C. *Janeway's immunobiology*. 8th edn, (Garland Science, 2012).

2 Taylor, P. R. *et al.* Macrophage receptors and immune recognition. *Annu Rev Immunol* **23**, 901-944, doi:10.1146/annurev.immunol.23.021704.115816 (2005).

3 Schenten, D. & Medzhitov, R. The control of adaptive immune responses by the innate immune system. *Adv Immunol* **109**, 87-124, doi:10.1016/B978-0-12-387664-5.00003-0 (2011).

4 Medzhitov, R. Toll-like receptors and innate immunity. *Nat Rev Immunol* **1**, 135-145, doi:10.1038/35100529 (2001).

5 Janeway, C. A., Jr. & Medzhitov, R. Innate immune recognition. *Annu Rev Immunol* **20**, 197-216, doi:10.1146/annurev.immunol.20.083001.084359 (2002).

6 Pancer, Z. & Cooper, M. D. The evolution of adaptive immunity. *Annu Rev Immunol* **24**, 497-518, doi:10.1146/annurev.immunol.24.021605.090542 (2006).

7 Carlson, C. M. *et al.* Kruppel-like factor 2 regulates thymocyte and T-cell migration. *Nature* **442**, 299-302 (2006).

8 Hart, G. T., Hogquist, K. A. & Jameson, S. C. Kruppel-like factors in lymphocyte biology. *J Immunol* **188**, 521-526, doi:10.4049/jimmunol.1101530 (2012).

9 Mescher, M. F. *et al.* Signals required for programming effector and memory development by CD8+ T cells. *Immunol Rev* **211**, 81-92, doi:10.1111/j.0105-2896.2006.00382.x (2006).

10 Carreno, B. M. & Collins, M. The B7 family of ligands and its receptors: new pathways for costimulation and inhibition of immune responses. *Annu Rev Immunol* **20**, 29-53, doi:10.1146/annurev.immunol.20.091101.091806 (2002).

11 Williams, M. A. & Bevan, M. J. Effector and memory CTL differentiation. *Annu Rev Immunol* **25**, 171-192, doi:10.1146/annurev.immunol.25.022106.141548 (2007).

12 Jameson, S. C. T cell homeostasis: Keeping useful T cells alive and live T cells useful. *Semin Immunol* **17**, 231-237 (2005).

13 Hamilton, S. E. & Jameson, S. C. CD8 T cell quiescence revisited. *Trends in Immunology* **33**, 224-230, doi:10.1016/j.it.2012.01.007 (2012).

14 Watts, C. Capture and processing of exogenous antigens for presentation on MHC molecules. *Annu Rev Immunol* **15**, 821-850, doi:10.1146/annurev.immunol.15.1.821 (1997).

15 Zhou, L., Chong, M. M. & Littman, D. R. Plasticity of CD4+ T cell lineage differentiation. *Immunity* **30**, 646-655, doi:10.1016/j.immuni.2009.05.001 (2009).

16 Bonelli, M. *et al.* Helper T Cell Plasticity: Impact of Extrinsic and Intrinsic Signals on Transcriptomes and Epigenomes. *Curr Top Microbiol Immunol*, doi:10.1007/82_2014_371 (2014).

17 Kaech, S. M. & Cui, W. Transcriptional control of effector and memory CD8+ T cell differentiation. *Nat Rev Immunol* **12**, 749-761, doi:10.1038/nri3307 (2012).

18 Mueller, S. N., Gebhardt, T., Carbone, F. R. & Heath, W. R. Memory T cell subsets, migration patterns, and tissue residence. *Annu Rev Immunol* **31**, 137-161, doi:10.1146/annurev-immunol-032712-095954 (2013).

19 Sallusto, F., Geginat, J. & Lanzavecchia, A. Central memory and effector memory T cell subsets: function, generation, and maintenance. *Annu Rev Immunol* **22**, 745-763, doi:10.1146/annurev.immunol.22.012703.104702 (2004).

20 Skon, C. N. *et al.* Transcriptional downregulation of S1pr1 is required for the establishment of resident memory CD8+ T cells. *Nature immunology* **14**, 1285-1293, doi:10.1038/ni.2745 (2013).

21 Schenkel, J. M., Fraser, K. A., Vezys, V. & Masopust, D. Sensing and alarm function of resident memory CD8(+) T cells. *Nature immunology* **14**, 509-513, doi:10.1038/ni.2568 (2013).

22 Schmitt, N. *et al.* The cytokine TGF-beta co-opts signaling via STAT3-STAT4 to promote the differentiation of human TFH cells. *Nature immunology* **15**, 856-865, doi:10.1038/ni.2947 (2014).

23 Harty, J. T. & Badovinac, V. P. Shaping and reshaping CD8+ T-cell memory. *Nat Rev Immunol* **8**, 107-119 (2008).

24 Lee, Y. J., Jameson, S. C. & Hogquist, K. A. Alternative memory in the CD8 T cell lineage. *Trends Immunol* **32**, 50-56, doi:10.1016/j.it.2010.12.004 (2011).

25 Sallusto, F., Geginat, J. & Lanzavecchia, A. Central memory and effector memory T cell subsets: function, generation, and maintenance. *Annu Rev Immunol* **22**, 745-763 (2004).

26 Akue, A. D., Lee, J. Y. & Jameson, S. C. Derivation and maintenance of virtual memory CD8 T cells. *J Immunol* **188**, 2516-2523, doi:10.4049/jimmunol.1102213 (2012).

27 Haluszczak, C. *et al.* The antigen-specific CD8+ T cell repertoire in unimmunized mice includes memory phenotype cells bearing markers of homeostatic expansion. *J Exp Med* **206**, 435-448 (2009).

28 Marleau, A. M. & Sarvetnick, N. T cell homeostasis in tolerance and immunity. *J Leukoc Biol* **78**, 575-584 (2005).

29 Surh, C. D. & Sprent, J. Regulation of mature T cell homeostasis. *Semin Immunol* **17**, 183-191 (2005).

30 Le Campion, A. *et al.* Naive T cells proliferate strongly in neonatal mice in response to self-peptide/self-MHC complexes. *Proc Natl Acad Sci U S A* **99**, 4538-4543 (2002).

31 Min, B. *et al.* Neonates support lymphopenia-induced proliferation. *Immunity* **18**, 131-140 (2003).

32 Hamilton, S. E., Wolkers, M. C., Schoenberger, S. P. & Jameson, S. C. The generation of protective memory-like CD8(+) T cells during homeostatic proliferation requires CD4(+) T cells. *Nature immunology* **7**, 475-481 (2006).

33 Hamilton, S. E. & Jameson, S. C. The nature of the lymphopenic environment dictates protective function of homeostatic-memory CD8+ T cells. *Proc Natl Acad Sci U S A* **105**, 18484-18489 (2008).

34 Zachariah, M. A. & Cyster, J. G. Thymic egress: S1P of 1000. *F1000 Biol Rep* **1**, 60, doi:10.3410/B1-60 (2009).

35 Cyster, J. G. & Schwab, S. R. Sphingosine-1-phosphate and lymphocyte egress from lymphoid organs. *Annu Rev Immunol* **30**, 69-94, doi:10.1146/annurev-immunol-020711-075011 (2012).

36 Pham, T. H., Okada, T., Matloubian, M., Lo, C. G. & Cyster, J. G. S1P1 receptor signaling overrides retention mediated by G alpha i-coupled receptors to promote T cell egress. *Immunity* **28**, 122-133, doi:10.1016/j.immuni.2007.11.017 (2008).

37 Matloubian, M. *et al.* Lymphocyte egress from thymus and peripheral lymphoid organs is dependent on S1P receptor 1. *Nature* **427**, 355-360, doi:10.1038/nature02284 (2004).

38 Preston, G. C., Feijoo-Carnero, C., Schurch, N., Cowling, V. H. & Cantrell, D. A. The impact of KLF2 modulation on the transcriptional program and function of CD8 T cells. *PloS one* **8**, e77537, doi:10.1371/journal.pone.0077537 (2013).

39 Hu, G. & Chen, J. A genome-wide regulatory network identifies key transcription factors for memory CD8(+) T-cell development. *Nat Commun* **4**, 2830, doi:10.1038/ncomms3830 (2013).

40 Goldrath, A. W., Bogatzki, L. Y. & Bevan, M. J. Naive T Cells Transiently Acquire a Memory-like Phenotype during Homeostasis-driven Proliferation. *J Exp Med* **192**, 557-564 (2000).

41 Cheung, K. P., Yang, E. & Goldrath, A. W. Memory-like CD8+ T cells generated during homeostatic proliferation defer to antigen-experienced memory cells. *J Immunol* **183**, 3364-3372, doi:10.4049/jimmunol.0900641 (2009).

42 La Gruta, N. L. *et al.* Primary CTL response magnitude in mice is determined by the extent of naive T cell recruitment and subsequent clonal expansion. *J Clin Invest* **120**, 1885-1894, doi:10.1172/JCI41538 (2010).

43 Hamilton, S. E., Schenkel, J. M., Akue, A. D. & Jameson, S. C. IL-2 Complex Treatment Can Protect Naïve Mice from Bacterial and Viral Infection. *J.Immunol.* **185**, 6584-6590 (2010).

44 Rudd, B. D. *et al.* Nonrandom attrition of the naive CD8+ T-cell pool with aging governed by T-cell receptor:pMHC interactions. *Proc Natl Acad Sci U S A* **108**, 13694-13699, doi:10.1073/pnas.1107594108 (2011).

45 Sosinowski, T. *et al.* CD8alpha+ Dendritic Cell Trans Presentation of IL-15 to Naive CD8+ T Cells Produces Antigen-Inexperienced T Cells in the Periphery with Memory Phenotype and Function. *J Immunol*, doi:10.4049/jimmunol.1203149 (2013).

46 Rifa'i, M., Kawamoto, Y., Nakashima, I. & Suzuki, H. Essential roles of CD8+CD122+ regulatory T cells in the maintenance of T cell homeostasis. *J Exp Med* **200**, 1123-1134 (2004).

47 Kim, H. J. *et al.* CD8+ T regulatory cells express the Ly49 Class I MHC receptor and are defective in autoimmune prone B6-Yaa mice. *Proc Natl Acad Sci U S A* **108**, 2010-2015, doi:10.1073/pnas.1018974108 (2011).

48 Sakuraba, K., Shibata, K., Iwamoto, Y., Yoshikai, Y. & Yamada, H. Naturally Occurring PD-1+ Memory Phenotype CD8 T Cells Belong to Nonconventional CD8 T Cells and Are Cyclophosphamide-Sensitive Regulatory T Cells. *J Immunol* **190**, 1560-1566, doi:10.4049/jimmunol.1202464 (2013).

49 Lin, S. J., Peacock, C. D., Bahl, K. & Welsh, R. M. Programmed death-1 (PD-1) defines a transient and dysfunctional oligoclonal T cell population in acute homeostatic proliferation. *J Exp Med* **204**, 2321-2333, doi:10.1084/jem.20062150 (2007).

50 Kim, H. J., Verbinnen, B., Tang, X., Lu, L. & Cantor, H. Inhibition of follicular T-helper cells by CD8(+) regulatory T cells is essential for self tolerance. *Nature* **467**, 328-332, doi:10.1038/nature09370 (2010).

51 Dillon, S. R., Jameson, S. C. & Fink, P. J. V beta 5+ T cell receptors skew toward OVA+H-2Kb recognition. *J Immunol* **152**, 1790-1801 (1994).

52 Zehn, D. & Bevan, M. J. T cells with low avidity for a tissue-restricted antigen routinely evade central and peripheral tolerance and cause autoimmunity. *Immunity* **25**, 261-270 (2006).

53 Seder, R. A. & Ahmed, R. Similarities and differences in CD4+ and CD8+ effector and memory T cell generation. *Nature immunology* **4**, 835-842 (2003).

54 Intlekofer, A. M. *et al.* Effector and memory CD8+ T cell fate coupled by T-bet and eomesodermin. *Nature immunology* **6**, 1236-1244 (2005).

55 Pearce, E. L. *et al.* Control of effector CD8+ T cell function by the transcription factor Eomesodermin. *Science* **302**, 1041-1043 (2003).

56 Banerjee, A. *et al.* Cutting edge: The transcription factor eomesodermin enables CD8+ T cells to compete for the memory cell niche. *J Immunol* **185**, 4988-4992, doi:10.4049/jimmunol.1002042 (2010).

57 Veiga-Fernandes, H. & Rocha, B. High expression of active CDK6 in the cytoplasm of CD8 memory cells favors rapid division. *Nature immunology* **5**, 31-37 (2004).

58 Munitic, I., Ryan, P. E. & Ashwell, J. D. T cells in G1 provide a memory-like response to secondary stimulation. *J Immunol* **174**, 4010-4018 (2005).

59 Latner, D. R., Kaech, S. M. & Ahmed, R. Enhanced expression of cell cycle regulatory genes in virus-specific memory CD8+ T cells. *J Virol* **78**, 10953-10959 (2004).

60 Surh, C. D. & Sprent, J. Homeostasis of naive and memory T cells. *Immunity* **29**, 848-862, doi:10.1016/j.immuni.2008.11.002 (2008).

61 Antia, R., Ganusov, V. V. & Ahmed, R. The role of models in understanding CD8+ T-cell memory. *Nat Rev Immunol* **5**, 101-111, doi:10.1038/nri1550 (2005).

62 Tough, D. F. & Sprent, J. Turnover of naive- and memory-phenotype T cells. *J Exp Med* **179**, 1127-1135 (1994).

63 Sullivan, B. M., Juedes, A., Szabo, S. J., von Herrath, M. & Glimcher, L. H. Antigen-driven effector CD8 T cell function regulated by T-bet. *Proc Natl Acad Sci U S A* **100**, 15818-15823, doi:10.1073/pnas.2636938100 (2003).

64 Brehm, M. A., Daniels, K. A. & Welsh, R. M. Rapid production of TNF-alpha following TCR engagement of naive CD8 T cells. *J Immunol* **175**, 5043-5049 (2005).

65 Kaech, S. M. & Wherry, E. J. Heterogeneity and cell-fate decisions in effector and memory CD8+ T cell differentiation during viral infection. *Immunity* **27**, 393-405 (2007).

66 Sallusto, F., Lenig, D., Forster, R., Lipp, M. & Lanzavecchia, A. Two subsets of memory T lymphocytes with distinct homing potentials and effector functions. *Nature* **401**, 708-712 (1999).

67 Masopust, D., Vezys, V., Marzo, A. L. & Lefrancois, L. Preferential localization of effector memory cells in nonlymphoid tissue. *Science* **291**, 2413-2417 (2001).

68 Masopust, D., Ha, S. J., Vezys, V. & Ahmed, R. Stimulation history dictates memory CD8 T cell phenotype: implications for prime-boost vaccination. *J Immunol* **177**, 831-839 (2006).

69 Jabbari, A. & Harty, J. T. Secondary memory CD8+ T cells are more protective but slower to acquire a central-memory phenotype. *J Exp Med* **203**, 919-932 (2006).

70 Pamer, E. G. Immune responses to Listeria monocytogenes. *Nat Rev Immunol* **4**, 812-823 (2004).

71 Dai, H. *et al.* Cutting edge: programmed death-1 defines CD8+CD122+ T cells as regulatory versus memory T cells. *J Immunol* **185**, 803-807, doi:10.4049/jimmunol.1000661 (2010).

72 Berg, R. E., Crossley, E., Murray, S. & Forman, J. Memory CD8+ T cells provide innate immune protection against Listeria monocytogenes in the absence of cognate antigen. *J Exp Med* **198**, 1583-1593 (2003).

73 Kambayashi, T., Assarsson, E., Lukacher, A. E., Ljunggren, H. G. & Jensen, P. E. Memory CD8+ T cells provide an early source of IFN-gamma. *J Immunol* **170**, 2399-2408 (2003).

74 Berg, R. E. & Forman, J. The role of CD8 T cells in innate immunity and in antigen non-specific protection. *Curr Opin Immunol* **18**, 338-343 (2006).

75 Miller, S. A., Mohn, S. E. & Weinmann, A. S. Jmjd3 and UTX play a demethylase-independent role in chromatin remodeling to regulate T-box family member-dependent gene expression. *Mol Cell* **40**, 594-605, doi:10.1016/j.molcel.2010.10.028 (2010).

76 Nolz, J. C. & Harty, J. T. Protective capacity of memory CD8+ T cells is dictated by antigen exposure history and nature of the infection. *Immunity* **34**, 781-793, doi:10.1016/j.immuni.2011.03.020 (2011).

77 Daniels, M. A. & Jameson, S. C. Critical role for CD8 in T cell receptor binding and activation by peptide/major histocompatibility complex multimers. *J Exp Med* **191**, 335-346 (2000).

78 Kedl, R. M., Schaefer, B. C., Kappler, J. W. & Marrack, P. T cells down-modulate peptide-MHC complexes on APCs in vivo. *Nature immunology* **3**, 27-32, doi:10.1038/ni742 (2002).

79 Anderson, K. G. *et al.* Cutting edge: intravascular staining redefines lung CD8 T cell responses. *J Immunol* **189**, 2702-2706, doi:10.4049/jimmunol.1201682 (2012).

80 Victora, G. D. & Nussenzweig, M. C. Germinal centers. *Annu Rev Immunol* **30**, 429-457, doi:10.1146/annurev-immunol-020711-075032 (2012).

81 Crotty, S. Follicular helper CD4 T cells (TFH). *Annu Rev Immunol* **29**, 621-663, doi:10.1146/annurev-immunol-031210-101400 (2011).

82 Vinuesa, C. G. & Cyster, J. G. How T cells earn the follicular rite of passage. *Immunity* **35**, 671-680, doi:10.1016/j.immuni.2011.11.001 (2011).

83 Liu, X., Nurieva, R. I. & Dong, C. Transcriptional regulation of follicular T-helper (Tfh) cells. *Immunol Rev* **252**, 139-145, doi:10.1111/imr.12040 (2013).

84 Moriyama, S. *et al.* Sphingosine-1-phosphate receptor 2 is critical for follicular helper T cell retention in germinal centers. *J Exp Med*, doi:10.1084/jem.20131666 (2014).

85 Haynes, N. M. *et al.* Role of CXCR5 and CCR7 in follicular Th cell positioning and appearance of a programmed cell death gene-1high germinal center-associated subpopulation. *J Immunol* **179**, 5099-5108 (2007).

86 Liu, X. *et al.* Transcription factor achaete-scute homologue 2 initiates follicular T-helper-cell development. *Nature* **507**, 513-518, doi:10.1038/nature12910 (2014).

87 Johnston, R. J., Choi, Y. S., Diamond, J. A., Yang, J. A. & Crotty, S. STAT5 is a potent negative regulator of TFH cell differentiation. *J Exp Med* **209**, 243-250, doi:10.1084/jem.20111174 (2012).

88 Oestreich, K. J., Mohn, S. E. & Weinmann, A. S. Molecular mechanisms that control the expression and activity of Bcl-6 in TH1 cells to regulate flexibility with a TFH-like gene profile. *Nature immunology* **13**, 405-411, doi:10.1038/ni.2242 (2012).

89 Ballesteros-Tato, A. *et al.* Interleukin-2 inhibits germinal center formation by limiting T follicular helper cell differentiation. *Immunity* **36**, 847-856, doi:10.1016/j.immuni.2012.02.012 (2012).

90 Pepper, M., Pagan, A. J., Igyarto, B. Z., Taylor, J. J. & Jenkins, M. K. Opposing signals from the Bcl6 transcription factor and the interleukin-2 receptor generate T helper 1 central and effector memory cells. *Immunity* **35**, 583-595, doi:10.1016/j.immuni.2011.09.009 (2011).

91 Kerdiles, Y. M. *et al.* Foxo transcription factors control regulatory T cell development and function. *Immunity* **33**, 890-904, doi:10.1016/j.immuni.2010.12.002 (2010).

92 Xiao, N. *et al.* The E3 ubiquitin ligase Itch is required for the differentiation of follicular helper T cells. *Nature immunology*, doi:10.1038/ni.2912 (2014).

93 Wang, H. *et al.* The transcription factor Foxp1 is a critical negative regulator of the differentiation of follicular helper T cells. *Nature immunology*, doi:10.1038/ni.2890 (2014).

94 Nurieva, R. I. *et al.* Bcl6 mediates the development of T follicular helper cells. *Science* **325**, 1001-1005, doi:10.1126/science.1176676 (2009).

95 Bai, A., Hu, H., Yeung, M. & Chen, J. Kruppel-like factor 2 controls T cell trafficking by activating L-selectin (CD62L) and sphingosine-1-phosphate receptor 1 transcription. *J Immunol* **178**, 7632-7639 (2007).

96 Takada, K. *et al.* Kruppel-like factor 2 is required for trafficking but not quiescence in postactivated T cells. *J Immunol* **186**, 775-783, doi:10.4049/jimmunol.1000094 (2011).

97 Weinreich, M. A. *et al.* KLF2 transcription-factor deficiency in T cells results in unrestrained cytokine production and upregulation of bystander chemokine receptors. *Immunity* **31**, 122-130, doi:10.1016/j.immuni.2009.05.011 (2009).

98 Grubin, C. E., Kovats, S., deRoos, P. & Rudensky, A. Y. Deficient positive selection of CD4 T cells in mice displaying altered repertoires of MHC class II-bound self-peptides. *Immunity* **7**, 197-208 (1997).

99 Hartley, S. B. *et al.* Elimination from peripheral lymphoid tissues of self-reactive B lymphocytes recognizing membrane-bound antigens. *Nature* **353**, 765-769, doi:10.1038/353765a0 (1991).

100 Cahalan, S. M. *et al.* Actions of a picomolar short-acting S1P(1) agonist in S1P(1)-eGFP knock-in mice. *Nat Chem Biol* **7**, 254-256, doi:10.1038/nchembio.547 (2011).

101 Tubo, N. J. *et al.* Single naive CD4+ T cells from a diverse repertoire produce different effector cell types during infection. *Cell* **153**, 785-796, doi:10.1016/j.cell.2013.04.007 (2013).

102 Fazilleau, N., McHeyzer-Williams, L. J., Rosen, H. & McHeyzer-Williams, M. G. The function of follicular helper T cells is regulated by the strength of T cell antigen receptor binding. *Nature immunology* **10**, 375-384, doi:10.1038/ni.1704 (2009).

103 Bankovich, A. J., Shiow, L. R. & Cyster, J. G. CD69 suppresses sphingosine 1-phosophate receptor-1 (S1P1) function through interaction with membrane helix 4. *J Biol Chem* **285**, 22328-22337, doi:10.1074/jbc.M110.123299 (2010).

104 Moran, A. E. *et al.* T cell receptor signal strength in Treg and iNKT cell development demonstrated by a novel fluorescent reporter mouse. *J Exp Med* **208**, 1279-1289, doi:10.1084/jem.20110308 (2011).

105 Zachariah, M. A. & Cyster, J. G. Neural crest-derived pericytes promote egress of mature thymocytes at the corticomedullary junction. *Science* **328**, 1129-1135, doi:10.1126/science.1188222 (2010).

106 Johnston, R. J. *et al.* Bcl6 and Blimp-1 are reciprocal and antagonistic regulators of T follicular helper cell differentiation. *Science* **325**, 1006-1010, doi:10.1126/science.1175870 (2009).

107 Arnon, T. I., Horton, R. M., Grigorova, I. L. & Cyster, J. G. Visualization of splenic marginal zone B-cell shuttling and follicular B-cell egress. *Nature* **493**, 684-688, doi:10.1038/nature11738 (2013).

108 Paliard, X. *et al.* Simultaneous production of IL-2, IL-4, and IFN-gamma by activated human CD4+ and CD8+ T cell clones. *J Immunol* **141**, 849-855 (1988).

109 Zhu, J., Yamane, H. & Paul, W. E. Differentiation of effector CD4 T cell populations. *Annu Rev Immunol* **28**, 445-489, doi:10.1146/annurev-immunol-030409-101212 (2010).

110 Hegazy, A. N. *et al.* Interferons direct Th2 cell reprogramming to generate a stable GATA-3(+)T-bet(+) cell subset with combined Th2 and Th1 cell functions. *Immunity* **32**, 116-128, doi:10.1016/j.immuni.2009.12.004 (2010).

111 Kanhere, A. *et al.* T-bet and GATA3 orchestrate Th1 and Th2 differentiation through lineage-specific targeting of distal regulatory elements. *Nat Commun* **3**, 1268, doi:10.1038/ncomms2260 (2012).

112 Cimmino, L. *et al.* Blimp-1 attenuates Th1 differentiation by repression of ifng, tbx21, and bcl6 gene expression. *J Immunol* **181**, 2338-2347 (2008).

113 Hart, G. T., Wang, X., Hogquist, K. A. & Jameson, S. C. Kruppel-like factor 2 (KLF2) regulates B-cell reactivity, subset differentiation, and trafficking molecule expression. *Proc Natl Acad Sci U S A* **108**, 716-721, doi:10.1073/pnas.1013168108 (2011).

114 Weinreich, M. A., Odumade, O. A., Jameson, S. C. & Hogquist, K. A. T cells expressing the transcription factor PLZF regulate the development of memory-like CD8+ T cells. *Nature immunology* **11**, 709-716, doi:10.1038/ni.1898 (2010).

115 Moon, J. J. *et al.* Tracking epitope-specific T cells. *Nat Protoc* **4**, 565-581, doi:10.1038/nprot.2009.9 (2009).

116 Lee, Y. J., Holzapfel, K. L., Zhu, J., Jameson, S. C. & Hogquist, K. A. Steady-state production of IL-4 modulates immunity in mouse strains and is determined

by lineage diversity of iNKT cells. *Nature immunology* **14**, 1146-1154, doi:10.1038/ni.2731 (2013).

117 Taylor, J. J. *et al.* Deletion and anergy of polyclonal B cells specific for ubiquitous membrane-bound self-antigen. *J Exp Med* **209**, 2065-2077, doi:10.1084/jem.20112272 (2012).

118 Pape, K. A., Taylor, J. J., Maul, R. W., Gearhart, P. J. & Jenkins, M. K. Different B cell populations mediate early and late memory during an endogenous immune response. *Science* **331**, 1203-1207, doi:10.1126/science.1201730 (2011).

119 Li, W. *et al.* Functional roles of enhancer RNAs for oestrogen-dependent transcriptional activation. *Nature* **498**, 516-520, doi:10.1038/nature12210 (2013).

120 Gerner, M. Y., Kastenmuller, W., Ifrim, I., Kabat, J. & Germain, R. N. Histo-cytometry: a method for highly multiplex quantitative tissue imaging analysis applied to dendritic cell subset microanatomy in lymph nodes. *Immunity* **37**, 364-376, doi:10.1016/j.immuni.2012.07.011 (2012).

121 Veiga-Fernandes, H., Walter, U., Bourgeois, C., McLean, A. & Rocha, B. Response of naive and memory CD8+ T cells to antigen stimulation in vivo. *Nature immunology* **1**, 47-53. (2000).

122 Seedhom, M. O., Jellison, E. R., Daniels, K. A. & Welsh, R. M. High frequencies of virus-specific CD8+ T-cell precursors. *J Virol* **83**, 12907-12916, doi:10.1128/JVI.01722-09 (2009).

123 Perona-Wright, G. *et al.* Persistent loss of IL-27 responsiveness in CD8+ memory T cells abrogates IL-10 expression in a recall response. *Proc Natl Acad Sci U S A* **109**, 18535-18540, doi:10.1073/pnas.1119133109 (2012).

124 Sun, J., Dodd, H., Moser, E. K., Sharma, R. & Braciale, T. J. CD4+ T cell help and innate-derived IL-27 induce Blimp-1-dependent IL-10 production by antiviral CTLs. *Nature immunology* **12**, 327-334, doi:10.1038/ni.1996 (2011).

125 Sun, J., Madan, R., Karp, C. L. & Braciale, T. J. Effector T cells control lung inflammation during acute influenza virus infection by producing IL-10. *Nat Med* **15**, 277-284, doi:10.1038/nm.1929 (2009).

126 Su, L. F., Kidd, B. A., Han, A., Kotzin, J. J. & Davis, M. M. Virus-specific CD4(+) memory-phenotype T cells are abundant in unexposed adults. *Immunity* **38**, 373-383, doi:10.1016/j.immuni.2012.10.021 (2013).

127 Choi, Y. S. *et al.* Bcl6 expressing follicular helper CD4 T cells are fate committed early and have the capacity to form memory. *J Immunol* **190**, 4014-4026, doi:10.4049/jimmunol.1202963 (2013).

128 Kerdiles, Y. M. *et al.* Foxo1 links homing and survival of naive T cells by regulating L-selectin, CCR7 and interleukin 7 receptor. *Nature immunology* **10**, 176-184, doi:10.1038/ni.1689 (2009).

129 Fabre, S. *et al.* FOXO1 regulates L-Selectin and a network of human T cell homing molecules downstream of phosphatidylinositol 3-kinase. *J Immunol* **181**, 2980-2989 (2008).

130 Sinclair, L. V. *et al.* Phosphatidylinositol-3-OH kinase and nutrient-sensing mTOR pathways control T lymphocyte trafficking. *Nature immunology* **9**, 513-521, doi:10.1038/ni.1603 (2008).

131 Gigoux, M. *et al.* Inducible costimulator promotes helper T-cell differentiation through phosphoinositide 3-kinase. *Proc Natl Acad Sci U S A* **106**, 20371-20376, doi:10.1073/pnas.0911573106 (2009).